UNIVERSITÀ DEGLI STUDI DI TRIESTE

XXVII CICLO DEL DOTTORATO DI RICERCA IN

**BIOMEDICINA MOLECOLARE**

# BRAF35 AS TARGET OF MID1/TRIM18 E3 LIGASE ACTIVITY

Settore scientifico-disciplinare: **BIO/18**


Dottoranda

**Melania Eva Zanchetta**

Coordinatore

**Prof. Guidalberto Manfioletti**

Supervisore di Tesi

**Prof.ssa. Germana Meroni**


**ANNO ACCADEMICO 2014 / 2015**

# TABLE OF CONTENTS

## SUMMARY

TRIM proteins are a family of ubiquitin E3 ligase enzymes characterized by the presence of a conserved N-terminus, the tripartite motif, which consists of a RING finger domain, one or two B-box motifs and an alpha-helical Coiled-coil region (RBCC). We focused our attention on TRIM18/MID1, the gene responsible for the X-linked form of Opitz G/BBB syndrome, a congenital disease characterized by defects in midline development and mental retardation. More recently, MID1 has also been found as overexpressed in some aggressive prostate cancers. The role of MID1 within the cell and the target(s) of its E3 ubiquitin activity during cellular processes are still not completely unravelled. In order to better investigate MID1 function and to find new cellular partners for this protein a two hybrid assay was performed in our laboratory. By means of this screening, *BR*CA2-*A*ssociated *F*actor 35 (BRAF35 or HMG20b) was identified as a novel MID1 interacting protein.

BRAF35 is a non-canonical High-Mobility-Group (HMG) protein that has a role in both neuronal differentiation and in cell cycle progression. Moreover BRAF35 sumoylation has been shown to be fundamental for its antineurogenic activity and is inhibited by the interaction with its homologue iBraf. The aim of the project was to characterise the functional role of MID1/BRAF35 interaction and to understand if MID1, as an E3 ubiquitin ligase, regulates BRAF35 during cytokinesis. The first evidence obtained from the preliminary screening was confirmed through MBP pull-down assay and co-immunoprecipitation, identifying the coiled-coil region of both proteins as responsible for the binding. We further investigated on a possible regulation of BRAF35 by the ubiquitin proteasome system and we recognized BRAF35 as a poly-ubiquitinated protein and we found that its abundance is regulated in a proteasome-dependent manner. In addition, overexpression of MID1 or its domain-deleted mutants altered BRAF35 stability and post-translational modification suggesting a MID1-dependent BRAF35 ubiquitination that implicates also K63-polyUb dependent signalling involvement.

Additionally, we found that MID1 and BRAF35 colocalize not only during interphase but also at the intercellular bridge during cytokinesis. Consistent with this observation, we observed a cell cycle-related regulation of BRAF35 protein level.

Moreover, MID1 depletion rescued the cytokinetic defect caused by BRAF35 silencing, leading to a decrease of binucleation, but promoted a blebbing phenotype in dividing cells.

This indicates that a fine regulation of the two proteins for the completion of cytokinesis is required and suggests an additional and new role for MID1 in cytokinesis regulation.

## LIST OF ABBREVIATIONS

| | |
|---|---|
| 4E-BP1 | Eukaryotic translation initiation factor 4E-binding protein 1 |
| ACID | Acid-rich region |
| ALIX | Apoptosis-Linked gene-2-Interacting protein X |
| AMSH | Associated Molecule with the SH3 domain of STAM |
| Aos1 | Activator of SUMO1 |
| APL | Acute Promyelocytic Leukaemia |
| AR | Androgen Receptor |
| ARF | ADP Ribosylation Factor |
| Arg, R | Arginine |
| ATG | Autophagy-Related Genes |
| ATG101 | Autophagy-related protein 101 |
| BECN1 | Beclin 1, autophagy related |
| BRAF35/HMG20B | BRCA2-associated factor 35 |
| BRCA2 | BReast CAncer 2 |
| BROMO | Bromodomain |
| BRUCE | BIR Repeat containing Ubiquitin-Conjugating Enzyme |
| C-term | C-terminus |
| CC | Coiled-coil |
| CCR4 | Chemokine (C-C Motif) Receptor 4 |
| Cdc20 | APC/C activator protein CDC20 |
| Cdh1 | APC/C activator protein CDH1 |
| CDK1 | Cyclin-Dependent Kinase 1 |
| CEP55 | Centrosomal Protein 55kDa |
| CHMP | CHarged Multivesicular body Protein |
| cIAP1 | Cellular inhibitor of Apoptosis Protein-1 |
| CLDN12 | Claudin 12 |
| CNOT7 | CCR4-NOT Transcription Complex, Subunit 7 |
| coREST/RCOR1 | REST corepressor 1 |
| COS | COS-box |
| CP | Core Particle |
| CPC | Chromosomal Passenger Complex |
| CTL | Cytotoxic T Lymphocyte |

| | |
|---|---|
| CUE | Coupling of Ubiquitin conjugation to ER degradation |
| Cul1 | Cullin 1 |
| CUL3 | Cullin 3 |
| CXADR | Coxsackie Virus snd Adenovirus Receptor |
| CYLD | Cylindromatosis (turban tumor syndrome) |
| Cys | Cysteine |
| DeSI | Desumoylating Isopeptidase |
| DMSO | Dimethylsulphoxide |
| DUB | Deubiquitinase |
| E1 | UBE1, Ubiquitin activating enzyme |
| E2 | UBE2, Ubiquitin conjugating enzyme |
| E3 | Ubiquitin ligase enzyme |
| ECT2 | Epithelial Cell Transforming 2 |
| EF1α | Elongation Factor-1α |
| EMT | Epithelial-to-Mesenchymal Transition |
| ERAD | Endoplasmic Reticulum-Associated Degradation |
| ESCRT | Endosomal Sorting Complex Required for Transport |
| FAT10/UBD | Ubiquitin-Like Protein FAT10 |
| FIL | Filamin-type I G domain |
| FN3 | Fibronection type III |
| Fu | Fused |
| FUB1 | Silencing boundary-establishment protein FUB1 |
| FYVE-CENT | Zinc Finger, FYVE Domain Containing 26 |
| GABARAP | GABA type A Receptor-Associated Protein |
| GEF | Guanine nucleotide Exchange Factor |
| GLI3 | GLI family zinc finger 3 |
| H3 | Histone 3 |
| HDAC | Histone Deacetylase |
| HECT | Homology to E6AP C Terminus |
| HMG | High-Mobility-Group |
| HOIL | Haem-Oxidized IRP2 ubiquitin Ligase |
| HOIP | HOIL-1L Inteacting Protein |
| HRS | Hepatocyte growth factor (HGF)-Regulated Tyr-kinase Substrate |

| | |
|---|---|
| HTT | Huntingtin |
| iBRAF/HMG20A | inhibitor of BRAF35 |
| ISG15 | Interferon Stimulated Gene product of 15 kDa |
| JAMM/MPN | Jab1/MPN domain-Associated Metalloisopeptidase |
| KIF4 | KInesin Family member 4 |
| KLCC | Kinesin-Like Coiled Coil |
| KLH22 | Kelch-like protein 22 |
| KLHDC8B | Kelch Domain Containing 8B |
| KRT18 | Keratin, type I cytoskeletal 18 |
| LIR | LC3-interacting region |
| LSD1/KDM1A | Lysine Demethylase 1A |
| LUBAC | Linear Ubiquitin Assembly Complex |
| Lys, K | Lysine |
| MAP | Microtubule-Associated Protein |
| MAP1LC3 | Microtubule-Associated Protein 1 Light Chain 3, LC3 |
| MAPK | Mitogen Activated Protein Kinase |
| MATH | Meprin and Tumor necrosis factor receptor-associated factor Homology |
| MB | Midbody |
| MBP | Maltose-Binding Protein |
| MBR | Midbody remnant |
| Mdmx | Transformed mouse 3T3 cell double minute 4 |
| Mdn2 | Transformed mouse 3T3 cell double minute 2 |
| Met | Methionine |
| MEX-3C | Mex-3 RNA Binding Family Member C |
| MHC-I | Major Histocompatibility Complex-I |
| MID1 | MIDline-1 |
| MID2 | MIDline-2 |
| MKLP1/KIF23 | Mitotic Kinesin-Like Protein 1 |
| MT | Microtubule |
| mTOR | mammalian Target of Rapamycin |
| mTORC1 | mammalian Target of Rapamycin Complex 1 |
| MVB | Multivescicular-body |
| NAE1 | NEDD8 Activating Enzyme 1 |

| | |
|---|---|
| NBR1 | Neighbor of BRCA1 gene 1 |
| NEDD8 | Neuronal-precursor-cell-Expressed Developmentally Downregulated protein-8 |
| NF-kB | Nuclear Factor of kappa light polypeptide gene enhancer in B-cells 1 |
| NHL | NCL-1, HT2A and Lin-41 |
| o/n | over-night |
| OCRL | Oculocerebrorenal syndrome of Lowe |
| OS | Opitz G/BBB Syndrome |
| OTU | Ovarian Tumour Proteases |
| PBS | Phosphate saline buffer |
| PCNA | Proliferating Cell Nuclear Antigen |
| PE | Phosphatidylethanolamine |
| PFA | Paraformaldehyde |
| PH | Plekstrin Homology |
| PHD | Plant HomeoDomain finger |
| PI3K | Phosphoinositide 3-Kinase |
| PIAS1 | Protein Inhibitor of Activated STAT, 1 |
| PIK3C3 | Phosphatidylinositol 3-Kinase Catalytic subunit type 3 |
| PLK1 | Polo-Like Kinase 1 |
| PML | Promyelocytic Leukemia |
| PP2A | Protein Phosphatase 2A |
| PP2ac | Protein Phosphatase 2, Catalytic Subuni |
| PRC1 | Protein Regulator of Cytokinesis 1 |
| Pru | Pleckstrin-like Receptor for Ubiquitin |
| PTM | Post-Translational Modification |
| RAD18 | E3 ubiquitin-protein ligase RAD18 |
| RAD6 | Ubiquitin-conjugating enzyme E2 2 |
| RanBP2 | RAN Binding Protein 2 |
| RAPTOR | Regulatory Associated Protein Of mTOR |
| RARα | Retinoic Acid Receptor alpha |
| RB1CC1/FIP200 | RB1 inducible Coiled-Coil 1 |
| RBCC | Ring Bbox Coiled-Coil |
| RBR | RING-between-RING |
| RBX1 | Ring-box 1, E3 ubiquitin protein ligase |

| | |
|---|---|
| REST | RE1 Silencing Transcription facto |
| RFP | Ret Finger Protein |
| RING, R | Really Interesting New Gene |
| RNF4 | Ring Finger Protein 4 |
| ROCK | Rho associated Coiled-coil containing protein Kinase 1 |
| RP | Regulatory Particle |
| Rpn1 | proteasome Regulatory Particle base subunit RPN1 |
| Rpn11 | proteasome Regulatory Particle lid subunit RPN11 |
| Rpn2 | proteasome Regulatory Particle base subunit RPN2 |
| RT | Room Temperature |
| S6K | Ribosomal Protein S6 Kinase |
| SCF | Skp, Cullin, F-box containing complex |
| SEM | standard error of the mean |
| SENP | sentrin-specific protease |
| SHARPIN | SHANK-Associated RH Domain Interactor |
| SIM | SUMO-interacting motifs |
| SKP1 | S-phase kinase-associated protein 1 |
| SNAI1 | Snail Family Zinc Finger 1 |
| SPRY | SPlA and RYanodine receptor |
| SQSTM1 | Sequestosome 1 |
| STAM | Signal Transducing Adaptor Molecule |
| SUMO | Small Ubiquitin-related MOdifier |
| TAE | Tris-acetate-EDTA |
| TBS | Tris-Buffered Saline |
| TGF-β | Transforming Growth Factor beta |
| TLS | Translesion Synthesis |
| TRAF6 | TNF Receptor- Associated Factor 6 |
| TRIM | TRIpartite Motif |
| TSG101 | Tumor Susceptibility Gene 101 |
| Ub | Ubiquitin |
| UBA | Ubiquitin-Associated Domain |
| UBA1 | Ubiquitin like modifier activating enzyme 1 |
| UBA6 | Ubiquitin like modifier activating enzyme 6 |

| | |
|---|---|
| UBC | Ubiquitin conjugating catalytic |
| UBD | Ubiquitin Binding Domain |
| UBE2D1 | Ubiquitin conjugating enzyme E2 D1 |
| UBE2E | Ubiquitin conjugating enzyme E2 E |
| UBE2G2 | Ubiquitin-conjugating enzyme E2G 2 |
| UBE2Z | Ubiquitin conjugating enzyme E2 Z |
| UBL | Ubiquitin-Like |
| UBPY | Ubiquitin-specific protease Y |
| UCH | Ubiquitin C-terminal Hydrolases |
| UCHL5 | Ubiquitin C-terminal Hydrolase L5 |
| UEV | ubiquitin E2 variant |
| UFD | Ubiquitin Fold Domain |
| UFM1 | Ubiquitin-Fold Modifier 1 |
| UIM | Ubiquitin-Interacting Motif |
| ULK1 | Unc-51 Like autophagy activating Kinase 1 |
| UPS | Ubiquitin-Proteasome system |
| URM1 | Ubiquitin Related Modifier 1 |
| USP | Ubiquitin-Specific Proteases |
| Usp14 | Ubiquitin Specific Peptidase 14 |
| USP2 | Ubiquitin Specific Peptidase 2 |
| USP5 | Ubiquitin Specific Peptidase 5 |
| USPL1 | Ubiquitin-Specific Protease-Like protein 1 |
| Wss1 | DNA-dependent metalloprotease WSS1 |
| ZnFn | Zinc Finger |
| α4 | Alpha 4 |

# 1. INTRODUCTION

## 1.1 The ubiquitin system

The ubiquitin-proteasome proteolytic system and ubiquitin and ubiquitin-like post-translational modification of proteins are both essential regulatory processes in all eukaryotes. Protein ubiquitination in fact can target a substrate for degradation, modify its cellular localization, modulate its activity, or alter its interaction with other proteins. The discovery of the ubiquitin-proteasome pathway emerged from the investigation on the mechanisms that were driving active intracellular protein degradation (Ciechanover et al., 1980) (Pickart and Eddins, 2004) (Hershko et al., 2000). The later identification of diverse ubiquitin chain topologies, of different fates of the targeted proteins, and of the presence of ubiquitin binding domains (UBD) in ubiquitin receptor proteins opened the ubiquitin system in the context of almost all cellular processes (Grabbe and Dikic, 2009) (Dikic et al., 2009).

### 1.1.1 The ubiquitination cascade

Ubiquitination is a post-translational modification that consists in the attachment of ubiquitin to target proteins. Substrates can be modified with a single ubiquitin (Ub) or with a polyubiquitin chain in which one ubiquitin is conjugated to the next. Ubiquitin is a highly stable and conserved protein that adopts a beta-grasp fold with a flexible six-residue C-terminal tail (figure 1.1). The most important features of ubiquitin are its N-terminus and its seven lysines, covering all surfaces of ubiquitin and pointing into distinct directions, and that represent the linkage residues involved in chain assembly (Komander and Rape, 2012). Linear chains formed by the linkage with the initial methionine were also reported (Walczak et al., 2012).

Ubiquitination occurs through sequential steps catalysed by activating (E1 or UBE1), conjugating (E2 or UBE2) and ligase (E3) enzymes that result in the formation of an isopeptide linkage between the C-terminus of ubiquitin and the $\varepsilon$-amino group of the target lysine (Pickart and Eddins, 2004). Less commonly than lysine, other residues including serine, threonine, and cysteine can be conjugated with ubiquitin via formation of oxyester and thioester bonds, respectively (McDowell and Philpott, 2013). In addition to conjugation to the side chain of amino acids, ubiquitin can also be conjugated to the N-terminal -NH2 group of some proteins. Interestingly, the E2 enzyme Ube2w has been identified as responsible for this kind of non-lysine modification (Scaglione et al., 2013) (Tatham et al., 2013).

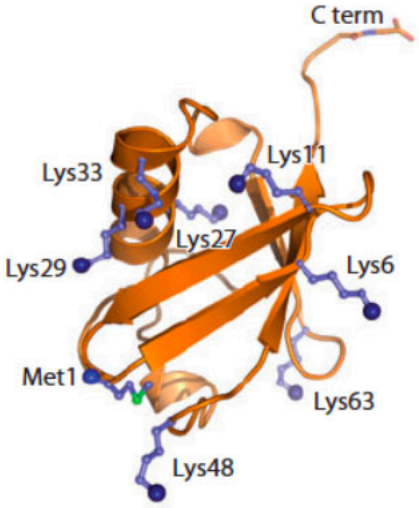


Figure 1.1: Structure of ubiquitin showing the seven Lys residues and Met1. Blue spheres indicate amino groups used in ubiquitin chain formation. (C term, C terminus) (Adapted from Komander and Rape, 2012)

Ubiquitin is activated in an ATP-dependent reaction by the E1 enzyme, which forms a thioester with the ubiquitin C-terminus, and is then transferred to the active site cysteine of the E2 enzyme to yield an E2~Ub thioester intermediate. The E3 ligase binds to both the E2~Ub thioester and the substrate, catalysing the transfer of ubiquitin from the active site cysteine of the E2 to the substrate lysine or N-terminus (Berndsen and Wolberger, 2014).

In humans, there are few E1s and tens of E2s but several hundreds E3s, reflecting the vast array of proteins and biochemical processes with which ubiquitin is associated.

In vertebrates the E1 family is composed of two distantly related members: UBA1 and UBA6. The major E1, UBA1, is one of the most abundant proteins in proliferative mammalian cells, while the minor one, UBA6, is required for embryonic development and is unique in its ability to specifically activate the E2 enzyme UBE2Z (Clague et al., 2015). Large conformational changes occur during the transfer of ubiquitin from the E1 to the E2 active site. The conformational flexibility of the E1 ubiquitin fold domain (UFD) may assist it in its ability to accommodate the binding and transfer of ubiquitin (or ubiquitin-like proteins) to multiple E2s (Tokgöz et al., 2012).

Although the E3s recognize and bind to the protein substrate, E2s bear the responsibility for catalysing the transfer of ubiquitin to the substrates for almost all ubiquitination reactions in

the cell (Kleiger and Mayor, 2014). Members of the family of ubiquitin-conjugating enzymes are characterized by the presence of a highly conserved 150–200 amino acid ubiquitin-conjugating catalytic (UBC) fold that provides a binding platform for E1s, E3s, and the activated Ub (Burroughs et al., 2008). E2s can be subdivided according to the presence of appendages to the catalytic cysteine-containing core: some E2s consist only of the catalytic domain (class I), others have additional N- or C-terminal extensions (classes II and III, respectively) or both (class IV) (figure 1.2) (van Wijk and Timmers, 2010).

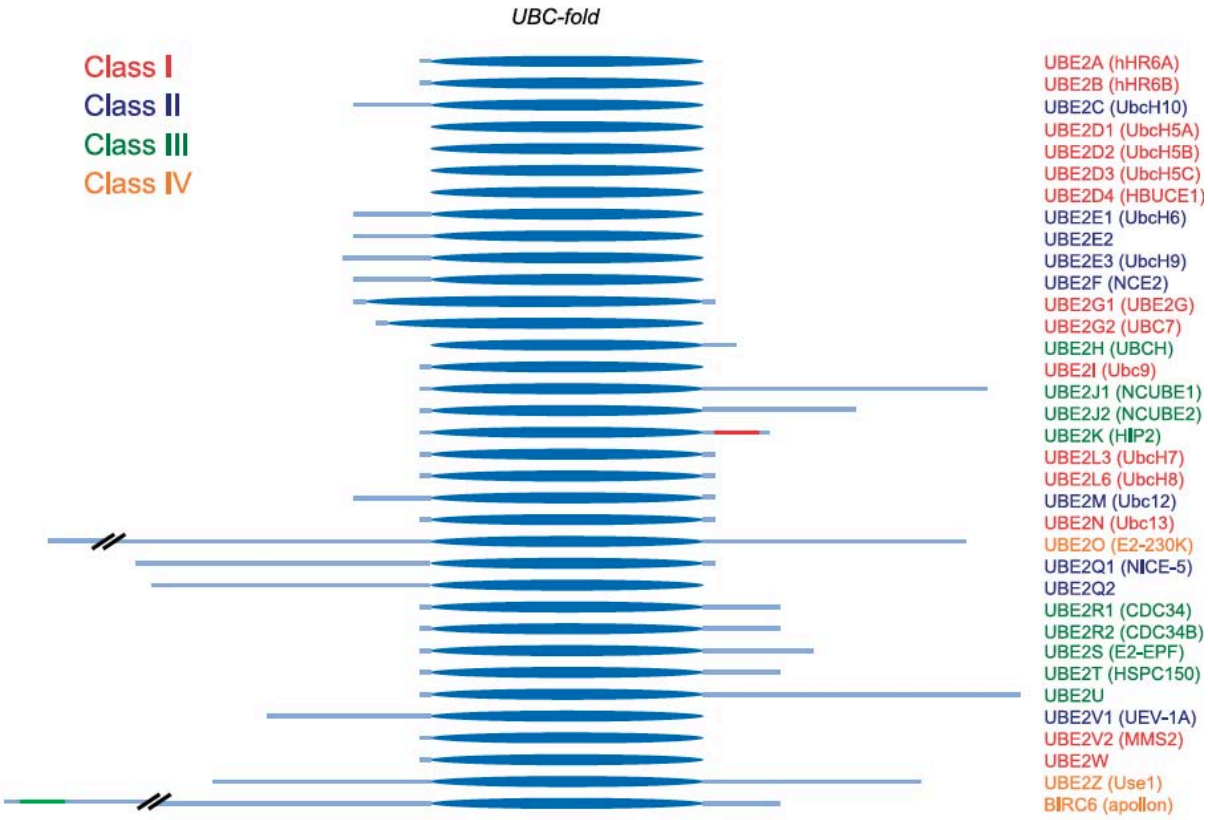


Figure 1.2: Schematic representation of human E2 enzymes. The UBC fold, the UBA domain of UBE2K and the BIR domain of apollon are indicated as a dark-blue ellipse, a red line and a green line, respectively. Different classes of E2 enzymes are indicated in different colours. (Adapted from van Wijk and Timmers, 2010)

The E3 ligases can be divided into three classes that utilize distinct conserved domains and mechanisms to transfer ubiquitin from E2 to substrate (figure 1.3). The really interesting new gene (RING) family catalyses direct transfer of ubiquitin from the E2 enzyme to the substrate, simultaneously binding both the E2~Ub thioester and the target protein. In contrast, the homology to E6AP C terminus (HECT) and the RING-between-RING (RBR) families of E3s ubiquitinate substrates in a two-step reaction in which ubiquitin is transferred from the E2 to an active site cysteine in the E3 and then from the E3 to the substrate (Deshaies and Joazeiro, 2009) (Huibregtse et al., 1995) (Wenzel and Klevit, 2012). When paired with RING E3s, the E2 partner dictates ubiquitin chain specificity. Some E2s have extensive flexibility in accommodating a variety of substrates leading either to monoubiquitination or to the production of short ubiquitin chains (chain initiation). A subset of E2s are incapable of adding ubiquitin to anything other than ubiquitin itself and are instead dedicated to the extension of chains with a specific linkage type (Clague et al., 2015). Although the molecular features that determine chain-building E2s versus those confined to monoubiquitination are poorly understood, it has been demonstrated for three members of the UBE2E subfamily (class II) restriction to monoubiquitination is imposed by their N-terminal domains, which may block access to an acceptor ubiquitin thus limiting chain assembly (Schumacher et al., 2013).

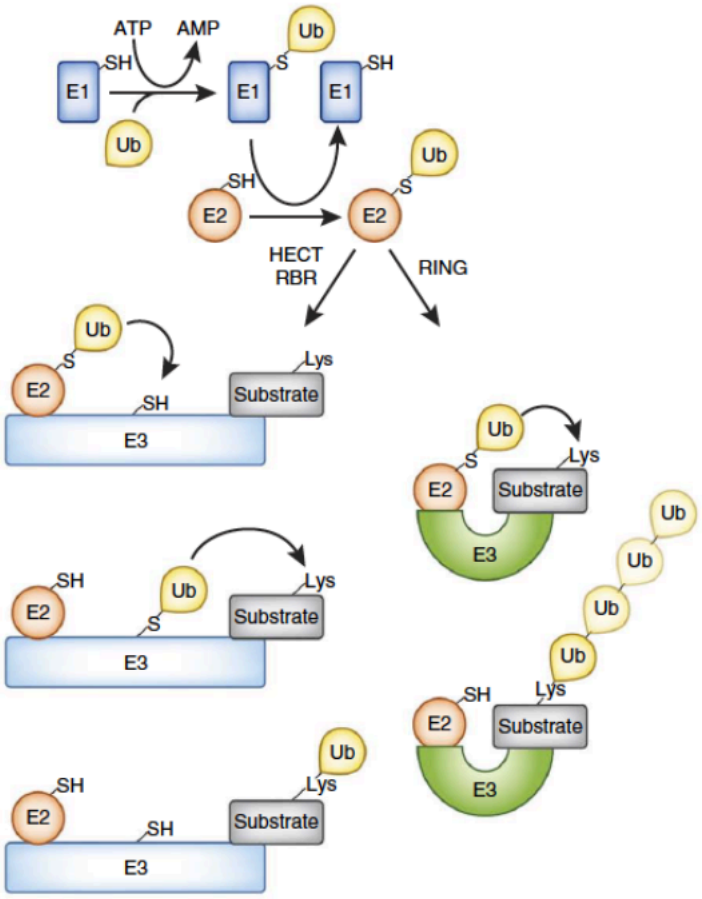


Figure 1.3: The ubiquitin cascade. Ubiquitination is initiated by the formation of a thiolester bond between the C-terminus of ubiquitin and the active-site cysteine residue of the E1. Ubiquitin is then transferred to the E2 active site cysteine in a transthioesterification reaction. The third step is dependent on the nature of the E3 ubiquitin ligase: RING E3s, which bind to both E2-Ub and substrate, catalyse transfer of the ubiquitin from the active site of the E2 to a target lysine on the substrate; HECT and RBR instead promote a two-step reaction, forming a thiolester linkage with ubiquitin before its transfer to the substrate. (Adapted from Berndsen and Wolberger, 2014)

#### 1.1.1.1 RING E3 ligases

RING E3 ligases contain a RING (or RING-like) domain that binds to ubiquitin-conjugating enzymes and promotes a direct transfer of ubiquitin to substrate. The RING domain is a type of zinc-finger domain that comprises 40–60 residues and is distinguished by the presence of a

Cys-$X_2$-Cys-$X_{(9-39)}$-Cys-$X_{(1-3)}$-His-$X_{(2-3)}$-Cys-$X_2$-Cys-$X_{(4-48)}$-Cys-$X_2$-Cys motif (where X can be any amino acid; histidines and cysteines are sometimes interchangeable). The 8 conserved cysteine and histidine residues coordinate two atoms of zinc in order to maintain the structure. In addition, semi-conserved residues are implicated either in forming the domain's hydrophobic core or in recruiting other proteins (Budhidarmo et al., 2012). Ubiquitin ligase activity is intrinsic in the RING domain, permitting directly binding to ubiquitin-conjugating enzymes. The E2-E3 interaction in fact is mediated by a surface on the RING domain that originates from two loop regions comprising the zinc coordination sites and the central helix that connects the first and second coordination sites of the RING (Deshaies and Joazeiro, 2009). Structural studies indicate that the E3-binding site on E2s may partially overlap with the E1-binding site. Binding of E1 or E3 to an E2 is mutually exclusive thus the E2-E3 interaction is transient (Eletr et al., 2005).

In addition to the E2-binding domain, RING E3 ligases contain multiple additional domains including those that recruit the substrate for ubiquitin conjugation. Although in many E3s the substrate-binding site resides in the same polypeptide as the RING domain, certain RING domain proteins belong to complexes where substrate recognition is mediated by a separate subunit. SCF complexes for example are RING-type E3s that consist of an adaptor protein (SKP1), a scaffold protein that recruits the E2 (cullin, Cul1), a substrate receptor protein (F-box protein), and a catalytic RING component (RBX1) (Zheng et al., 2002). Sometimes RING domain proteins form homo- or hetero-oligomers to create a larger complex in which the RING is stabilized. In the case of heterodimers, in some instances only one of the two RING proteins binds the E2 and has E3 ligase activity, while the other has only a structural role. An example is given by Mdm2, that can homodimeryze, heterodimeryze with MdmX, or can build a multimeric RING assembly (Poyurovsky et al., 2007).

Recently, using a stabilized E2 linked to ubiquitin, the crystal structure of a RING-E2-ubiquitin complex has been determined (Plechanovova et al., 2012) (Dou et al., 2012). This effort originated a model that can explain the mechanism by which ubiquitin is transferred from the E2 to the substrate by the RING (either as monomer or dimer). In the crystal structures an arginine side chain of a RING monomer bridges the E2 protein and the C-terminal tail of ubiquitin; the opposite RING subunit contacts ubiquitin through, for example, a highly-conserved tyrosine or phenylalanine residue. Moreover, a zinc-bound histidine interacts with ubiquitin through a hydrogen bond. Therefore, RING binding reduces the conformational heterogeneity of E2-ubiquitin and immobilize ubiquitin's C-terminal tail in a

structurally conserved cleft within the E2 protein. As a result, the thioester bond becomes suitably positioned for attack by the substrate protein's lysine while several residues of the E2 protein are rearranged to promote the transfer reaction (Lima and Schulman, 2012).

The linkage of one ubiquitin molecule to the substrate is a slow and unspecific reaction. Differently from chain initiation, the chain elongation process is faster and E2-specific. This step corresponds to the formation of an ubiquitin-ubiquitin isopeptide bond to attach the n+1 ubiquitin to a chain that contains n ubiquitin peptides. The interaction of a RING ligase with distinct initiating and elongating E2 can promote monoubiquitination and subsequent polyubiquitination in a "tag team E2s" manner. Interestingly, polyubiquitin chains can be built directly on the substrate but also preformed on the E2 and then transferred. An example is given by the RING ligase gp78, which promotes polyubiquitination of the substrates preassembling the ubiquitin chains at the catalytic cysteine of the E2 Ube2g2 (Li et al., 2007).

### 1.1.2 The ubiquitin code

Both monoubiquitination and polyubiquitination are important modifications that trigger a well-defined outcome depending on the E2, the E3 or a particular substrate-E3 interaction. Differently from HECT domain ligases, which determine the chain linkages of the ubiquitination reaction, single RING can recruit different E2s that have different linkage specificities. In this case, the output of the reaction is determined by the known specificity of the E2. Determinants in the catalytic core of E2s, Ub and structural features distant from the catalytic site, are important for Ub lysine specificity during polyubiquitination. For example, studies with UBE2D1, which can generate K11, K48 and K63 poly-Ub chains, demonstrate that mutation of residues near the catalytic cysteine can modulate linkage specificity of this E2 enzyme. This results in the altered preference of the E2 enzyme towards K63-linked Ub chains formation at the expense of K11-linked Ub chains (Ye and Rape, 2009) (Bosanac et al., 2011).

Attachment of a single or several Ubs onto substrate lysine(s) results in monoubiquitination or multiubiquitination, respectively (figure 1.4). These modifications can regulate cellular processes such as DNA repair, regulation of histone function, gene expression and receptor endocytosis. Considering the seven lysines (K6, K11, K27, K29, K33, K48 and K63) present on the surface of the ubiquitin molecule, different structural topologies of poly-Ub chains, homogeneous or mixed ubiquitin chains and even branched chains, can be obtained. An

alternative type of ubiquitin chain is the linear head-to-tail poly-Ub chain. In that case, the C-terminal glycine of ubiquitin is attached to the α-amino group of the N-terminal methionine residue of another Ub. Ubiquitin chains adopt either compact conformation, where adjacent moieties interact with each other, or open conformations, where no interfaces are present except for the linkage site. The canonical K48-linked chains and K6- and K11- linked poly-Ub chains adopt a relatively compact conformation. In contrast, Met1- and K63-linked chains mostly display open conformations (Komander and Rape, 2012). Moreover, distinct chain types, although structurally similar, exhibit different flexibility (e.g. K63- and Met1-linked chains) or can be specifically recognized because of their compactness (K48-linked) (Suryadinata et al., 2014).

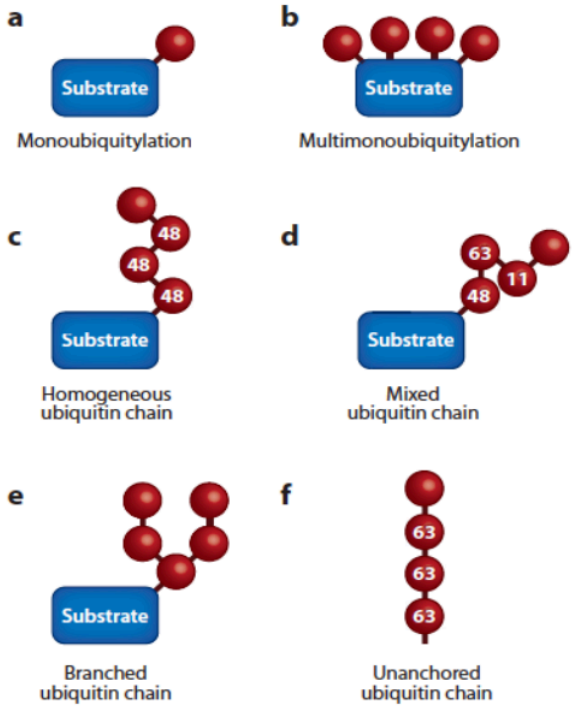


Figure 1.4: Ubiquitin chain topology indicating monoubiquitination (a), multimonoubiquitination (b), homogeneous (c) and mixed (d) ubiquitin chains, branched (e) and unanchored chains (f). (Adapted from Komander and Rape, 2012)

Different ubiquitin binding proteins can then recognize different chain types, targeting the substrate protein to specific signalling pathways. These downstream proteins can interact directly with monoubiquitinated and/or polyubiquitinated proteins through ubiquitin-binding domains (UBDs) (figure 1.5). Generally UBDs are rather small and diverge in both structure

and patterns of ubiquitin recognition. The majority of the UBDs fold into α-helical based structures, including the UBA (ubiquitin-associated domain), UIM (ubiquitin-interacting motif) and CUE (coupling of ubiquitin conjugation to ER degradation). Non-helical UBDs are also frequent and can be exemplified by the different ubiquitin binding zinc fingers (ZnFn), the ubiquitin conjugating (UBC) domain present in E2 enzymes, or plekstrin homology (PH) folds (Dikic et al., 2009) (Grabbe and Dikic, 2009).

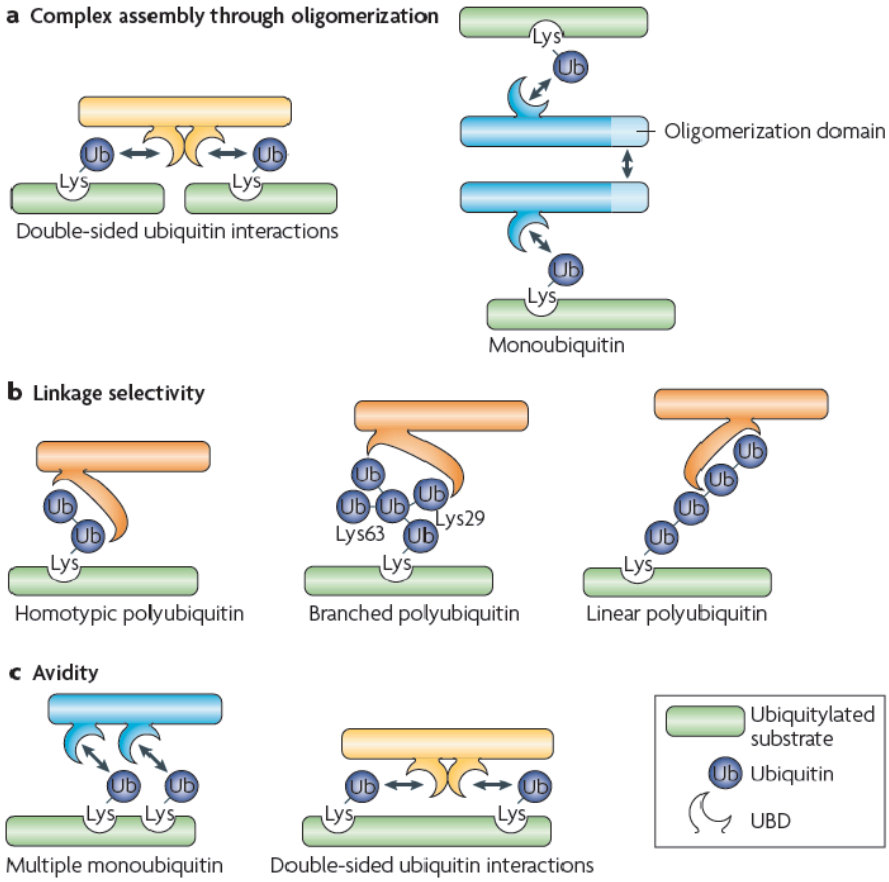


Figure 1.5: the ubiquitin-UBD network. Ubiquitin attached on target substrates can be recognized by specialized sets of ubiquitin-binding domains (UBDs) mediating different outputs depending o the protein in which they are embedded. A) Two UBDs in the same protein can bridge two ubiquitinated substrates. Alternatively, two proteins carrying oligomerization domains and UBDs can indirectly bridge the same ubiquitinated substrate to form protein complexes. B) Specialized UBDs can selectively discriminate between different types of ubiquitin chain. C) The presence of two or more UBDs in a protein or the attachment of multiple ubiquitin moieties on the same substrate can increase the avidity of and promote ubiquitin–UBD interactions, despite the low affinities of the individual interactions. (Adapted from Dikic, 2009).

The molecular event triggered by the ubiquitin signal is therefore the result of the interaction between UBDs of effector proteins and different ubiquitin chains produced on the substrate. For example, polyubiquitination through Ub K48 (and similarly K11-linked), with a chain of at least 4 Ub molecules, generally targets proteins for proteasomal degradation. K63-linked poly-Ub chains instead lead to non-proteasomal degradative cellular processes. Alternatively, Met-1 chain linkage by the RBR E3 ligase HOIL/HOIP/SHARPIN linear Ub chain assembly E3 ligase complex (LUBAC) is important for activation of the NF-κB transcription factor (Niu et al., 2011).

### 1.1.3 Deubiquitinases

In order to regulate protein ubiquitination and to avoid constitutively activation of the ubiquitin pathway, some UBD-containing protein called deubiquitinases (DUBs) can reverse the ubiquitination process. Specificity is required also in the deubiquitination process, therefore DUBs must discriminate chains of distinct linkage, topology, and length.

DUBs can be classified into five families based on the architecture of their catalytic domain. Ubiquitin-specific proteases (USPs), ubiquitin C-terminal hydrolases (UCHs), Josephins, and ovarian tumour proteases (OTUs) are cysteine-dependent proteases, while the fifth family, Jab1/MPN domain-associated metalloisopeptidase (JAMM/MPN), is composed of zinc-dependent metalloenzymes (Clague et al., 2013). Housekeeping proteasome-associated DUBs are essential for maintaining a sufficient level of free ubiquitin chains that can be used for chain assembly. Another group of DUBs, including most members of the USP family, selectively recognize the target but disassembles chains independently from the linkage. These DUBs regulate many cellular reactions, including splicing, protein trafficking, or chromatin remodelling (Komander and Rape, 2012) (Clague et al., 2013). In contrast, several DUBs display specificity toward one or a few linkages. For example, DUBs USP5 and USP2 readily cleave K48- and K63-linked chains, but they have scarse activity towards linear chains. By contrast, the DUB cylindromatosis tumour suppressor (CYLD) cleaves linear and K63-linked but not K48-linked chains (Dikic et al., 2009).

### 1.1.4 Cellular functions of ubiquitination

The combinatorial action of ubiquitination, deubiquitination and ubiquitin-binding proteins determines the fate of the modified target. Therefore the function of ubiquitination depends on chain topology, but also on the enzymes or substrate localization and interactions between E3s and effectors protein.

#### 1.1.4.1 Protein degradation pathways

There are three major ubiquitin-dependent degradation pathways that collaborate within the cell to regulate protein turnover and degradation, all characterized by specific ubiquitin receptors. Although the ubiquitin-proteasome system (UPS) was considered as the major route for ubiquitin-driven degradation, it has been successively discovered that ubiquitin tagging also provides a signal to drive lysosomal degradation pathway and, more recently, to mark autophagy.

##### 1.1.4.1.1 Proteasomal degradation

Proteasomal targeting requires a K48-linked ubiquitin chain consisting of at least four conjoined ubiquitin molecules. New evidence however indicates that an array of different ubiquitin chains can determine targeting to the proteasome. In yeast, K63 was shown to be the only linkage that does not have a role in proteasomal degradation, and this selection is possibly due to K63- preferential binding to non-proteasomal UBDs. Moreover, K11-linkages have been associated with the endoplasmic reticulum-associated degradation (ERAD) pathway, a quality control pathway in which misfolded or improperly assembled proteins of the ER are ubiquitinated, translocated to the cytosol if necessary, and degraded by the proteasome (Xu et al., 2009) (Christianson and Ye, 2014).

The 26S proteasome is an ATP dependent protease containing two major assemblies, the 20-subunit core particle (CP) and a 19S regulatory particle (RP) subunit (Finley, 2009). The CP is made of two β-rings that contain the catalytic sites, each of which is made of seven subunits (β1–7), flanked on both sides by two α-rings, which are also made of seven subunits each. Thus, the structure of the 20S CP is α1–7β1–7β1–7α1–7. The RP includes a base and a lid and regulates substrate access to the core through a substrate translocation channel (figure 1.6) (Weissman at al., 2010). The six ATPase subunits of the RP are responsible for substrate unfolding, permitting its entrance in the core. Two subunits of the RP, Rpn10 and Rpn13 interact with ubiquitinated substrates through their UIM and Pru (pleckstrin-like receptor for

ubiquitin) domain, respectively (Finley, 2009). Moreover, proteins of the UBL/UBA family, which bind proteasomes only weakly with the UBL domain and are usually substoichiometric components of the complex, recognize ubiquitin-conjugates through one or more UBA domains. In addition to ubiquitin receptors, the largest proteasome subunits Rpn1 and Rpn2 bind three deubiquitinases Rpn11, UchL5 and Usp14 that cooperate to provide effective processing of ubiquitin chains showing specificity for diverse chain linkages (Finley, 2009). RPN11 is thought to specifically disassemble K63-linked chains, as well as cleave the isopeptide bond that links the substrate and the proximal ubiquitin, allowing for en bloc removal of an ubiquitin chain. In addition it regulates entry into the central proteolytic chamber, thereby coupling substrate degradation to recycling of ubiquitin. Usp14 and UchL5 instead account for all activity directed toward K48-linked chains and also contribute to K63-linked chain disassembly (Clague and Urbe, 2010). It has been proposed that rapid deubiquitination of K63-polyUbs could cause inefficient degradation because the conjugates are released from the proteasome before being unfolded for translocation and degradation (Jacobson et al., 2009).

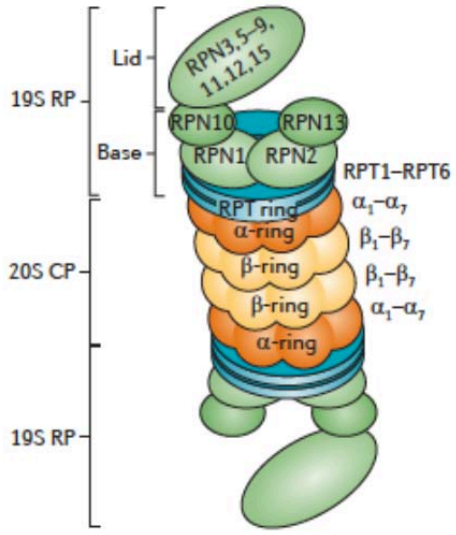


Figure 1.6: Structure of the 26S proteasome, indicating the core 20S catalytic particle (CP) and the 19S regulatory particle (RP). The substrate is bound to specific subunits in the 19S RP, then unfolded by the ATPases in the RPT ring and inserted via an open gate in the α-ring of the 20S CP into the proteolytic chamber. The structure of the CP is α 1–7 β 1–7 β 1–7 α 1–7 The RP contains deubiquitylating enzymes that recycle ubiquitin (adapted from Weissman at al., 2010).

1.1.4.1.2 Lysosomal degradation

The degradation of plasma membrane proteins such as receptors or channels occurs in lysosomes and substrates are targeted to this proteolytic compartment through monoubiquitination or K63-linked chains. Ubiquitin is recognized as an internalization signal by a receptor, but can also serve after internalization as localization signal. Ubiquitinated membrane proteins are recognized by different endosomal sorting complexes required for transport (ESCRTs). Monoubiquitination is sufficient for initial internalization but efficient sorting at the endosome by the ESCRT machinery requires K63-linked polyubiquitin. Endocytosed proteins are either recycled to the plasma membrane or captured into multivesicular bodies (MVB) that mature into late endosomes and lysosomes, where they are degraded (figure 1.7) (Wright et al., 2011). The evolutionary conserved ESCRT-dependent processes are important also during cytokinesis and HIV budding and are coordinated by modular setup of the machinery with five distinct ESCRT complexes (ESCRT-0, -I, -II, -III and the Vps4 complex) (Schmidt and Teis, 2012). In contrast to the early ESCRT complexes (ESCRT-0, -I and -II), which form stable protein complexes in the cytoplasm, the ESCRT-III complex only transiently assembles on endosomes. In the cytoplasm, Vps4 is an inactive protomer (monomer or dimer) that is recruited onto ESCRT-III. ESCRT-0 that is composed by HRS (Vps27 in yeast) and STAM (Hse1 in yeast) is responsible for the initial selection of ubiquitinated cargo at the endosomal membrane. HRS interacts with the ESCRT-I component TSG101, which in addition binds ubiquitin through its N-terminal UEV domain (Williams and Urbè, 2007). The ESCRT-I complex engages ESCRT-II, which then nucleates ESCRT-III polymerization via the activation of the ESCRT-III subunit Vps20. Vps4 (ESCRT-IV) ultimately disassembles the ESCRT-III complex to recycle its subunits (Schuh and Audhya, 2014). The ESCRT machinery is associated with at least two DUB activities, AMSH and UBPY, belonging to the JAMM/MPN+ and USP families, respectively, that provide ubiquitin recycling (Wright et al., 2011).

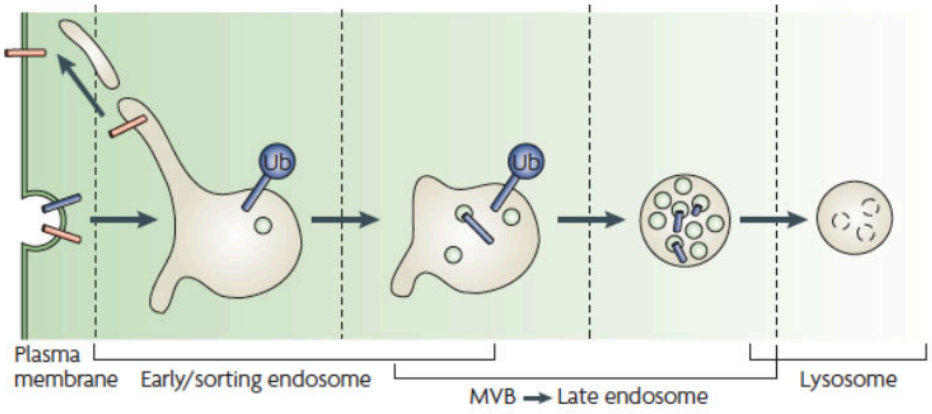


Figure 1.7: Overview of the endocytic pathway. Membrane proteins are removed from the plasma membrane by incorporation into endocytic vesicles that fuse with an early endosomal compartment. Ub directs cargo incorporation into intralumenal vesicles to form MVBs, that fuse with the late endosome and mature into lysosomes, where proteins are degraded (adapted from Williams and Urbè, 2007).

1.1.4.1.3 Selective autophagy

Although autophagy has long been viewed as a random cytoplasmic degradation system, several lines of evidence suggest the existence of different types of selective autophagic degradation pathways. In fact, certain structures such as protein aggregates or ribosomes and organelles, that are incompatible with unfolding by the proteasome, are selectively removed from the cytoplasm by this pathway. Autophagy is characterized by the formation of a double-membrane compartment derived from the preautophagosomal structure in which cytosol and organelles are captured. The autophagosome can then directly fuse with late endosomes or lysosomes to form the autolysosome, wherein the double-membrane structure is digested (figure 1.8) (Kraft et al., 2010). Over 30 autophagy-related genes (ATG) involved in the process of autophagosome formation have been identified to date. The 'core' ATG proteins can be categorised into four subgroups: Atg1/ULK1 kinase complex (ULK1, ATG13, RB1CC1, ATG101), PI3K complex (PIK3C3-BECN1), and two Ubiquitin-like (UBL, see below) systems comprised by the ATG12-ATG5-ATG16L and MAP1LC3/GABARAP modifiers. ATG12 and LC3 modifiers share a common ubiquitin-like beta-grasp superfold and show similarities to the ubiquitin conjugation system. UBLs such as the LC3 modifier interact to a short hydrophobic sequence, termed LC3-interacting region (LIR) motif. The molecular characterisation of ubiquitin binding proteins such as p62/SQSTM1 and NBR1 has demonstrated that an ubiquitin-dependent sensor system is

responsible for substrate specificity. p62, which contains both a UBA and a LIR motif in fact has been previously implicated in the clearing of protein aggregates, which are known to be concentrated in ubiquitin. Interestingly, K48- and K63-linked polyubiquitination, as well as monoubiquitin modifications, all contributed to the biogenesis of inclusion bodies, but only K63-linked chains induced autophagic degradation of these inclusions (Shaid et al., 2013).

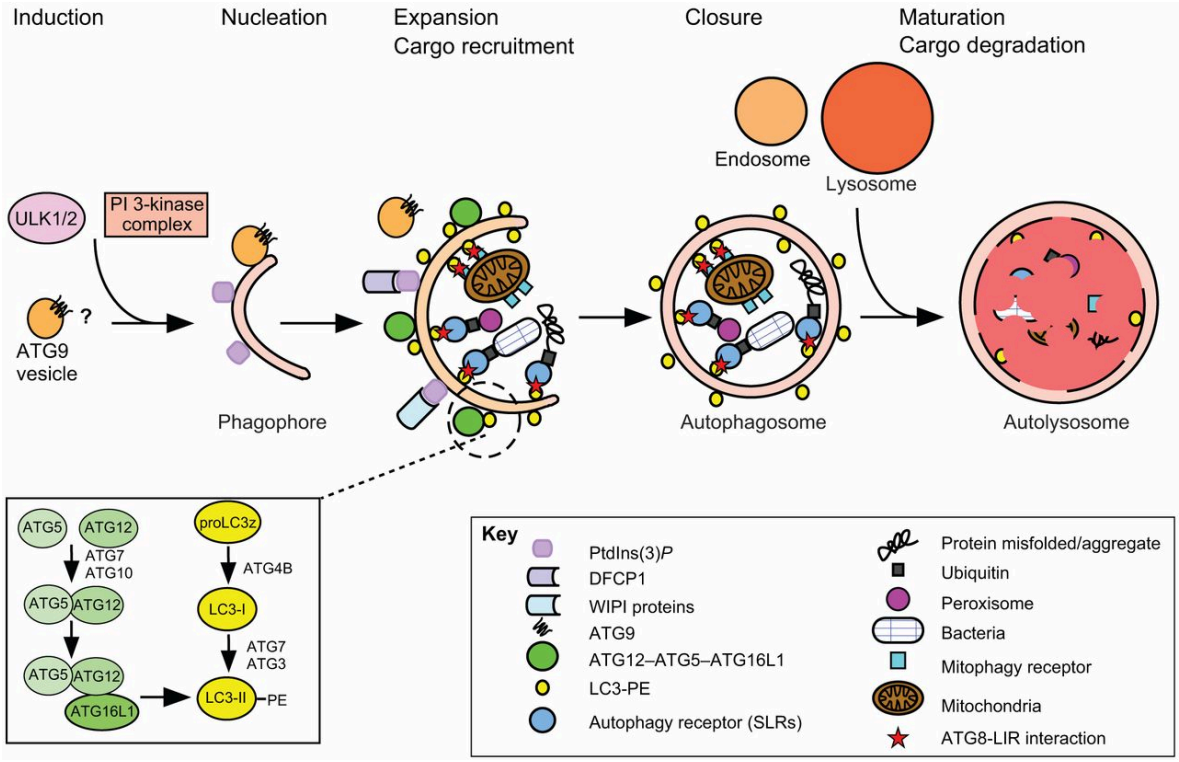


Figure 1.8: Overview of selective autophagy. Selective autophagy is induced by activation of the ULK1/ATG complex that includes the scaffold proteins ATG13, FIP200 and ATG101. During nucleation, protein and lipids are recruited to the phagophore. Expansion of the phagophore depends on two UBL complexes: conjugation of ATG5 to ATG12, requires the E1 enzyme ATG7 and the E2 enzyme ATG10, generating an oligomeric complex between the ATG12–ATG5 conjugate and ATG16L1; proLC3 is cleaved by ATG4, LC3 is then activated by ATG7, transferred to ATG3 and conjugated to PE by ATG12–ATG5–ATG16 complex. Autophagy receptors interact with lapidated-LC3 and with the cargo, recruiting the latter into the inner surface of the phagophore.h The phagopgore expands and encloses its cargo to form the double-membrane autophagosome; fusion of autophagosomes with late endosomes or lysosomes forms autolysosomes where the enclosed cargo is degraded (adapted from Birgisdottir et al., 2013).

1.1.4.2 Non-proteolytic function of ubiquitination

The role of ubiquitination in non-proteolytic pathways has been long investigated during years. The non-proteolytic functions of the ubiquitin code are often the consequence of monoubiquitination or Met1- and K63-linked chain formation. For example, ubiquitination can regulate protein interaction recruiting a protein in a defined cellular location, as it happens for the proliferating cell nuclear antigen (PCNA). In response to DNA damage, the E3 ligase RAD18 is recruited to the stalled replication fork; RAD18 and RAD6 then monoubiquitinate PCNA, which recruits the translesion synthesis (TLS) polymerases to replace the high-fidelity replicative polymerases. Following the successful repair of the damaged DNA, the recruitment signal for Y family polymerases is turned off by Usp1-dependent deubiquitination, allowing the replication machinery to return to its normal state. Protein interactions can also be regulated by K63-linked chains that can function as scaffolds during the cellular response to DNA damage (Chen and Sun, 2009).

Ubiquitination can also affect protein activity, as in the case of protein kinases. In the NF-κB pathway that is usually activated in response to external stimuli, binding of the tumour necrosis factor α to its membrane receptor initiates a variety of ubiquitination events, such as formation of K63-linked chains by TRAF6, mixed K11/K63-linked chains by the RING E3 ligase cIAP1 or Met1-linked chains by LUBAC, thus inducing allosteric activation of a core regulator and recruitment of upstream activating enzymes (Komander and Rape, 2012).

Additionally, ubiquitination is important for protein localization. Ubiquitination of Polo-like kinase 1(PLK1) mediated by the E3 ubiquitin ligase complex that contains cullin 3 (CUL3) and its adaptor protein Kelch-like protein 22 (KLHL22) for example promotes the release of PLK1 from kinetochores during chromosome alignment, in order to successfully proceed through mitosis (Beck et al., 2013).

Interestingly, a role for ubiquitin in the degradation of mRNA has also been identified. MEX-3C, a member of the recently described family of RNA-binding ubiquitin E3-ligases, associates with the cytoplasmic deadenylation complexes, and ubiquitinates CNOT7, the main deadenylase subunit of the CCR4-NOT machinery promoting its activity leading to MHC-I mRNA degradation (Cano et al., 2015).

1.1.5 Ubiquitin-like modifiers

Besides ubiquitin, other ubiquitin-like proteins (UBLs) can be attached to a target protein to modulate its function. In total, 17 human UBLs, within 9 phylogenetic classes, have been

reported. Like ubiquitin, nine UBLs have been shown to covalently modify other macromolecules, usually proteins, sometimes lipids. All UBLs display a common overall fold, but, in general, the different UBLs have their own E1-E2-E3 cascades, and they impart distinct functions to their targets. The first identified UBL was an interferon-stimulated gene product of 15 kDa (ISG15). The most studied UBLs are neuronal-precursor-cell-expressed developmentally downregulated protein-8 (NEDD8) and small ubiquitin-related modifier (SUMO) family members. Other UBLs are FAT10, FUB1, UFM1, URM1, Atg12, and Atg8 (see also above). NEDD8 conjugation is initiated by its dedicated E1, the heterodimeric NEDD8 activating enzyme 1 (NAE1)-ubiquitin activating enzyme 3 (UBA3) complex. Attachment of NEDD8 to its predominant targets, cullins, enhances enzymatic activity of cullin-RING E3 ubiquitin ligases. Mammalian cells express four SUMO paralogs: SUMO1, the nearly identical SUMO2/3 and SUMO4. SUMOs 1–3 are ubiquitously expressed, and SUMO3 is the predominant isoform, whose absence in mice causes lethality. Sumoylation occurs often on lysines within specific consensus sites. The consensus sequence for SUMO2/3 is ΨKX(D/E), in which Ψ is a large hydrophobic amino acid, and X is any amino acid. SUMO proteins are activated by a common E1, Aos1-UBA2 complex. SUMO attachment often alters the interaction of a target with other proteins, via interactions between SUMO and SUMO-interacting motifs (SIM) (Schulman and Harper, 2009) (Hochstrasser, 2009). Substrate specificity in the sumoylation pathway is poorly understood because only a single E2 enzyme (Ubc9) and relatively few E3 ligases have been identified. The best-characterized SUMO E3 ligases are the Siz/PIAS (SP) family of RING-related E3 ligases and RanBP2. Recently a new family of SUMO2/3-specific E3 ligase with E4 elongase activities in SUMO-chain assembly have been discovered (Eisenhardt et al., 2015).

Sumoylation is highly dynamic and can be reversed by the action of desumoylating enzymes. In vertebrates, these isopeptidases include a family of six sentrin-specific proteases (SENPs) defined by a conserved cysteine protease domain, distinct-subcellular localizations and non-redundant functions. In addition, several unique desumoylating enzymes have more recently been identified, including the metalloprotease Wss1, the PPPDE–domain containing proteins DeSI-1 and DeSI-2, and the ubiquitin-specific protease-like protein 1 (USPL1) (Nayak and Muller, 2014). SUMO is predominantly found in the nucleus and has a crucial role in many nuclear processes, such as gene expression, genome stability, the DNA damage response, protein trafficking, and cell cycle control. In many instances, sumoylation may play a role in facilitating the assembly of large multiprotein complexes between proteins that are either

covalently modified by SUMO and/or contain SIM, as exemplified by PML nuclear bodies. In these sub-nuclear structures, SUMO acts as a scaffold to mediate interactions between the PML protein and other associated factors. Other complexes are assembled on chromatin, including repressive complexes organized around sites of DNA methylation, as well as transcriptional regulatory complexes at gene promoters, indicating a role for sumoylation in the regulation of chromatin structure and function (Cubenas-Potts and Matunis, 2013).

The SUMO and the ubiquitin pathways communicate acting in concert or opposing their activities. Some SUMO-targeted Ub ligase (e.g. RNF4 family) in fact can target for ubiquitination a protein after its sumoylation through direct recognition of the SUMO moiety with a SIM (Tatham et al., 2008). Moreover, the same lysine of a substrate protein can be both subjected to ubiquitination and sumoylation, in a way that one modification excludes the other, resulting in an antagonistic or agonistic effect (Denuc and Marfany, 2010). Additionally, SUMO itself can be ubiquitinated (Tatham et al., 2008).

## 1.2 The TRIM family

TRIM/RBCC-containing proteins could be defined as E3 ubiquitin ligases as they contain a N-terminal tripartite motif composed by a RING domain (R), followed by one or two b-boxes (BB) and a coiled coil (CC) region (Reymond et al., 2001) (Ozato et al., 2008) (Nisole et al., 2005). This modular structure is conserved among protein family members although few non-orthodox TRIMs lack the RING domain. The tripartite motif (RING-BBox-CC), which is invariably present at the N-terminal portion of these proteins, is usually associated with a variable C-terminal that confers activity-specificity (figure 1.9). The TRIM family can be considered as one of the largest gene families in humans, comprising about 70 members. From an evolutionary point of view, TRIM proteins can be divided into two groups: the first, composed of 34 proteins (29 TRIM and 5 TRIM-like proteins), includes conserved members with a tripartite-module in combination with all the C-terminal domains found in TRIM proteins and is present in invertebrates. Genes of the second group instead are absent in invertebrates and are rapidly evolving, possibly acting as a TRIM genes "reservoir" to develop novel functions (Sardiello et al., 2008).

The RING domain plays a critical role in ubiquitination by binding to E2 enzymes and promoting the transfer of ubiquitin to the substrates (see par. 1.1.1.1). Many TRIMs have a single B-box (B-box type 2) domain; however, some have tandem domains with a type 1 B-box domain (B-box1) and the B1B2 order of tandem B-box domains is conserved. The two types of B-box domains coordinate two zinc atoms in a cross-brace fashion and adopt RING-like folds even though they share little sequence homology with RING domains besides being Cys-His rich domains as well (Meroni and Diez-Roux, 2005). Structure analysis suggests that B-box1 could acts as a RING-E3 enhancer and it is possible that the B-box2 domain functions to regulate B-box1, when present, or the RING domain although the specific function for B-box domains is still unclear (Tao et al., 2008). A coiled-coil region of about 100 residues invariably follows the B-box2 in all TRIMs. This region, sometimes broken into two or three coiled-coil motifs, is mainly involved in homo and hetero-interactions and in promoting the formation of high molecular weight complexes (Napolitano and Meroni, 2012). Recently, the structure of several isolated TRIM coiled-coil regions has been solved showing a basic dimer formation in an antiparallel arrangement (Sanchez et al., 2014) (Li et al., 2014).

As mentioned above, the tripartite motif can be found in combination with a variety of C-terminal domains, including the NHL (NCL-1/HT2A/LIN-41 repeat), immunoglobulin,

MATH (meprin and tumor necrosis factor receptor-associated factor homology), B30.2-like/RFP (Ret finger protein)/ SPRY (SplA and ryanodine receptor), ARF (ADP ribosylation factor), PHD (plant homeodomain finger), and BROMO domains (Short and Cox, 2006). Approximately two-thirds of the TRIM proteins possess the PRY-SPRY domain, a 200-amino acid-long sequence that assumes an immunoglobulin-like fold (figure 1.9) (James et al., 2007).

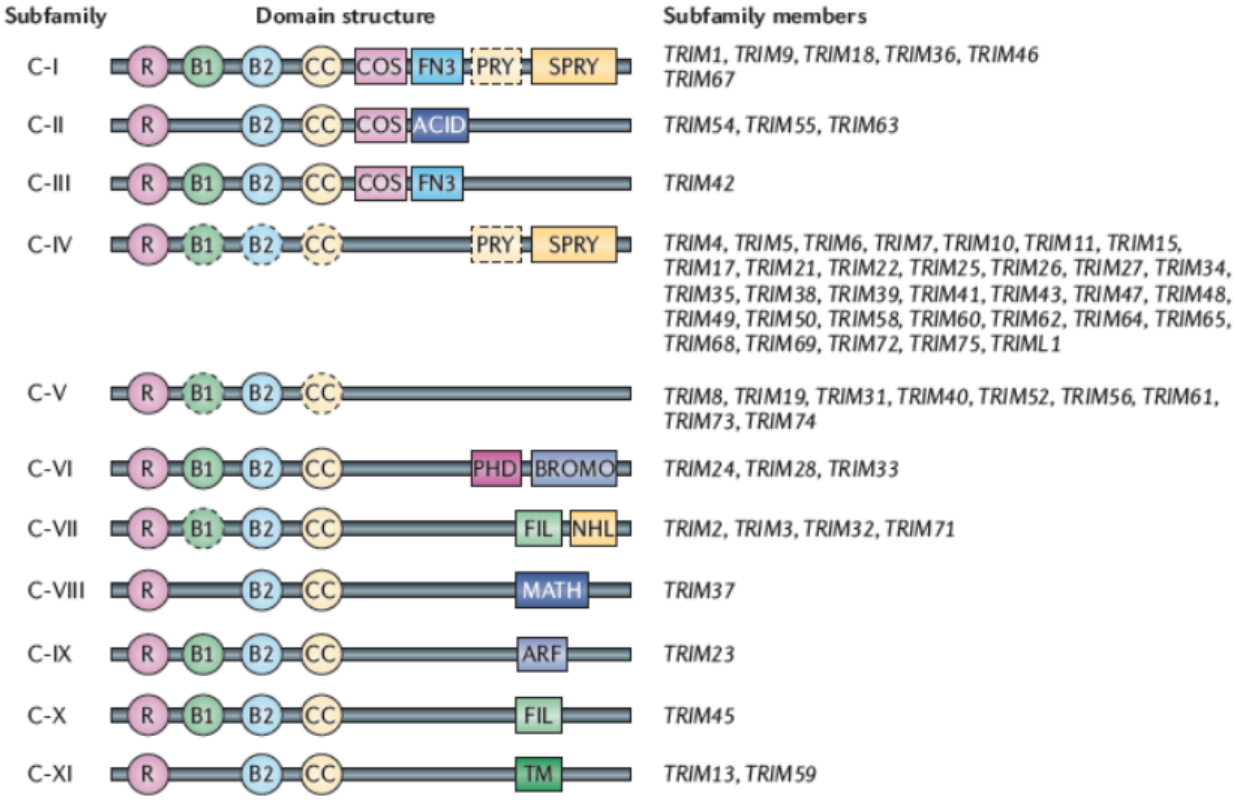


Figure 1.9: Subclassification of TRIM family protein members (C-I to C-XI). Almost all TRIM proteins have a RING-finger domain (R), one or two B-box domains (B) and a coiled-coil domain (CC). ACID, acid-rich region; ARF, ADP-ribosylation factor family domain; BROMO, bromodomain; COS, cos-box; FIL, filamin-type I G domain; FN3, fibronection type III repeat; MATH, meprin and TRAF-homology domain; NHL, NCL1, HT2A and LIN41 domain; PHD, PHD domain; PRY, PRY domain; SPRY, SPRY domain. (Adapted from Hatakeyama, 2011)

TRIM proteins are often present as dimer thanks to their ability to homointeract through their CC region. TRIM25 is likely an obligate dimer and the dimer architecture is similar to TRIM5α (Sanchez et al., 2014). Interestingly, heterointeractions have been also observed among closely related TRIM family members. TRIM18/MID1 interacts with its homologue TRIM1/MID2 supporting the idea of a regulatory mechanism between the two proteins (Short et al., 2002). TRIM24 was found to interact with TRIM28 and TRIM33 (all members of the TIF1-related subfamily) to form two different complexes: the major TRIM24/TRIM28 and the minor TRIM24/TRIM28/TRIM33 containing complexes having a role in liver tumour formation (Herquel et al., 2011).

Considering their role as E3 ligases, TRIM proteins have been shown to bind directly to E2 enzymes and to interact preferentially with the evolutionary close D and E classes, but not with the L class of UBE2. Moreover, several TRIM proteins interact with UBE2N, and, in addition, two highly specific interactions between TRIM9 and UBE2G2 and between TRIM32 and UBE2V1 and V2 were also observed (Napolitano et al., 2011).

TRIM proteins have been associated to many diverse cellular processes, such as cell cycle progression, apoptosis, transcriptional regulation, and antiviral response (Reymond et al., 2001) (Ozato et al., 2008) (Nisole et al., 2005) (Meroni and Diez-Roux, 2005). Several TRIM family genes are involved in chromosomal translocations generating oncogenic fusions. For example, TRIM19, which is encoded by the promyelocytic leukaemia (PML) gene, is characterized by its involvement in the t(15;17) translocation that specifically occurs in acute promyelocytic leukaemia (APL), resulting in a PML–RARα fusion protein. TRIM28, TRIM24 and TRIM33 negatively regulate several transcriptional complexes through histone modification and binding. The PHD-finger domain and bromodomain of TRIM33 specifically bind H3 tails that are unmethylated at K4 and R2 but that are acetylated at K18 and K23 and this interaction seems to be necessary for its E3 ubiquitin ligase activity (Hatakeyama, 2011).

A series of studies revealed the potent antiviral and antimicrobial activities of some TRIM family members. One of the best characterized TRIMs with direct antiviral activity is TRIM5α, which is the largest isoform encoded by the TRIM5 gene containing the B30.2 domain required for its anti-HIV-1 function. The molecular mechanism of TRIM5α viral restriction is still not well understood although it is known that TRIM5α recognizes and promotes premature disassembly of the viral capside lattice, blocking reverse transcription, nuclear entry, and integration (Lascano et al., 2015).

Several TRIM proteins are implicated in developmental processes and in hereditary disorders and in many cases the disease is caused by a loss of their E3 ligase activity against a crucial target (Napolitano and Meroni, 2012). For example X-linked Opitz syndrome is a multiple congenital anomaly of midline structures caused by mutations in the TRIM18/MID1 gene, whose product controls the level of the catalytic subunit of PP2A (Trockenbacher et al., 2001) (see below). Other TRIMs are involved in neuronal architecture, such as TRIM46, that forms parallel microtubule arrays in the axon to drive neuronal polarization (van Beuningen et al., 2015).

Interestingly, but not surprisingly, TRIM proteins have been also recorded as SUMO E3 ligase. This is true for TRIM19/PML but also for TRIM27, TRIM32 and other family members (Chu and Yang, 2010).

Lastly, TRIM proteins have been shown to regulate selective autophagy. Some family members (TRIMs 5α, 6, 16, 17, 20, 22, 49, and 55) interact with autophagic regulators and effectors (ULK1, Beclin 1, Atg8 and p62/sequestosome 1) acting as scaffold or, in the case of TRIM5α, as a cargo receptor (Mandell et al., 2014) (Kimura et al., 2015).

### 1.2.1 MID1/TRIM18

The *MID1* gene is located on the short arm of the X chromosome (Xp22.2) and is composed of 9 coding exons (figure 1.10) (Quaderi et al., 1997). It spans approximately 400 kb, is transcribed from multiple promoters and uses alternative 5'untranslated (5'UTR) exons in different combinations (Landry et al., 2002).

The *MID1* gene encodes a 667 amino acid product (MID1/TRIM18) that belongs to the tripartite motif (TRIM/RBCC) subfamily of zinc finger proteins (Quaderi et al., 1997). MID1, like the other components of this family of proteins, is characterized by the presence of the tripartite motif at the N-terminus, which consists of a RING finger domain, two B-box motifs and an alpha-helical Coiled-coil region (RBCC) (Reymond et al., 2001). At the C-terminus there are: a COS domain, a Fibronectin type III (FN3) repeat and a PRY-SPRY domain (B30.2-like) (Figure 1.10). The coiled-coil region of MID1 is confined within 120 amino acids from the end of the B-box2 and mediates MID1 self-interaction (Meroni and Diez-Roux, 2005) (Sardiello et al., 2008). The coiled-coil is also responsible for MID1 hetero-interaction with other TRIM family members such as TRIM1/MID2 and TRIM16 (Short and Cox, 2006) (Bell et al., 2012).

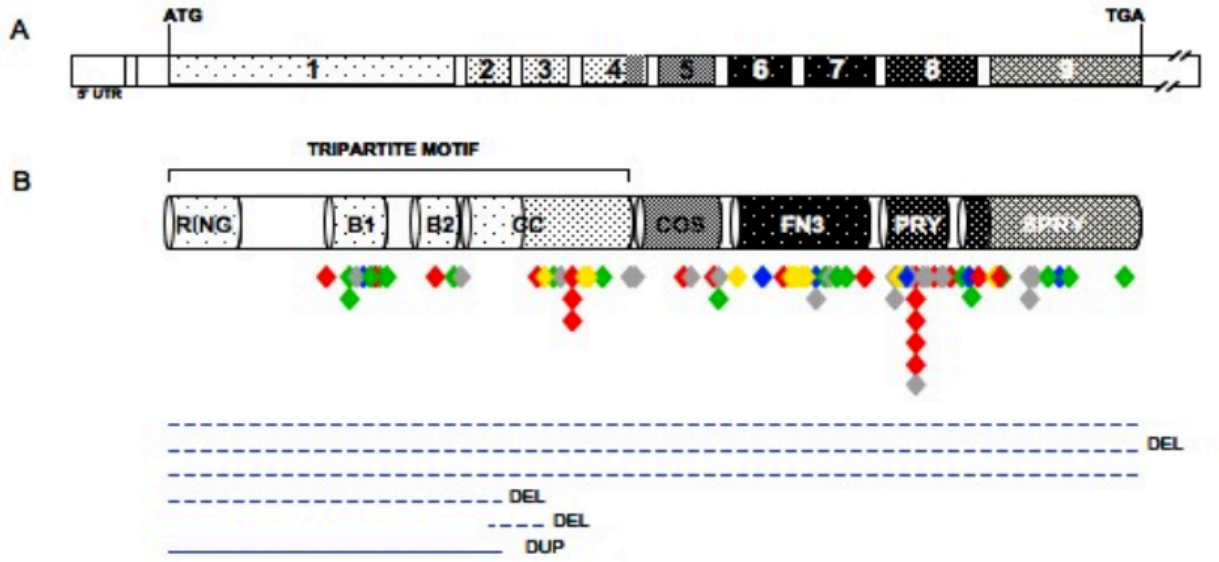


Figure 1.10: Schematic representation of the *MID1* gene (A) and its protein product (B) indicating the different mutations and the most localization. RING, RING finger domain; B1 and B2, B-Box1 and B-Box2 domains, respectively; CC, Coiled-coil region; COS, COS domain; FN3, fibronectin type III repeat; PRY and SPRY form the PRY-SPRY domain. Colours indicate the different effect of the mutation: red, nonsense mutations; green, missense mutations; gray, frameshift mutations; blue, small in-frame insert mutations or deletions; yellow, splice-site consensus mutations. Dotted lines indicate large deletions. Continuous blue line represents a large duplication (Adapted from Fontanella et al., 2008).

1.2.1.1 *MID1* mutations in X-linked Opitz syndrome patients

Mutations in *MID1* gene have been associated with the human X-linked Opitz G/BBB (OS) syndrome (Quaderi et al., 1997). OS is a multiple congenital disorder characterized by developmental defects of the midline (Opitz, 1987). OS patients present characteristic craniofacial, genitourinary, cardiovascular malformations such as cleft lip/palate, laryngeal cleft, hypertelorism and hypospadias. In addition, developmental delay, mental retardation, and brain defects are frequent. Mutation analysis of isolated and familial cases of OS revealed the presence of more than 80 different mutations in the *MID1* gene. Pathogenetic mutations include nonsense, missense, indels, duplications, and splice-site changes as well as partial or complete gene deletions. The mutations are distributed along the entire length of the gene, although the majorities are concentrated in the 3' region. All the protein domains

are affected, with the exception of the RING domain, which is only affected if the entire gene is deleted. Therefore the distribution and type of mutations indicate that loss-of-function is the mechanism underlying the pathogenesis of OS (Fontanella et al., 2008). To study the pathological processes that occur during embryogenesis, leading to the clinical manifestations observed in OS patients, a *Mid1* knock-out mouse line has been generated. This mouse is viable and do not present evident midline defects but present cerebellar anatomical abnormalities (cerebellar vermis hypoplasia) and coordination and learning impairment, recapitulating the neurological defects observed in OS patients (Lancioni et al., 2010).

1.2.1.2 MID1 protein functions

MID1 is localized in the cytoplasm of the cell and associates with the microtubules along their length and throughout the cell cycle through the COS domain (Cainarca et al., 1999) (Short and Cox, 2006). Interestingly, MID1 is bi-directionally transported along the microtubules in a kinesin and dynein-dependent manner. This mechanism is finely regulated by MID1 phosphorylation and dephosphorylation via mitogen activated protein kinase (MAPK) and protein phosphatase 2A (PP2A) (Aranda-Orgilles et al., 2008). MID1 in fact interacts with alpha4, the rapamycin-sensitive regulatory subunit of PP2A, and through this recruits the latter to microtubules (Trockenbacher et al., 2001) (Short et al., 2002). As a TRIM protein, the main property of MID1 is to participate in the ubiquitination process as an E3 ubiquitin ligase (Napolitano et al., 2011) (Han et al., 2011). Interestingly, MID1 functions as E3 ubiquitin ligase for mono-ubiquitination of α4, the regulatory subunit of PP2A. Monoubiquitination of α4 triggers calpain-mediated cleavage and degradation of its C-terminal domain that contains the MID1 binding region. Therefore α4 cleavage disrupts the MID1-mediated association of α4/PP2A to microtubules thus influencing PP2Ac stability and phosphatase activity on microtubule-associated proteins (MAPs) such as Tau (Liu et al., 2001) (Short et al., 2002) (Watkins et al., 2012). Deregulation of PP2A activity and hyperphosphorylation of MAPs are observed in OS-derived cells (Trockenbacher et al., 2001). *In vitro* assays also indicate that MID1 catalyzes the ubiquitination of PP2Ac (Du et al., 2013). It has been also reported that the MID1/alpha4 complex interacts through the PRY-SPRY domain with elongation factor-1α (EF-1α), the 40S ribosomal S6 kinase (S6K). Through this association, MID1 is able to bind RNA and form a microtubular ribonucleoprotein complex and together with PP2Ac controls the activity of the mTOR kinase (Aranda-Orgilles et al., 2008). High levels of PP2Ac activity in MID1-deficient cells

have demonstrated to abolish the interaction between mTOR and Raptor, which is an essential cofactor of mTOR activity. mTOR-dependent phosphorylation of S6K and 4E-BP1 supports protein translation, while their dephosphorylation by PP2A inhibits it (Liu et al., 2011). Since MID1 depletion reduces mTORC1 activity, MID1 is a positive regulator of translation. By this mechanism, MID1-PP2A complex regulates the translation of mRNAs with CAG repeat expansions such as HTT and therefore is likely implicated in Huntington's Disease (Krauss et al., 2013).

Another function of the MID1/α4/PP2A complex is the ability to regulate the nuclear localization of the activator form of the GLI3 transcription factor. It was demonstrated that an increase of PP2A activity mediated by a downregulation of MID1/α4 results in cytosolic retention of GLI3 and its reduced transcriptional activity (Krauss et al., 2009). It has been shown that MID1 interact also with Fu, an essential component of Hedgehog signalling, and through this interaction likely controls the subcellular localization and transcriptional activity of GLI3 in cancer cell line, promoting K6-, K48- and K63-linked ubiquitination of Fu. As a result the kinase domain of Fu is cleaved-off permitting nuclear translocation of GLI3 and transcriptional activation (Schweiger et al., 2014).

Recently, new findings on MID1 protein role in neuronal development, immunity and cancer have been demonstrated, providing a broader role in context-specific functions of this E3 ligase. A role for MID1 in axon development has been proposed: depletion of MID1 in cultured neurons results in PP2Ac accumulation in the axon shaft and causes abnormal corpus callosum development in mice. Therefore MID1-dependent PP2Ac turnover controls axon growth and branching *in vitro* and regulates axon elongation and projection *in vivo* (Lu et al., 2013).

Furthermore MID1 has been shown to primarily localize to the uropod of migrating Cytotoxic T lymphocytes (CTLs), a structure that is retracted in an actin and actomyosin dependent way (Boding et al., 2014a). It has been also demonstrated that MID1 controls polarization and migration of CTLs, probably by affecting microtubule dynamic (Boding et al., 2014b).

Recent works indicate an involvement for MID1 not only in development but also in cancer. MID1 binds androgen receptor (AR) mRNA and enhances its translation. Moreover, AR in turn decreases MID1 levels in response to androgen stimulation, creating a regulatory loop between AR and MID1. AR is a transcription factor that regulates androgen-dependent gene expression during prostate development, but is also aberrantly activated in prostate cancer.

High levels of MID1 protein in prostate cancer tissues have been found along with high AR expression level, reflecting a mechanism that contributes to tumour progression (Demir et al., 2014) (Kohler et al., 2014).

1.2.1.2 Novel partners of MID1 protein: BRAF35

Despite findings about MID1 involvement are increasing rapidly, not only in the pathogenesis of Opitz syndrome but also in other cellular processes that regulate adult tissue function, a complete overview on its role within the cell and the target(s) of its E3 ligase activity are still not completely unravelled. Our group has been for long time investigating MID1 protein and gene, thus, to elucidate MID1 function in different pathways, we decided to search for new cellular partners for this protein. As described in this thesis work, the BRCA2-associated factor 35 (BRAF35) was identified as a novel MID1 interacting protein.

BRAF35, also known as HMG20b, is a non-canonical High-Mobility-Group (HMG) protein that contains an HMG-box domain and a kinesin-like coiled coil region (KLCC) (figure 4.1 in Results section). The HMG-box of BRAF35 is a non-sequence-specific DNA-binding domain, as it does not exhibit selectivity towards DNA sequence (Lee et al., 2002) (Stros et al., 2007). Recent bioinformatic analysis revealed that the initial predicted KLCC is in reality more extended, forming a bundle of a-helices that may provide interfaces for the dynamic assembly of protein complexes (Lee and Venkitaraman, 2014). BRAF35 has been isolated in two different complexes within the cell: the BRAF-histone deacetylase complex (BHC, also called HDAC-coREST) and the BRCA2-containing complex (Hakimi et al., 2002) (Marmorstein et al., 2001). Working with different partners of the two complexes, BRAF35 has a role in both neuronal differentiation and in cell cycle progression. BRAF35 is modified through SUMO conjugation at 4 lysines and sumoylation has been shown to be fundamental for its anti-neurogenic activity and to be inhibited by the interaction with its paralogue iBRAF (inhibitor of BRAF35). BRAF35 and iBRAF are mutually exclusive subunits of the coREST-LSD1 complex and promote an antagonist repressor and activator effect on neuronal REST target genes (Ceballos-Chavez et al., 2012) (Wynder et al., 2005). Furthermore, BRAF35 C-terminus strongly binds to the BRC5 repeat of BRCA2; the two proteins associate with chromatin during early phases of mitotic chromosome condensation and are needed for the completion of cell division. In fact, cells lacking BRAF35 can initiate cleavage furrow formation but are inefficient in separating after cytokinesis, and often

become binucleate (Lee et al., 2011). By means of its coiled coil region, BRAF35 is also able to bind KIF4, a kinesin that is required for microtubule organization of spindle midzone and midbody during cytokinesis (Lee and Kim, 2003) (Kurasawa et al., 2004). A recent paper demonstrated that BRAF35 is recruited to the cytokinetic midbody during telophase. In this context, a cancer-associated mutation in the C-terminal region of BRAF35 has been shown to interfere with BRCA2 binding and midbody localization, inducing cytokinesis failure (Lee and Venkitaraman, 2014).

## 1.3 Mammalian cytokinesis

Initial findings on MID1 and BRAF35 proteins obtained in our lab suggest an involvement of the two proteins in the cytokinetic process.

Cytokinesis is the last step of the cell cycle that consists in the physical separation of one cell into two upon chromosome separation in two identical sets. It requires coordinated actions of the cytoskeleton, membrane systems, and the cell cycle engine, which are precisely controlled in space and time.

Simplifying a very complex process, cytokinesis can be divided in different sub-processes: the central spindle assembly, the division plane specification, the contractile ring assembly, the cytokinetic furrow ingression and the abscission (Eggert et al., 2006).

### 1.3.1 Central spindle assembly

Cytokinesis is initiated during anaphase, when the decline of Cyclin-dependent kinase 1 (CDK1) activity leads to a stabilization of microtubules and reorganization of the mitotic spindle. The central spindle is built from antiparallel bundles of microtubules overlapping at a central region, where microtubule-associated proteins, motor proteins and protein kinases accumulate (figure 1.11). Microtubules of the central spindle (midzone) partly derive from microtubules of the metaphase spindle but they are also assembled de novo during anaphase through non-centrosomal microtubule nucleation. The principal microtubule-interacting proteins implicated in morphogenesis of the midzone are bundling factors and kinesins. A conserved bundling factor, PRC1/Fascetto/spd-1 accumulates at the centre of the midzone. It is inhibited until anaphase onset by CDK1-mediated phosphorylation. As mitosis progresses and CDK1 activity decreases, PRC1 is dephosphorylated and becomes active (figure 1.11). Two classes of plus-end-directed kinesins have been implicated in midzone assembly: a kinesin-6 family member (MKLP1/KIF23) and a member of the kinesin-4 family (KIF4). At anaphase, KIF4 relocalizes to microtubule bundles and accumulates at the midzone where it binds dephosphorylated PRC1 helping its corrects localization. MKLP1 together with Rho-family GTPase activating protein (GAP) CYK-4 (also termed MgcRacGAP) form a tetrameric complex called centralspindlin. MKLP1 affinity to the central spindle is regulated by phosphorylation by CDK1 and Aurora B. Aurora B is part of a third complex that regulates central spindle assembly called chromosomal passenger complex (CPC) (Fededa and Gerlich, 2012). At anaphase the CPC moves from the centromeres to the midzone where its function is needed for phosphoregulation of other central spindle components such as

PRC1. The E3 ligase Cul3 promotes the removal of Aurora B from the anaphase chromatin. The localization of central spindle core components, such as PRC1, centralspindlin and the CPC, is mutually interdependent, therefore various microtubule bundling factors may be required in cells to stabilize the midzone. In summary, reduction of CDK1 activity at the metaphase–anaphase transition leads to dephosphorylation of multiple central spindle components resulting in the activation of a self-assembly process that organizes microtubules (figure 1.11) (Eggert et al., 2006) (Fededa and Gerlich, 2012).

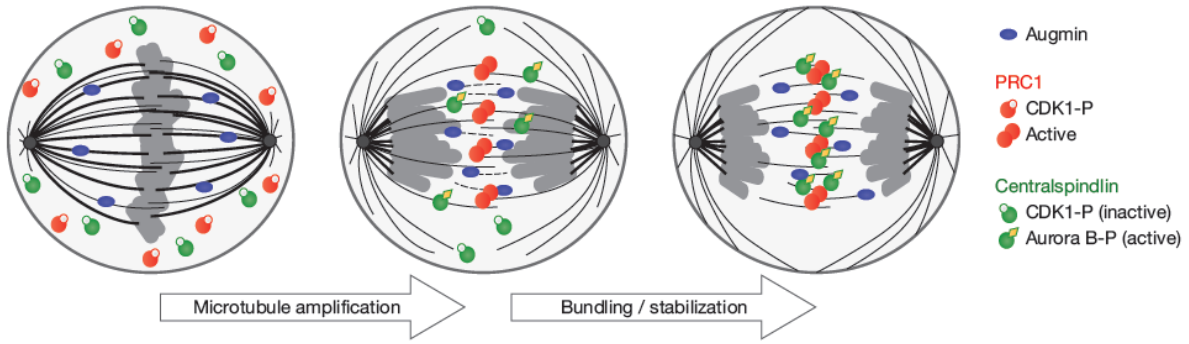


Figure 1.11: Central spindle assembly. During anaphase, *de novo* assembled and interpolar microtubules form an array of antiparallel microtubules at the central spindle. The overlap is stabilized by dephosphorylated PRC1 (red). Dephosphorylation of a CDK1 site and phosphorylation of an Aurora B site on MKLP1 (a component of the centralspindlin complex, green) promotes its binding and bundling of central spindle microtubules (adapted from Fededa and Gerlich, 2012).

### 1.3.2 Division plane specification

The mitotic spindle defines the division plane position and transmits a position signal to the cell cortex during early anaphase by promoting concentration and activation of the small GTPase RhoA at the equatorial cortex. After CDK1 inactivation PLK1 phosphorylates MgcRacGAP that binds ECT2 (mammalian Rho GEF). This interaction is necessary for ECT2 activation and transport to the equatorial cortex, where this GEF associates with the plasma membrane and activates RhoA, The C1 domain of MgcRacGAP associates with the plasma membrane by interacting with polyanionic phosphoinositide lipids thus linking central spindle and plasma membrane. The formation of an active zone of RhoA at the equatorial cortex is thought to be the key event that triggers cleavage furrow formation and ingression (Yuce et al., 2005) (Petronczki et al., 2007).

### 1.3.3 Contractile ring assembly

The RhoA pathway promotes assembly of the actomyosin ring (figure 1.12) by stimulating nucleation of unbranched actin filaments by activation of Diaphanous-related formins and promoting myosin II activation by the kinase ROCK. Besides actin and myosin II, the contractile ring contains the scaffolding protein anillin and citron kinase (CIT-K). Anillin binds to actin, myosin, RhoA and MgcRacGAP, and thereby links the equatorial cortex with the signals from the central spindle. CIT-K is required for proper RhoA localization and has been reported to control the localization of other contractile ring components, anillin, actin, myosin, and three central spindle MAPs, KIF14, KIF23, and PRC1 (Lekomtsev et al., 2012) (D'Avino et al., 2015).

### 1.3.4 Furrow ingression

After the actomyosin ring assembly, its contraction leads to ingression of the attached plasma membrane, which partitions the cytoplasm into two emerging sister cells (figure 1.12). Efficient furrow ingression requires reduction of contractility at polar cortex regions and stabilization of the cytokinetic furrow position, involving cortex fluctuations by plasma membrane blebbing. It has been shown that misregulated polar cortex contractility leads to unstable and oscillating furrows. Despite its central importance in cell division, the force-generating mechanism of actomyosin ring contraction is still not well understood (Fededa and Gerlich, 2012).

As furrowing progresses, the spindle midzone transforms into an intercellular bridge that connects the two dividing cells. The intercellular bridge contains antiparallel bundles of microtubules that overlap at a central zone termed midbody, which appears as a dense structure in electron micrographs. The midbody is considered as a targeting platform for the abscission machinery. The midbody is not a static structure, but it undergoes a series of morphological changes during the late stages of cytokinesis and after mitosis it persists for a long time until abscission occurs (Agromayor and Martin-Serrano, 2013).

### 1.3.5 Abscission

After furrowing completion, two symmetric constrictions form at both sides of the midbody ring (figure 1.12); at this stage, the chromosomes are almost completely de-condensed. Subsequently, the microtubule bundles become progressively thinner, an event most likely

mediated by microtubule depolymerizing factors, such as katanin and spastin. Before abscission occurs, a secondary ingression site develops that decreases the thickness of the midbody from 1.5–2 mm to approximately 100–200 nm. Once the midbody has thinned, the ESCRT machinery is recruited to mediate the final membrane scission event that separates the daughter cells (figure 1.12). First, the centrosomal protein CEP55 recruits the ESCRT-I subunit TSG101 and the ESCRT-associated protein apoptosis-linked gene-2-interacting protein X (ALIX) to the midbody, then, ESCRT-III subunits (CHMPs) are recruited to mediate abscission. ESCRT-III subunits form filaments at the plasma membrane of the midbody, which curves progressively reducing the membrane neck for fission by AAA ATPase vacuolar protein sorting 4 (VPS4), the enzymatic component of the ESCRT machinery (Agromayor and Martin-Serrano, 2013). It has been demonstrated that BRCA2 is recruited on the midbody through an interaction with Filamin A and regulates CEP55-ALIX and CEP55-TSG101 complexes (Mondal et al., 2012).

Also the abscission timing is highly regulated: PLK1 phosphorylates CEP55 to prevent its interaction with MKLP1 during furrow ingression in order to avoid premature accumulation of CEP55 and, in turn, the ESCRT proteins at the midbody ring (D'Avino et al., 2015). Moreover, Aurora B activity controls abscission timing functioning as a checkpoint that delays abscission in response to DNA trapped in the intercellular bridge (Kitagawa and Lee, 2015).

In order to permit complete cortical constriction at the abscission site, the PKCε–14-3-3, GTPase Rab35 and its effectors, and the phosphatidylinositol-4,5-bisphosphate 5-phosphatase OCRL regulate actin filament disassembly. Disassembly of microtubule bundles inside the intercellular bridge instead depends on the microtubule severing protein spastin, which binds to midbody-localized ESCRT-III-associated protein CHMP1B (Fededa and Gerlich, 2012). It was shown that two ESCRT-modulating deubiquitinating enzymes UBPY/USP8 and AMSH were recruited to the MB during cytokinesis and depletion of either DUBs led to cytokinesis failure. The localization of DUBs to the central spindle and midbody is an indication of the presence of a large amount of ubiquitinated proteins that are to be deubiquitinated by these DUBs during cytokinesis. Interestingly, the level of protein ubiquitination rises strikingly and transiently in the Aurora B-positive region of the central spindle during cytokinesis, suggesting an ubiquitination-mediated regulation of this cellular event (Mukai et al., 2008). Aurora B itself subject to extensive posttranslational modification throughout the cell cycle: is ubiquitinated by the APC cofactors Cdh1 and Cdc20, which

regulate its degradation, or by Cul3-KLK21. Another E3 ligase, the SCF- FBXL2 targets Aurora B polyubiquitination and degradation promoting its depletion from the midbody (Chen et al., 2013).

Moreover, another giant protein possessing E2/E3 ubiquitin ligase activity, BRUCE, localizes on the midbody and interacts with midbody components, such as MKLP1, and if depleted, it blocks abscission (Pohl and Jentsch, 2008).

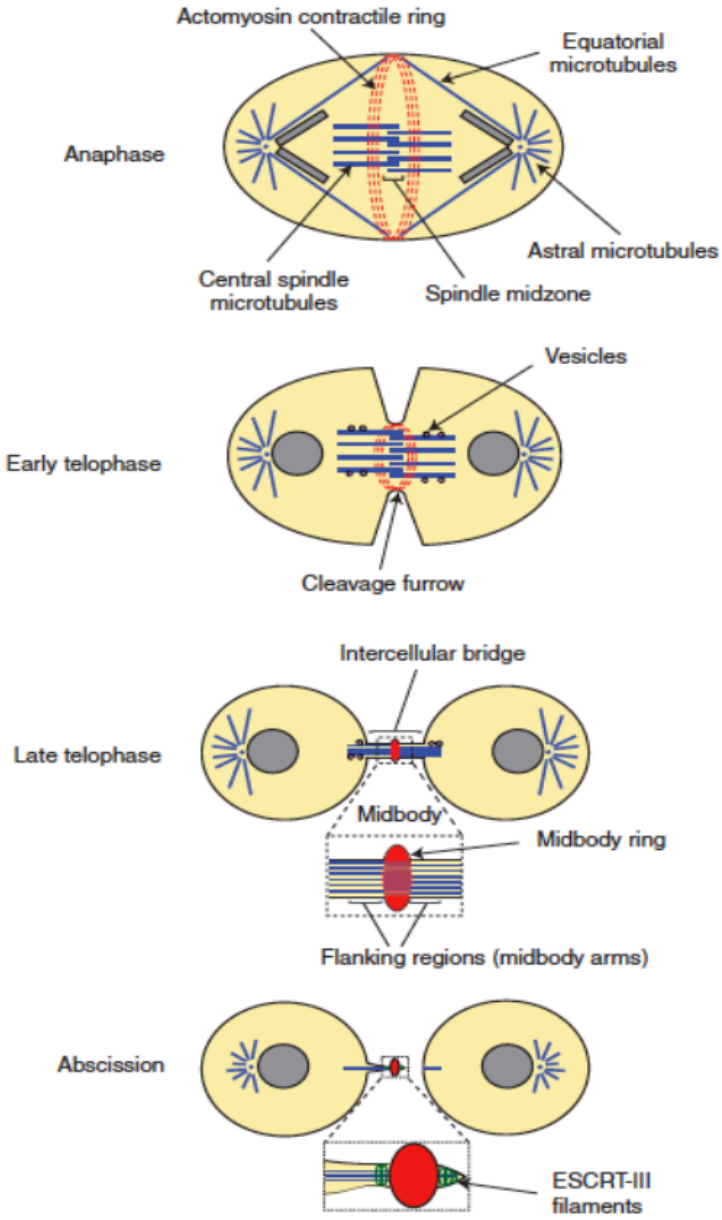


Figure 1.12: Schematic diagram illustrating the different stages of cytokinesis in animal cells. Microtubules are depicted in blue, the actomyosin contractile ring and the midbody ring in red, ESCRT-III spiral filaments in green. (Adapted from D'Avino et al., 2015)

### 1.3.6 Midbody fate

Following abscission, the residual midbody structure (midbody remnant, MBR) that remains attached to one daughter cell has different fates depending on the cell type. The midbody derivative is either released to the extracellular medium, degraded by selective autophagy or persists in the cytoplasm (figure 1.13). Interestingly, evidences suggest that MBs are also involved in non-mitotic functions such as dorso-ventral axis patterning, cell differentiation and cancer. Midbodies can act as asymmetrically-positioned scaffolds that transfer signalling molecules to one daughter cell. Therefore in the event of asymmetric abscission, a daughter cell inherits the MB, whereas during symmetric abscission MB is released into the extracellular space. It was shown that daughter cells with the older mother centriole tend to inherit the MB and possess a more stem-like phenotype, although the role of MB inheritance/accumulation in regulating cell 'stemness' likely depends on the cell and tissue type, as well as conditions that induce cell differentiation. Intriguingly, cancer cells contain the highest level of MB accumulation. Given that secreted MBs can be engulfed by these cells, it is plausible that cancer cells that come in contact with secreted MBs at the extracellular matrix could potentially uptake and accumulate MBs to acquire 'stemness' (Chen et al., 2013) (Dionne et al., 2015) (Kuo et al., 2011) (Pinheiro and Bellaiche, 2014).

Figure 1.13: (see following page) Schematic representation of cytokinesis progression, abscission, and the fate of the post-mitotic midbody (MB). (a) A representative drawing of "Zwischenkorper" (midbody) by Walther Flemming. The black dot between the two reforming nuclei (N) represents the MB. (b) Progression from early to late cytokinesis is shown from left to right. (c) Enlargement of inset in (b), showing the process of abscission and the fate of the post-mitotic MB. From left: As the cell approaches the final stage of abscission, the density of MTs decreases and different vesicle types again appear in vicinity of the MB. Meanwhile, ESCRT complexes are recruited to the constriction zone, and interact with the MT-severing protein. Abscission requires the orchestration of these pathways (e.g., vesicle trafficking and fusion, ESCRT machinery, and MT severing). After abscission, the post-mitotic MB is either released after a secondary bridge-severing event (bottom left panel) or inherited by one of the two daughter cells (bottom middle and right panels). The inherited MBs may be retained freely in the cytoplasm (bottom middle panel) or degraded in the autolysosome after being recognized by autophagic receptors (grey ovals) and engulfed by autophagosomes (bottom right panel). Thus, two major mechanisms for MB clearance are autophagy and MB release. (Adapted from Chen et al., 2013)

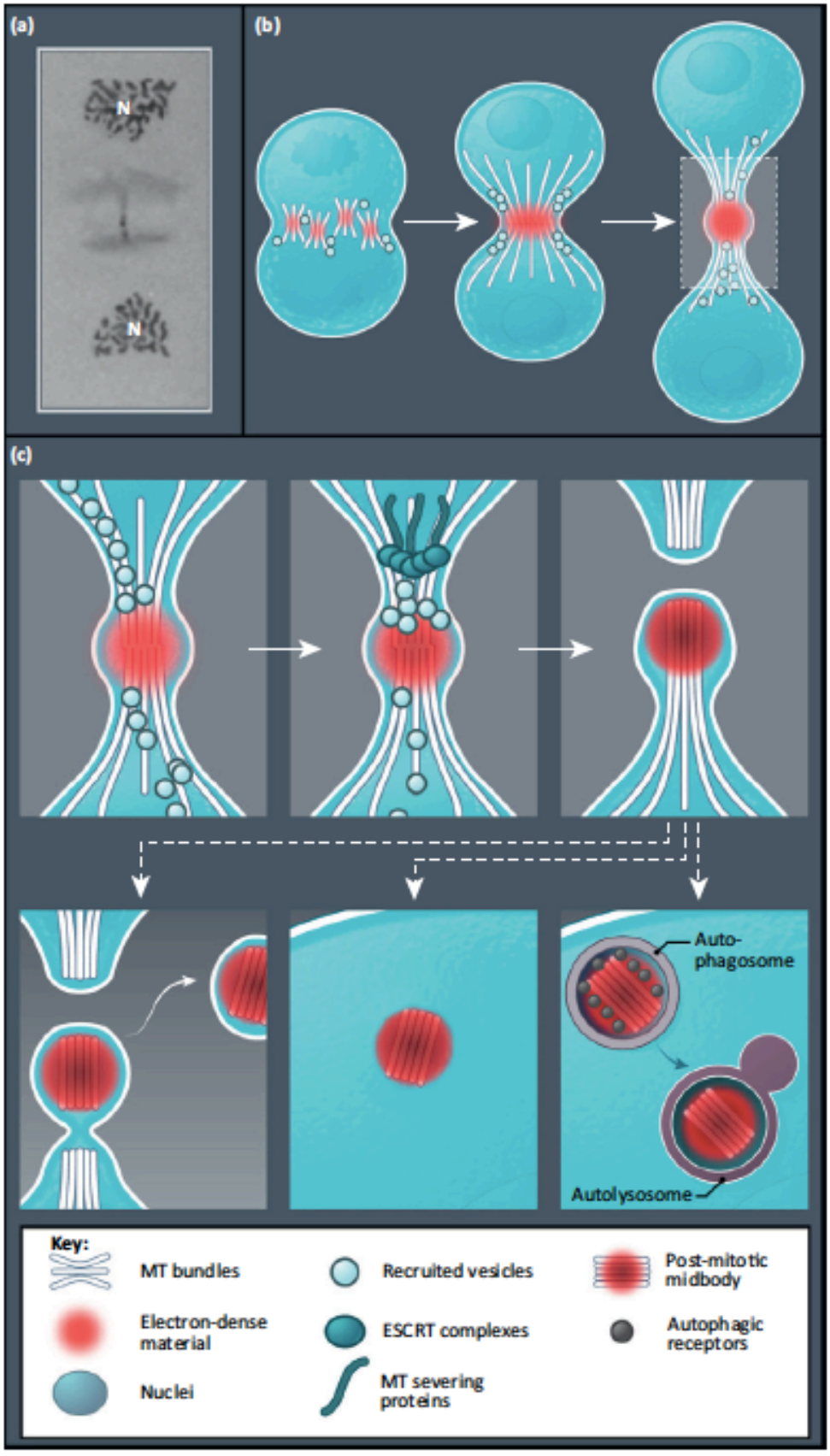
(a)
N
N
(b)
(c)
Auto-
phagosome
Autolysosome
Key:
MT bundles
Recruited vesicles
Post-mitotic
midbody
Electron-dense
material
ESCRT complexes
Autophagic
receptors
Nuclei
MT severing
proteins

### 1.3.7 Cytokinesis and cancer

Cytokinesis failure results in tetraploid cells with extra centrosomes that are genetically instable owing to perturbed chromosome segregation in subsequent cell divisions. DNA trapped in the cytokinesis furrow potentially perturbs abscission, and chromatin bridges between sister chromatids in anaphase, owing to the presence of chromosome fusion or unresolved DNA catenae, become an obstacle to the cleavage furrow ingression. Cytokinesis failure also gives rise to an extra copy of the centrosome, which can end up with twice the centrosomes in the next mitosis following centrosome duplication during S phase. The number of centrosomes that are present in a cell determines the number of spindle poles. So, in the case of extra centrosomes, the cell will have multipolar spindles and in the case of failure in centrosome separation, the cells will have monopolar asters. Such super-numerical centrosomes during mitosis are frequently found in many cancer cell lines. Cells that have failed cytokinesis in the previous cell cycle frequently generate lagging chromosomes and micronuclei, and are thus predisposed to suffer from DNA damage associated with those failures (Hayashi and Karlseder, 2013). Multiple cytokinetic regulators have been found mutated in various cancers. PLK1 is overexpressed in human leukemia cell lines as well as in cell samples from individuals with acute myelogenous leukemia and acute lymphoblastic leukemia; the *KLHDC8B* protein product localizes to the midbody and a translocation disrupting this gene has been characterized in a family in which multiple individuals developed Classical Hodgkin lymphoma. Furthermore, the cytokinesis regulator FYVE-CENT is found mutated in breast cancer samples and depletion of this protein results in an increased number of binuclear and multinuclear profiles, as well as cells arrested in cytokinesis, indicating its important role in this process (Sagona and Stenmark, 2010).

All these evidences suggest that aberrant cytokinesis may lead to aneuploidy, which may in turn develop into cancer. Considering that cytokinesis failure should be an early event that triggers carcinogenesis, detection of mutations in cytokinetic regulators might help to detect earlier such aberrations.

Further investigation on new proteins involved in the regulation of this cellular mechanism will provide new insights on cell division-dependent processes such as differentiation and tumourigenesis.

## 2. AIM OF THE STUDY

.

MID1/TRIM18 is a microtubule-associated protein that is mutated in the X-linked Opitz G/BBB syndrome (OS). OS is characterized by several physical defects and developmental delay (Cainarca et al., 1999). During the past years, some of the targets of MID1 activity have been identified. MID1 interacts and mono-ubiquitinates alpha4 (α4), the rapamycin-sensitive regulatory subunit of PP2A, influencing protein phosphatase PP2Ac stability (Watkins et al., 2012). Moreover, MID1 interact with Fu, a component of the Hh pathway, and catalyses its ubiquitination and cleavage (Schweiger et al., 2014). Recent works indicate an involvement for MID1 not only in development but also in cancer. In fact, high levels of MID1 protein in prostate cancer tissues have been found along with high androgen receptor (AR) expression level, likely contributing to tumour progression (Kohler et al., 2014). Nevertheless, the role of MID1 within these different pathways and the function exerted during development and in other non-physiological conditions is still to be unravelled. For this reason, we decided to search for new interacting partners of MID1, in order to get additional information about its cellular role.

We identified the BRCA2-associated factor 35 (BRAF35) as a novel MID1 binding protein. Interestingly, data form literature described BRAF35 as either part of the LSD1-CoREST neuronal repressor complex or in a complex together with BRCA2, which is linked to familial breast and ovarian cancer, regulating cell cycle progression (Hakimi et al., 2002) (Marmorstein et al., 2001). Despite that, little is known about its function and regulation during these processes.

The thesis work was based on the hypothesis that BRAF35 represents a novel MID1 E3 ligase substrate and that, through an ubiquitination-dependent mechanism, MID1 can regulate BRAF35. The aim of the project was to i) characterise MID1/BRAF35 interaction, ii) to understand if MID1, as an E3 ubiquitin ligase, regulates BRAF35 and iii) to investigate the functional role of the MID1/BRAF35 complex during cytokinesis.

Given that many of the cellular processes involved in embryonic development such as proliferation, adhesion, migration, and differentiation are mediated by factors that frequently are abnormally regulated in cancer, we think that understanding the functions and the relationship between MID1 and BRAF35 will deepen our knowledge of the pathogenesis of Opitz syndrome and tumourigenesis.

# 3. MATERIALS AND METHODS

3.1 Composition of the Buffers and solutions employed

- TAE buffer 50x: 242 g Tris base, 57,1 mL glacial acetic acid, 100 mL EDTA 0,5 M pH 8.0, $H_2O$ up to 1 L.
- PBS buffer 10x pH 7.4: 8 g NaCl, 0,2 g KCl, 1,44 g Na2HPO4 • 2 H2O, 0,24 g KH2PO4, $H_2O$ up to 1L. Adjust pH 7.4 with NaOH 10 M.
- 1.5 M Tris-HCl, pH 8.8: 54.45 g Tris, $H_2O$ up to 300 mL, adjust pH to 8.8 with HCl.
- 0.5 M Tris-HCl pH 6.8: 6g Tris, $H_2O$ up to 100 mL, adjust pH to 6.8 with HCl
- TBS buffer 10x: 24 g Tris base, 88 g NaCl. Dissolve in 900 mL distilled $H_2O$ and adjust pH to 7.6 with HCl. Add $H_2O$ to a final volume of 1 L.
- TBST (Tris-buffered saline, 0.1% Tween 20): for 1 L 100 mL of TBS 10x, 900 mL distilled $H_2O$ and 1 mL Tween 20.
- Sample Buffer 1x: 62.5 mM Tris-HCl pH 6.8, 20% Glycerol, 2% SDS, 5% beta-Mercaptoethanol, 0.02 % w/v bromophenol blue.
- Tris-Glycine Running Buffer 1x: 25 mM Tris, 192 mM Glycine, 0.1% SDS.
- Transfer buffer 1x: 25 mM Tris, 192 mM Glycine, 20% v/v methanol.
- Pull down lysis buffer: 20 mM Tris-HCl pH 7.5, 20% glycerol, 50 mM NaCl, 5 mM EDTA, 0.1% Triton X- 100, 1.5 mM PMSF and 5 µL/mL protease inhibitors cocktail (P8340 Sigma).
- Lysis buffer: 20mM Tris-HCl pH 7.4, 150mM NaCl, 1mM EDTA, 0.5% Triton X-100, 10% glycerol, 0.5% NP-40, 1mM DTT, 1mM PMSF, 5 µL/mL protease inhibitors cocktail (P8340 Sigma).
- Denaturing lysis buffer: 50mM Tris-HCl pH 7.4, 5 mM EDTA, 1% SDS, 10mM DTT, 1mM PMSF, 15U/mL DNAseI.
- IP buffer: 50 mM Tris-HCl pH 7.4, 300 mM NaCl, 5 mM EDTA, 1%Triton X-100, 5 µL/mL protease inhibitors cocktail (P8340 Sigma).
- Wash buffer IP: 50mM Tris-HCl pH 7.4, 300 mM NaCl, 5mM EDTA, 0.1% Triton X-100.
- RIPA buffer: 30mM Tris-HCl pH 8, 0.1% SDS, 150 mM NaCl, 0.5% NaDOC, 1% NP-40, 5 µL/mL protease inhibitors cocktail (P8340 Sigma).
- TBST 20 mM Tris-HCl pH 7, 50 mM NaCl and 0.1% Tween-20.

3.2 Constructs

MycGFP-tagged TRIM9, TRIM27, UBE2D1 and UBE2G2 were already available in the lab (Reymond et al., 2001) (Napolitano et al., 2011). MycGFPpCDNA3-tagged MID1 full length and domain-deleted mutants were either available in the lab (Cainarca et al., 1999) or produced by subcloning the cDNA from HApCDNA3-MID1 plasmids into EcoRI-XhoI sites of MycGFPpCDNA3 vector. pRSV-FLAG-BRAF35, pRSV-FLAG-BRAF354KR and pRSV-HA-iBRAF were kindly provided by Dr. Reyes, CABIMER, Sevilla, Spain. pRK5-HA-ubiquitin wt, K48 and K63 were kindly provided by Dr. Zucchelli, SISSA, Trieste.

HA-BRAF35 was produced by PCR using NIH3T3 cDNA as template for SmaN and SmaC amplification. The reaction was assembled as indicated below:

| | |
|---|---|
| cDNA 100 ng/μL | 2 μL |
| 10x Buffer | 5 μL |
| Fw primer 200 ng/μL | 1 μL |
| Rev primer 200 ng/μL | 1 μL |
| dNTPs mix 10mM | 1 μL |
| Pfu DNA Polymerase (Promega) 2.5 U/μL | 0.5 μL |
| $H_20$ | up to 50 μL |

| | |
|---|---|
| 2’ at 95°C | |
| 30’’ at 95°C | |
| 30’’ at 95°C | |
| 30’’ at 58°C | Repeated for 35 cycles |
| 1’ at 72 °C | |
| 10’’ at 72°C | |

The amplification fragment was precipitated with NaAc 3M in 100% ethanol and digested with EcoRI and XhoI restriction enzymes (Roche).

Digested fragments were separated by electrophoresis on 1% agarose gels in TAE 1x containing GelRed 1x (Biotium), excised from the gel and purified using the QIAquick gel

extraction kit (QIAGEN). The DNA was then eluted in 30 μL of EB buffer (Tris-Cl 10 mM, pH 8.5) and final concentration was evaluated by spectrophotometer (Nanodrop ND-1000). BRAF35 fragment was cloned into EcoRI and XhoI sites of HApDCNA3 vector (digested and purified from 0.8 % agarose gel as described above).

Ligation reaction was performed as described below using a 1:3 molar ratio of insert:vector and incubated o/n at 4°C:

Vector DNA 100 ng
Insert DNA x ng
10x T4 DNA ligase buffer (Promega) 2 μL
T4 Ligase (Promega) 1 μL
$H_20$ up to 20 μL

HA-BRAF35 C1 was produced by PCR as indicated above using HA-BRAF35 as template (100 ng) and SmaN/SmadelC1 oligonucleotides (annealing temperature 55 °C).
Primer sequences:
SmaN 5'-GAATTCATGTCCCACGGTCCCCG-3'
SmadelC1 5'-CACTCGAGTCAGAAGATGGGCACATC-3'
SmaC 5'-CTCGAGTCACAGGTGCTCG-3'

Competent E. coli DH5α cells were transformed with ½ of the ligation reaction (or with 100-250 ng of plasmid) and grown on LB-agar containing the appropriate antibiotic o/n at 37°C.

3.3 Plasmid DNA preparation
For miniprep and midiprep preparation, single colonies were picked from plates and grown o/n at 37°C in 2 mL or 100 mL, respectively, of LB broth containing the appropriate antibiotic. Pellet was obtained after centrifugation for 10' at 4000 g and plasmid DNA was prepared using QIAGEN plasmid Mini or Midi kit, following manufacturer's indications.

3.4 Two hybrid screening and interaction mating assays

The two-hybrid screening was performed using MID1ΔRBB fused with in the LexA DNA-binding domain in the pEG202 vector. The bait was transformed into the yeast strain EGY48 that was subsequently transformed with an NIH3T3 cDNA library cloned into pJG4-5, in frame with the B42 activation domain. Transformants were seeded on plates containing either X-gal or lacking Leucine to select positive clones that have activated both LexA driven reporter genes (lacZ and LEU2). Interaction mating assay to confirm the positivity was performed using the same system and two different yeast mating types (EGY48 MAT α and EGY42 MAT a) transformed with the different LexA-MID1 clones and B42-clones, respectively as described (Finley and Brent, 1994).

3.5 Cell culture and transfections

HeLa, HEK293T and hTERT-RPE1 cell lines were maintained in Dulbecco's Modified Eagle Medium (DMEM) supplemented with 10% Fetal Bovine Serum (FBS), 4mM L-Glutamine, 10 U/mL Penicillin /Streptomycin, at 37°C with 5% CO2.

Plasmid transfections were performed with standard calcium phosphate method (Graham and van der Eb, 1973).

3.6 siRNA-mediated depletion

Specific transcript ablation was performed upon treatment of cells with 10 nM of non-targeting or specific siRNA.

Three siRNAs targeting MID1 and a GFP positive control siRNA were transfected in hTERT-RPE1 cells with Lipofectamine3000 (Invitrogen). After 24 hours medium was replaced and cells were transfected with MycGFP-MID1. After a total of 72 hours of silencing, cells were lysed in lysis buffer and MycGFP-MID1 depletion was tested by immunoblot analysis with anti-myc antibody (figure 3.1A and B). The best siRNA was used for subsequent experiments in HeLa cells (figure 3.1C and D).

Two siRNAs targeting BRAF35 were transfected in HeLa cells with lipofectamine 3000 (Invitrogen). Silencing efficiency was evaluated after 72h on protein lysates with immunoblot analysis with anti-BRAF35 antibody (figure 3.2A and B). siBRAF35 was used to perform subsequent experiments. siRNA sequences were:

- Non-targeting, Stealth RNAi™ siRNA Negative Control, Med GC (Ambion)
- Stealth RNAi™ siRNA GFP Reporter Control (Ambion)
- siMID1_1, sense 5'CAUCACUGUGCAUUGGACCUCCGAU 3'antisense 5'AUCGGAGGUCCAAUGCACAGUGAUG 3' (MID1 HSS181108 Invitrogen)
- siMID1_2, sense 5'GGAGUCAGAACUGACCUGCCCUAUU3' antisense 5' AAUAGGGCAGGUCAGUUCUGACUCC 3' (MID1 HSS106544, Invitrogen)
- siMID1_5n, sense 5'AUUACAACUUUUAGGAAUUtt 3' antisense 5'AAUUCCUAAAAGUUGUAAUcc 3' (Ambion)
- siB35_5, sense 5' GCAUCCCUUUAGCUUUCAAtt 3' antisense 5' UUGAAAGCUAAAGGGAUGCUg 3' (Ambion)
- siBRAF35, sense 5'GCUUCGGCGCUUGCGGAAGAUGAAU 3' antisense 5' AUUCAUCUUCCGCAACGCCCGAAGC 3' (HMG20B BHSS145582 Invitrogen)

3.7 SDS-PAGE and immunoblotting

Protein samples and immunoprecipitated proteins were separated on either 10% or 12% SDS PAGE and blotted onto PVDF membranes (Millipore). The membranes were rinsed in methanol and incubated with Ponceau solution, then washed and blocked in 5% dry milk in TBST for 1 hour. Incubation with primary antibodies was performed for 1-3 hours at room temperature (RT) or over-night (o/n) at 4°C. Membranes were washed 5 times in TBST and

incubated for 1h with HRP-conjugated secondary antibodies. After washing, signal was detected with ECL substrate (Pierce or Millipore).

Relative quantification of blots was performed with ImageJ software (http://rsb.info.nih.gov/ij/index.html). Briefly, blots were scanned and .tif images were used to compare the density of the bands. Bands were selected to generate a profile plot of each lane in which the area of the peak corresponds to the density of the band.

3.8 Antibodies:

anti actin (WB1:2000, Sigma), anti-BRAF35 clone 4.21 (WB 1:2000, IF 1:200, Upstate), anti-beta tubulin (WB 1:4000, IF 1:400, Sigma), anti-Cyclin B1 (WB 1:500, Santa Cruz), anti-Cyclin A (WB1:500, Santa Cruz), anti-cMyc 9e10 (WB 1:5000, M4439 Sigma), anti-MID1 (WB 1:2000, A302-227A Bethyl), anti-FLAG M2 (WB 1:2000, F3163 Sigma), anti-FLAG M2 (F1804 Sigma, for IP), anti-GAPDH (WB 1:10000, G8795 Sigma), anti-Nuclear matrix p84 (WB 1:500, Abcam), anti-HA (WB 1:1500, Babco), anti-HA (IF 1:100, Roche).

3.9 Pull-down assay

HeLa cells were seeded and the day after transfection with MycGFP–UBE2D1 and G2 plasmids was performed. MBP-MID1, -TRIM9 and –TRIM27 proteins (Napolitano et al., 2011) were immobilized on amylose resin (New England Biolabs) and incubated with HeLa lysate for 4 h at 4◦C. The resin was washed three times with pull-down lysis buffer; bound proteins were separated by SDS-PAGE and UBE2 enzymes were visualized by immunoblotting using anti-cmyc antibody. Endogenous BRAF35 was revealed with anti-BRAF35 clone 4.21 (Upstate) antibody. MBP–TRIM proteins were visualized by Coomassie Blue staining.

3.10 Co-immunoprecipitation

HeLa or HEK293T were lysed in IP buffer 48h after transfection. Cell lysates were incubated with 1µg of anti-cmyc 9e10 or anti-FLAG M2 antibodies o/n at 4°C. The immunocomplexes were incubated with protein G sepharose beads (P3296 Sigma) and collected by centrifugation. The beads were washed two times with IP buffer and 3 times with IP wash buffer. Immunoprecipitated (IP) proteins were eluted with 2× sodium dodecyl sulphate (SDS) sample buffer, boiled and analysed by western blot.

3.11 *In vivo* ubiquitination assays

For *in vivo* ubiquitination assays, HEK293T cells were seeded on 60mm or 100mm plates and transfected with a total amount of 7 μg or 15 μg of the indicated constructs. 40 h after transfection, cells were incubated with 5μM MG132 for 4h and lysed in denaturing lysis buffer. Samples were boiled and centrifuged for 30' at 10000g. SDS sample buffer 2x was added, followed by immunoblot analysis.

For the immunoprecipitation, samples were prepared as described above. After centrifugation, 9/10 of clear lysates were diluted 1:10 with IP buffer and incubated with HA-affinity matrix (Roche) or 1 μg of anti-FLAG M2 antibody and protein G sepharose (Sigma) o/n at 4°C. Beads were washed in IP buffer and IP wash buffer two times each and IP protein were eluted in 2x SDS sample buffer. Immunoblot analysis was performed with the indicated antibodies.

3.12 Subcellular fractionation

HeLa cells were transfected with the indicated siRNAs as described above. After 72 hours cells were collected from plates and split into two. For total lysate cells preparation, cells were lysed in lysis buffer. Subcellular fractions were prepared with NE-PER™ Nuclear and Cytoplasmic Extraction Reagent (ThermoScientific) following the manufacturer's indications. All lysates were diluted with SDS sample buffer 4x. Immunoblot analysis with anti-BRAF35, anti-beta Tubulin and anti p84 was performed.

3.13 Cycloheximide (CHX) treatment

Cells were seeded on 35mm plates in complete medium. 24 hours later cells were either non-treated or incubated with siRNAs for the indicated period. For CHX-chase cells were incubated with 50μg/mL CHX (stock 100 mg/mL in DMSO) alone or together with 10μM MG132, and collected at the indicated time points. Lysates were prepared in lysis buffer and analysed by immunoblot with anti-BRAF35 and anti-beta Tubulin antibodies.

3.14 Cell cycle synchronization

For double thymidine block procedure cells were seeded on 35mm plates and the day after were incubated with 2mM thymidine (stock 100 mM, Sigma) for 19h. Cells were then washed in PBS and released in complete fresh medium for 10h. The second block was performed incubating cells with 2mM thymidine for other 14h and releasing in fresh medium

after washing two times in PBS. Cells were collected at the indicated time points for lysis in RIPA buffer.

For mitotic shake-off HeLa cells were seeded on 35mm plates and treated with 2mM thymidine for 24h, then washed in PBS and released for 6h in complete fresh medium. Cells were then incubated with 40 ng/ml nocodazole (stock 200 μg/mL, Sigma) for 12h and mitotic cells were detached from plates with gentle shaking. Cells were collected by centrifugation, resuspended and washed two times in PBS and then re-seeded for releasing in fresh medium. Samples were collected at the indicated time points and cells were lysed in RIPA buffer.

Immunoblot was performed with anti-actin, anti-BRAf35, anti-CyclinB1 and anti-CyclinA antibodies.

### 3.15 Immunofluorescence

For immunofluorescence analysis cells were seeded on coverslips or in chamber slides and transfected as indicated. 24h or 48h after transfection cells were fixed with paraformaldehyde (PFA) 4% in PBS, permeabilized with 0.2% Triton X-100 in PBS and blocked with 10% goat or pig serum in 0.1% Triton X-100 in PBS. Cells were stained with anti-HA, anti-BRAF35 or anti-beta tubulin antibodies and Cy3- or FITC-conjugated secondary antibodies. Coverslips were mounted with Vectashield mounting medium with DAPI and analysed by epifluorescent microscopy.

### 3.16 Bright-field imaging

Cells were seeded on 35 mm plates and treated with the indicated siRNAs. After 24 hours cells were trypsinized, and split 1:4 or re-seeded in 12-well plates. 72h after siRNA transfection cells were fixed with PFA 4% in PBS. Random images were acquired with NIKON ECLIPSE TS100 inverted microscope. To determine the percentage of bi/multinucleated cells, ~400 cells per condition were evaluated and cells with two or more nuclei were counted. To determine the percentage of cells with membrane blebs the same images were analysed. Three independent experiments were performed; data are presented as mean ± sem. T-test was performed using excel (Microsoft Corporation).

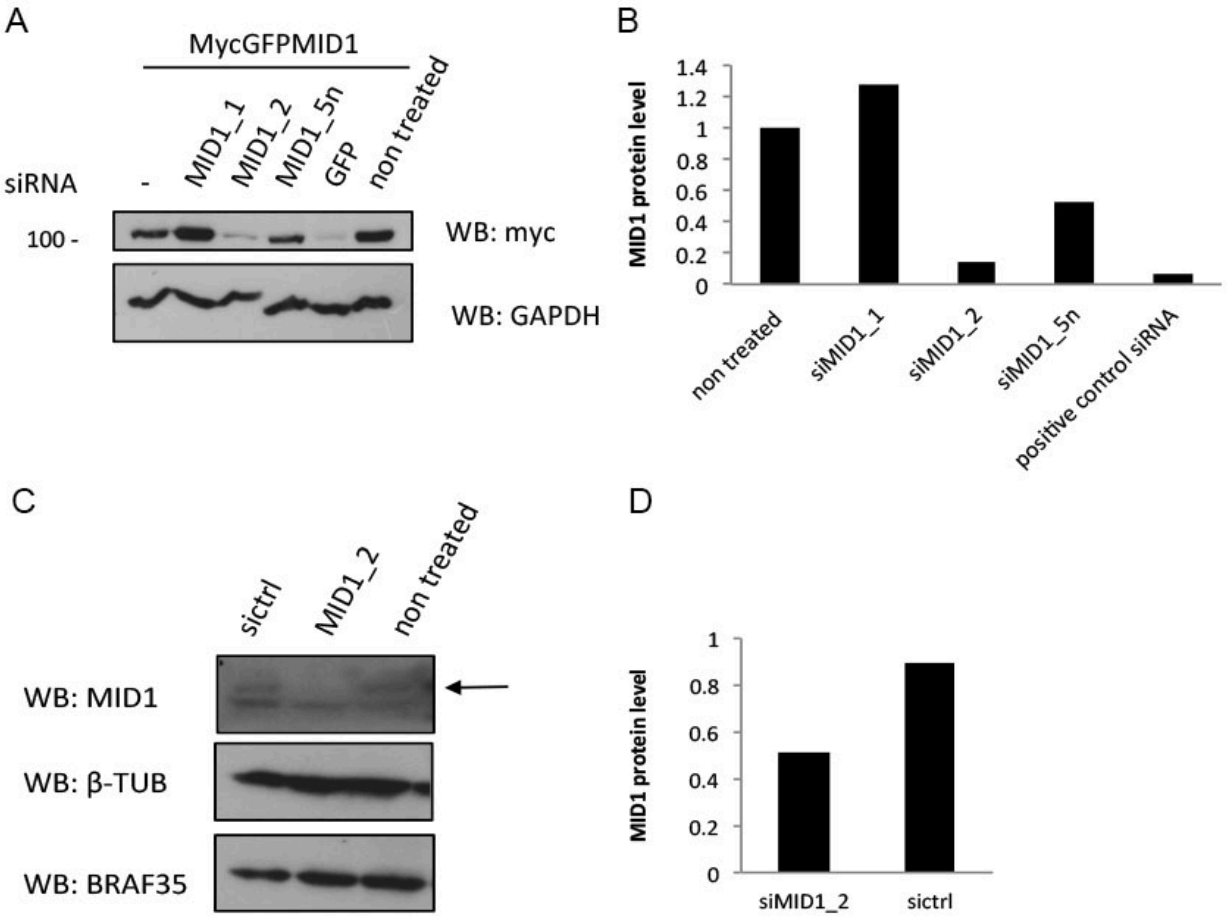


Figure 3.1: MID1 siRNAs. A) htert-RPE cells were transfected with three different MID1 siRNA (siMID1_1, siMID1_2, siMID1_5n) and a positive control GFP siRNA. After 24h, cells were transfected with MycGFP-MID1. Immunoblot analysis with anti-myc antibody and gapdh was performed to assess MycGFP-MID1 down-regulation. Quantification is shown in B). C) Immunoblot analysis of HeLa cells transfected with non-targeting siRNA (sictrl) or MID1 siRNA (siMID1_2) with the indicated antibodies. D) Quantification of MID1 level relative to tubulin after 40h of incubation of HeLa cells with MID1 (siMID1_2) or non-targeting (sictrl) siRNA.

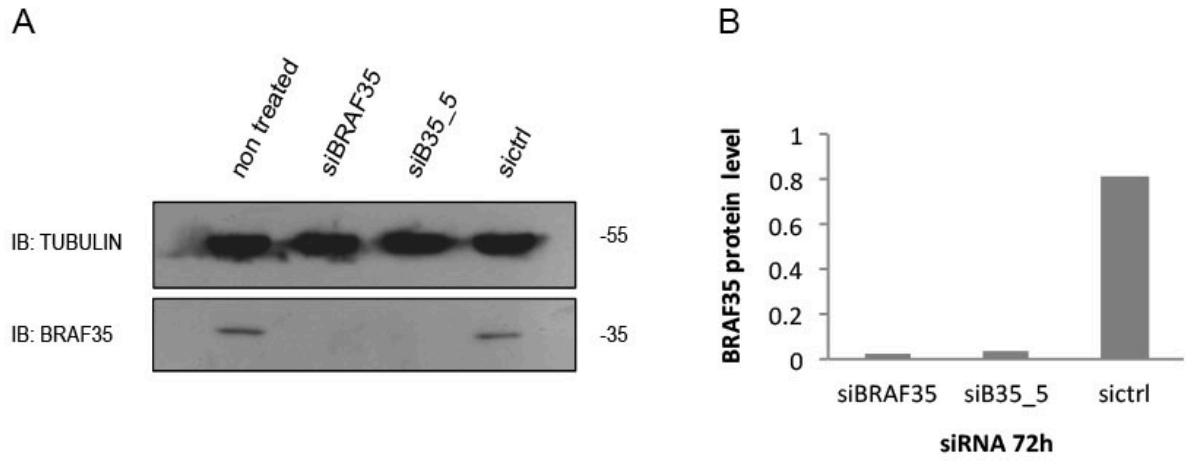


Figure 3.2: BRAF35 siRNAs. Representative immunoblot (A) and quantification (B) of BRAF35 level relative to tubulin after 72 hours of non-targeting (sictrl) and two different BRAF35 siRNAs (siBRAF35 and siB35_5) transfection in HeLa cells.

# 4. RESULTS

## 4.1 The BRCA2 associated factor 35 (BRAF35) is a new interaction partner of the TRIM protein MID1

The TRIM protein family member MID1 (also called TRIM18) is a microtubule-associated protein that is mutated in a developmental disorder, the X-linked Opitz G/BBB syndrome (Cainarca et al., 1999) (Quaderi et al., 1997). Moreover, MID1 is implicated in different processes, as T cell migration (Boding et al., 2014b) and axon development (Lu et al., 2013), or diseases like neurodegeneration (Krauss et al., 2013) and cancer (Demir et al., 2014). Nevertheless, the role of MID1 within the cell and the pathogenetic mechanisms that cause the diseases are still not completely unravelled. In order to discover new targets of its E3 ubiquitin activity during cellular processes we decided to perform a screening with an unbiased approach. We took advantage of the two-hybrid technique to identify new binding partners for MID1. A construct encompassing the coiled-coil (CC), the fibronectin-type 3 (FN3) and the PRY-SPRY domains of MID1 (ΔRBB) was used as a bait in the assay (figure 4.1A). The cDNA library obtained from mouse NIH3T3 cells was screened with the bait and, among others, 6 independent clones were found to contain inserts corresponding to the transcript of the HMG box-containing protein, HMG20B, also known as BRCA2 associated factor 35 (BRAF35) (Lee et al., 2002). BRAF35 has previously been reported as being part of two different large cellular complexes, the BRCA2-containing complex and the BRAF-histone deacetylase complex (BHC) (Hakimi et al., 2002) (Marmorstein et al., 2001). The shortest of the six clones identified, clone M37, contains the C-terminal coiled-coil region and represents the common minimum region for MID1 binding (figure 4.1B). To confirm the binding, an interaction-mating assay was performed. A BRAF35 reconstructed full length (FL) and a truncated construct that lacks the N-terminal P-rich region (M8) were tested for the interaction with MID1 full length or domain-deleted constructs consisting of CC domain only (CC), PRY-SPRY domain only (RFP) and Tripartite Motif only (RBCC) (figure 4.1A). As shown in the summarizing table in figure 4.1C, strong positive interaction between FL and M8 and MID1 CC was observed. The assay also showed a positive interaction between M8 and MID1 full length and RBCC but lack of binding between BRAF35 FL and M8 with MID1 RFP. A second interaction mating was performed combining M37 with MID1, RBCC, CC, RFP, ΔRBB, BB and ΔPRY-SPRY constructs-containing vectors. Interaction was observed in correspondence with M37 clone and MID1 RBCC, ΔRBB and CC (figure 4.1C).

Therefore, we discovered a new interaction between MID1 and BRAF35. The coiled-coil domain represented by the M37 clone resulted as the minimum region of BRAF35 required for MID1 binding. Moreover, the yeast data collected suggested that the CC domain of both proteins is necessary for the reciprocal binding.

A


B

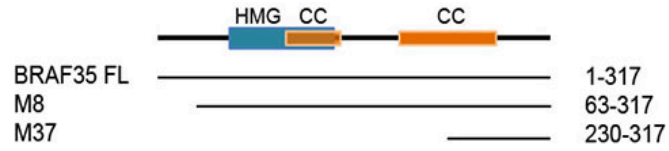


C

| | FL | M8 | M37 |
|---|---|---|---|
| MID1 | - | + | - |
| RBCC | + | + | + |
| CC | ++ | ++ | + |
| RFP | - | - | - |
| ΔRBB | | | + |
| BB | | | - |
| ΔPRYSPRY | | | - |

Figure 4.1: Identification of a novel MID1 partner, BRAF35. A) Schematic representation of MID1 full length and domain-deleted proteins. R, RING domain; B1, B-box1; B2, B-box2; CC, coiled-coil domain; FN3, Fibronectin type 3. B) Schematic representation of BRAF35 full length and truncated proteins. HMG, high-mobility group domain; CC, coiled-coil region. C) Summary of the interaction between BRAF35 and MID1 clones observed in the yeast mating assays.

### 4.1.1 MID1 interacts with BRAF35

In order to confirm the preliminary interaction data obtained from the yeast interaction-mating assay, an in vitro pull-down assay was performed. HeLa cell extracts were incubated with MBP-MID1 or with other two MBP-TRIM proteins and bound proteins were separated and analysed by immunoblotting using anti-BRAF35 antibody. As shown in the immunoblot in figure 4.2A, only MBP-MID1 interacts with endogenous BRAF35 present in the lysate. TRIM9 and TRIM27 were used as controls for the specificity of the MID1-BRAF35 interaction because they belong to the TRIM family. In particular, TRIM9 belongs to the same TRIM subfamily as MID1 (class C-I) whereas TRIM27 is part of a different TRIM subclass (C-IV) (Short and Cox, 2006). Moreover, MycGFP-tagged UBE2 enzymes (UBE2D1 and UBE2G2) were transiently overexpressed and correctly pulled-down as a positive control of the assay. Indeed, both MBP-MID1 and MBP-TRIM27 bind to their specific E2 enzyme UBED1 *in vitro* and, similarly, MBP-TRIM9 specifically recognizes its cognate UBEG2 protein (figure 4.2A) (Napolitano et al., 2011). Thus, the observation that MID1 binds BRAF35 obtained from the two-hybrid screening was validated *in vitro*. To further confirm that the interaction between MID1 and BRAF35 occurs *in vivo*, an immunoprecipitation (IP) assay was performed. MycGFP-tagged MID1 was overexpressed in HeLa cells and immunoprecipitated with anti-myc antibody. As for the MBP-pull down assay, MycGFP-TRIM9 and MycGFP-TRIM27 were used as controls for the specificity of the interaction. Immunoblot with anti-BRAF35 antibody revealed the exclusive co-IP of endogenous BRAF35 only with MID1 (figure 4.2B).

Therefore, these data support the findings that MID1 binds to BRAF35 *in vitro* and *in vivo*.

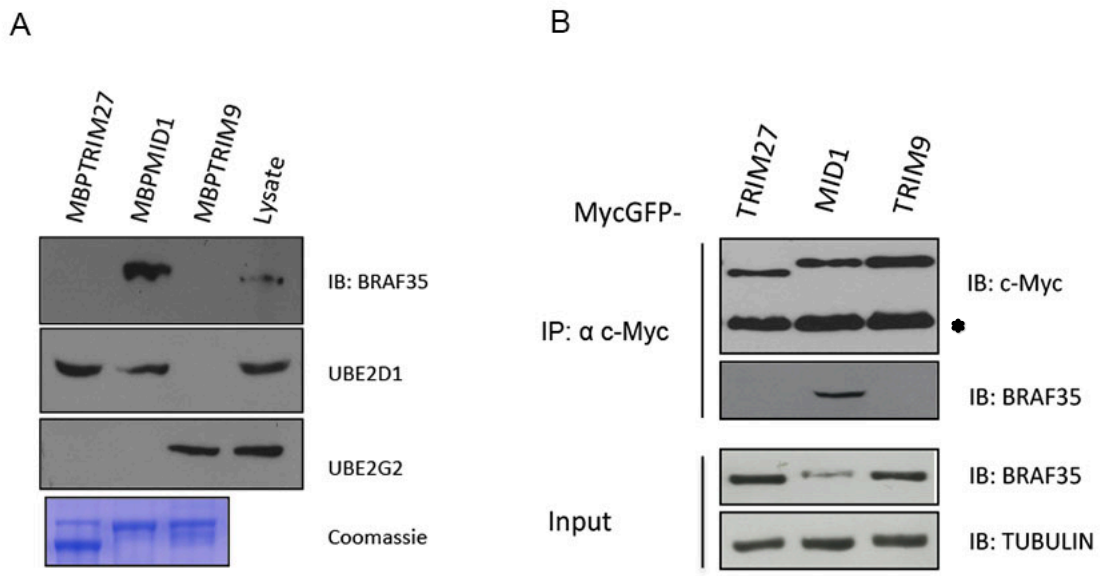


Figure 4.2: MID1 interacts *in vitro* and *in vivo* with BRAF35. A) Immunoblot of a pull-down assay of MBP-MID1 and endogenous BRAF35 from HeLa whole cell lysate. MBP-TRIM9, TRIM27 and their binding partners (UBE2D1 and UBE2G2) are used as controls. Bottom panel, Coomassie staining of the MBP-TRIM proteins employed. B) MycGFP-tagged MID1 but not TRIM9 and TRIM27 co-immunoprecipitate with endogenous BRAF35 in HeLa cell lysate. * indicates IgG heavy chain.

### 4.1.2 MID1 domains involved in the interaction

The data collected in the interaction mating screening indicated that the minimal region of BRAF35 required for the interaction with MID1 is comprised in its C-terminal coiled-coil domain. In order to define MID1 domain(s) implicated in the association with BRAF35, a series of MycGFP-tagged MID1 deleted mutants were used to perform a co-IP experiment in HEK293T cells (figure 4.1A and figure 4.3). In parallel with full-length MID1, the constructs lacking one or both B-boxes domain (ΔB2 and ΔB1B2, respectively), the RING and B-boxes (ΔRBB), the coiled-coil region (ΔCC), the COS and FN3 regions (Δtdn) or comprising only tripartite motif RING/B-boxes/coiled-coil (RBCC) or the PRYSPRY domain (RFP) were co-overexpressed with FLAG-BRAF35. Anti-FLAG antibody was used to immunoprecipitate BRAF35 and immunoblot with anti-myc was performed to reveal MycGFP-tagged proteins. As shown in figure 4.3, all constructs but ΔCC and RFP are retrieved in the IP, indicating that the coiled-coil region of MID1 mediates the interaction with BRAF35.

Taking the above results together we conclude that BRAF35 binds MID1 *in vitro* and *in vivo*, and their respective coiled-coil domain mediates the interaction.

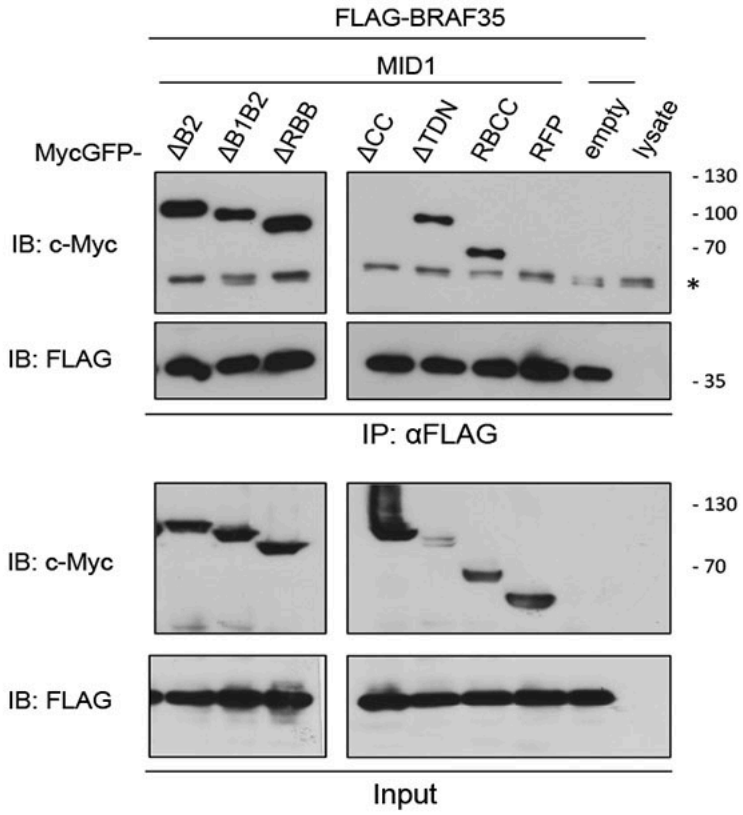


Figure 4.3: The coiled-coil domain of MID1 mediates the interaction with BRAF35. HEK293T cells overexpressing FLAG-BRAF35 and the MycGFP-tagged MID1 deleted mutants indicated on top were subjected to immunoprecipitation using FLAGM2 antibody. As control, the IP was also performed with non-transfected (lysate) and pCDNA3 vector (empty) transfected HEK293T cell lysates. The bottom panel shows the input extracts. Immunoblotting analysis with the indicated antibodies showing that the coiled-coil domain of MID1 is necessary for the interaction between the two proteins. * indicates IgG heavy chain.

## 4.2 BRAF35 as a substrate for MID1 activity

Given the biochemical function of TRIM proteins and of MID1, the binding between the TRIM protein MID1 and BRAF35 may reflect an E3 ligase-substrate relationship. Therefore, to start investigating this hypothesis we decided to follow up on a possible regulation of BRAF35 by the ubiquitin-proteasome system.

### 4.2.1 MID1 regulates BRAF35 level

To investigate whether BRAF35 is subjected to regulated degradation, we treated HeLa cells with cycloheximide (CHX) for increasing time periods and evaluated BRAF35 protein level after immunoblotting with anti-BRAF35 and anti-tubulin antibodies. Initial experiments on cycling cells indicated that BRAF35 is a relatively unstable protein. In fact, our experiments showed a reduction of BRAF35 protein level after 2 hours of CHX treatment, suggesting a regulated degradation mechanism (figure 4.4A). Analogous experiments were performed in HEK293T cells that show the same trend of degradation although the protein seems slightly more stable than in HeLa cells, with a half-life of about 4 hours (figure 4.4B). Thus, taking into account the small difference concerning BRAF35 half-life between HeLa and HEK293T cells, subsequent experiments were performed in both cell lines. To address if BRAF35 undergoes specific degradation by the ubiquitin-proteasome system, cells were treated for four hours with the proteasome inhibitor MG132. As shown in figure 4.4C, simultaneous block of translation elongation and proteasomal degradation (CHX + MG132) led to a rescue of BRAF35 protein level. BRAF35 level tends to further increase when proteasome function alone is inhibited (Figure 4.4C and 4.4D).

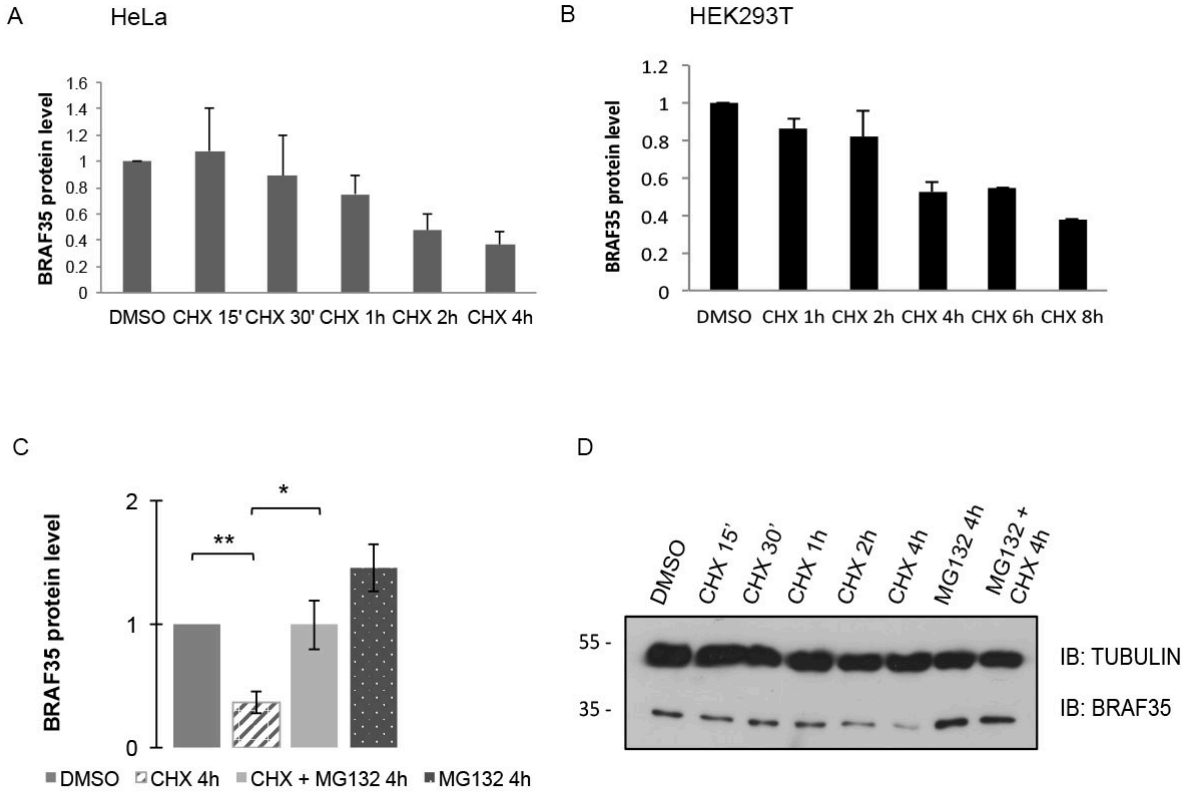


Figure 4.4: BRAF35 undergoes proteasomal degradation in HeLa and HEK293T cells. A) Cycling HeLa cells were treated with cycloheximide (CHX) for the time indicated and then lysates were analysed by immunoblotting. Mean intensity of BRAF35 levels of four different independent experiments were quantified relative to tubulin levels. BRAF35 level of dimethylsulphoxide (DMSO) treated cells was set as 1 (bars= sem). B) Cycling HEK293T cells were incubated for the indicated periods with CHX and lysed. Immunoblot was performed with BRAF35 and tubulin antibodies and mean intensity of BRAF35 levels of two different independent experiments were quantified relative to tubulin. Results were plotted taking BRAF35 levels in DMSO treated cells as 1 (bars=sem). C) Exponentially growing HeLa cells were mock-treated (DMSO) or incubated with CHX or the proteasome inhibitor MG132 or with the combination of the two drugs. Samples were collected after 4 hours and lysates were analyses by immunoblotting. BRAF35 levels relative to tubulin levels were quantified with imageJ software. Results from three independent experiments were plotted considering BRAF35 levels of mock-treated cells as 1 (bars = sem; t-test: *$p<0.05$ and **$p<0.001$). D) Representative immunoblot image for CHX–chase and MG132 treatment experiments described in A and C. Used antibodies are indicated.

To address whether MID1 contributes to BRAF35 degradation, we treated HeLa cells with either non-targeting or MID1 specific short interfering RNA (siRNA) for 40 hours. Levels of MID1 silencing were evaluated by immunoblot with specific anti-MID1 antibody (figure 3.1 in the Material and Methods section). As shown in the immunoblot quantification depicted in figure 4.5A, MID1 depletion results in an increase of BRAF35 protein level with respect to mock-treated (sictrl) cells. Moreover, treatment with CHX upon 40h of MID1 silencing shows a delayed trend of degradation particularly evident in the range of 1 to 4 hours with respect to control silencing (figure 4.5B).

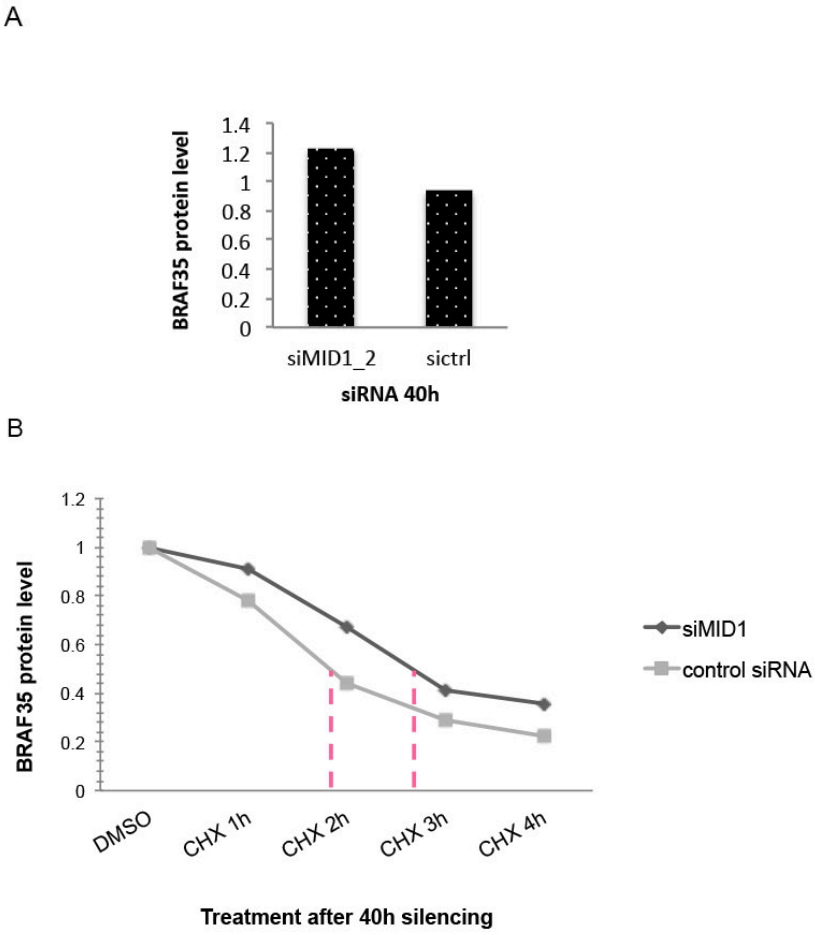


Figure 4.5: MID1 influences BRAF35 stability. A) HeLa cells were treated with either non-targeting (sictrl) or MID1 siRNA (siMID1_2); after 40 hours lysates were prepared and subjected to immunoblot analysis with anti-BRAF35 and anti-tubulin antibodies. Quantification of BRAF35 level relative to tubulin is shown. Protein level in non-treated cells was set as 1. B) HeLa cells were transfected with non-targeting (sictrl) or MID1 siRNA (siMID1_2) for 40 hours and then treated with DMSO or CHX for the indicated period. Samples were collected and immunoblot was performed to quantify BRAF35 levels relative to tubulin. Results were plotted taking as 1 BRAF35 levels of mock-treated (DMSO) cells in both non-targeting and MID1 siRNA lysates.

The results depicted in figure 4.5A and 4.5B suggest an involvement of MID1 in regulating BRAF35 protein level. To better understand the consequences of this regulated degradation we decided to look at BRAF35 level in different subcellular compartments. Data from the literature indicate BRAF35 as a predominantly nuclear protein associated with nuclear matrix and avoiding nucleoli. BRAF35 in fact contains a nuclear localization signal (NLS) in its N-terminus (Marmorstein et al., 2001) (Lee et al., 2002). Our immunofluorescence (IF) experiments performed in HeLa either overexpressing HA-tagged BRAF35 or detecting endogenous BRAF35 using a specific antibody confirmed its localization in the nucleus (figure 4.6A) but also showed the presence of a cytoplasmic fraction of BRAF35 in some cells, forming aggregates (figure 4.6B). Occasionally, BRAF35 was expressed almost only in the cytoplasm even assuming a filamentous staining (Figure 4.6C). Ectopically expressed BRAF35 showed a similar pattern of expression in Cos-7 cells: the protein was mainly present in the nucleus but also appeared concentrated in the perinuclear region and distributed in the cytoplasm (figure 4.6D).

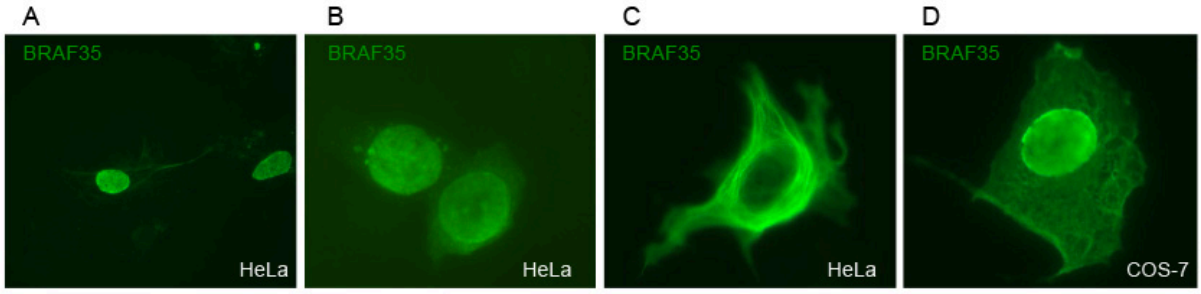


Figure 4.6: BRAF35 subcellular localization. A-C) HeLa cells Immunofluorescence experiments showing HA-BRAF35 localization in the nucleus (A), both in the nucleus and forming aggregates in the cytoplasm (B), with a filamentous staining in the cytoplasm. D) HA-BRAF35 localization in the nucleus and cytoplasm of COS-7 cells

MID1 is usually associated with microtubules but when dephosphorylated it detaches from them and it is observed in cytoplasmic bodies (Liu et al., 2001). Figure 4.7 shows an example of this dynamic distribution of MycGFP-MID1 in transfected cells with the co-localization with tubulin (red) and displaying a punctate staining, indicating microtubules detachment.

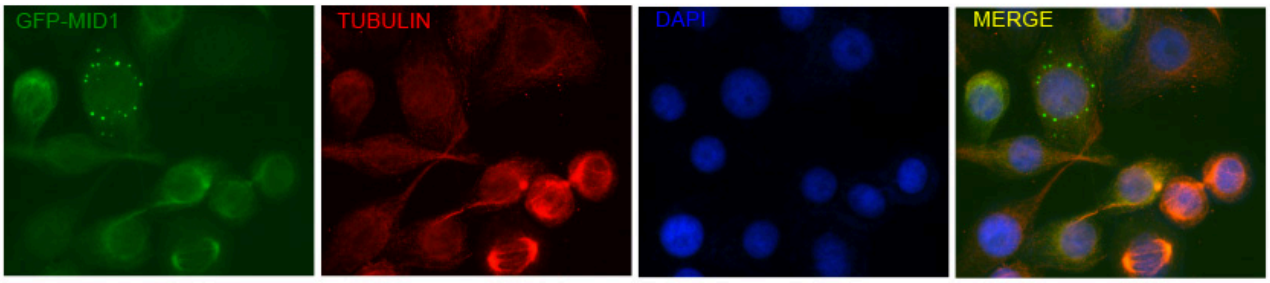


Figure 4.7: MID1 subcellular localization. MycGFPMID1 (green) co-localizes with the microtubules of the mitotic spindle and the midbody region of dividing HeLa cells. Green dots indicate MID1 detachment from microtubules in an interphase cell. Tubulin antibody and DAPI were used to stain microtubules (red) and nuclei (blue), respectively.

To add information on MID1/BRAF35 interaction we decided to analyse reciprocal localization of the two proteins in HeLa and Cos-7 cells. Consistently with previous studies (Cainarca et al., 1999) (Marmorstein et al., 2001) and our IF experiments (figure 4.6 and 4.7), we observed the typical pattern of microtubular and nuclear distribution for MID1 and BRAF35, respectively (figure 4.8A). In the largest fraction of cells analysed the two proteins maintained a distinct localization between cell compartments (figure 4.8A). An interesting observation was that when BRAF35 was concentrated at the periphery of the nucleus, likely near the nuclear envelope or the perinuclear region, it partially colocalized with MID1 (figure 4.8B). The colocalization became more evident in cells where BRAF35 showed a predominantly cytoplasmic staining and MID1 detached from microtubules forming cytoplasmic bodies where the two proteins co-localized (4.8C). An identical pattern of colocalization was noticed in Cos-7 cells. Confocal images of IF experiments confirmed the co-localization between the two proteins in the perinuclear region, stronger when BRAF35 diffuses in the cytoplasm and when MID1 loses its microtubular localization. In addition, the two proteins form aggregates in the cytoplasm (figure 4.9).

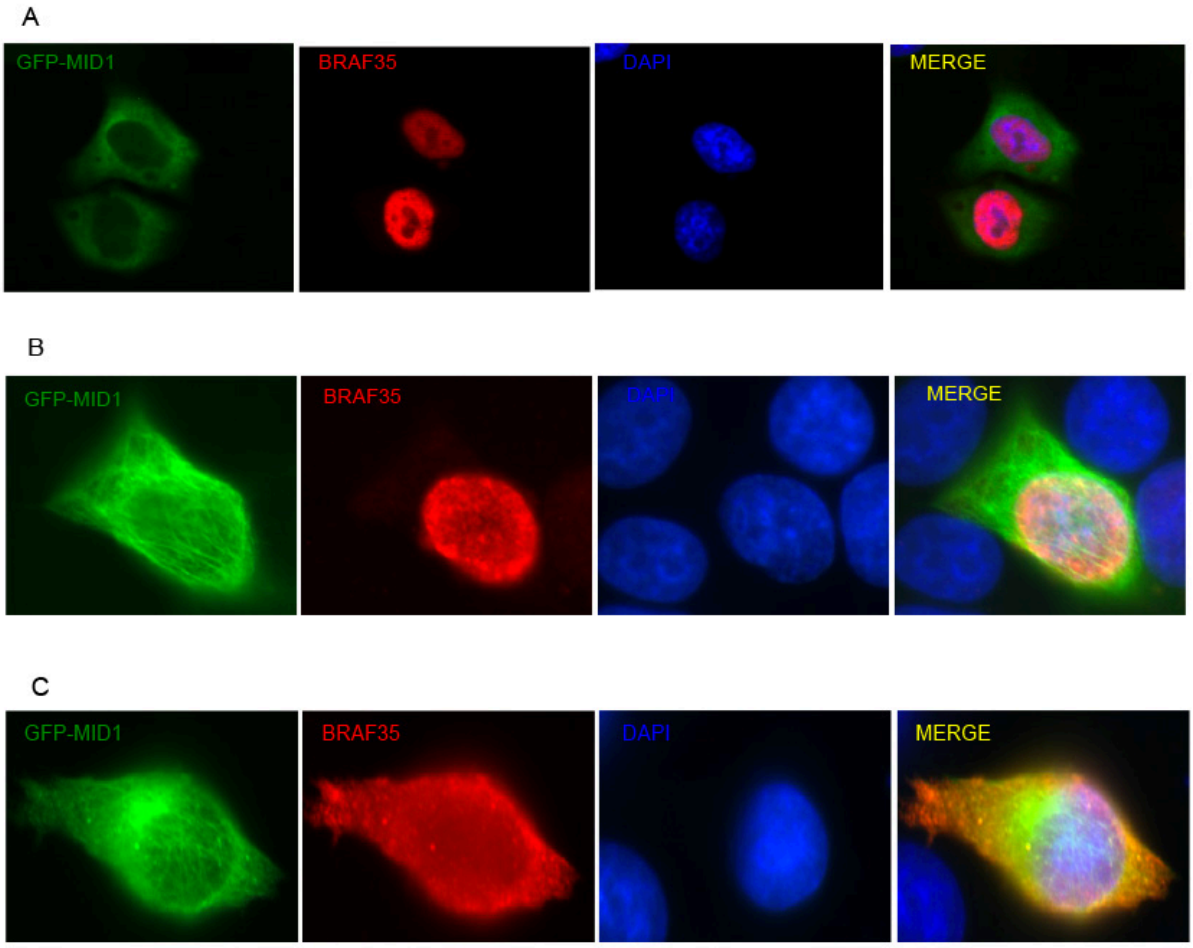


Figure 4.8: MID1 and BRAF35 partially co-localize during interphase in HeLa cells. A) IF experiments showing nuclear and cytoplasmic localization of HA-BRAF35 (red) and MycGFP-MID1 (green), respectively, in HeLa cells. B) Ectopically expressed BRAF35 stained with HA antibody (red) localizes in the nucleus (blue). Merged images show a partial overlap with MycGFP-MID1 (green) in the perinuclear region of HeLa cells. C) Immunofluorescence experiment in HeLa cells showing co-localization of HA-BRAF35 (red) and MycGFP-MID1 (green) in the cytoplasm.

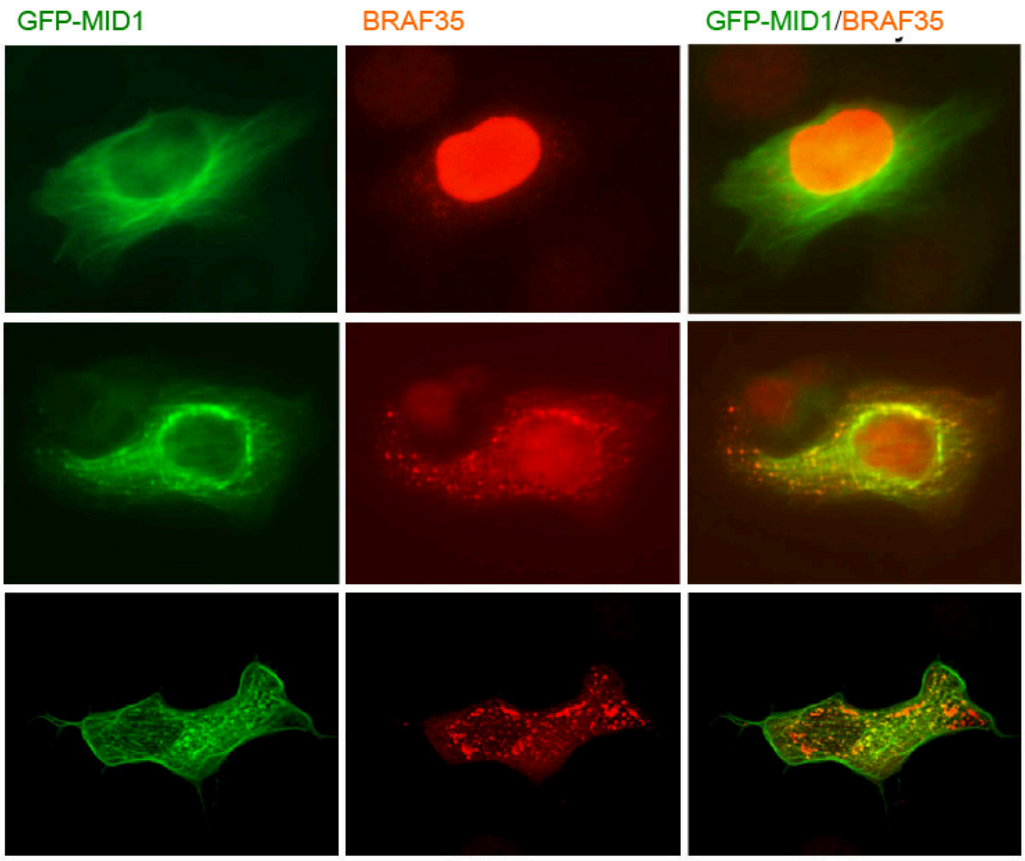


Figure 4.9: MID1 and BRAF35 partially co-localize during interphase in COS-7 cells. Immunofluorescence experiment showing co-localization of overexpressed MycGFP-MID1 and endogenous BRAF35 (red) in the cytoplasm and perinuclear region of interphase COS-7 cells.

Therefore we asked if the influence of MID1 exerted on the regulation of BRAF35 abundance was limited to a precise subcellular fraction of the protein.

For this purpose nuclear and cytoplasmic extracts from HeLa cells treated with non-targeting or MID1 siRNA were prepared and subsequently analysed by immunoblot to quantify BRAF35 protein amounts in the different cellular fractions. In order to verify the correct fraction separation, anti-nuclear matrix protein p84 and anti-tubulin antibodies were used as nuclear and cytoplasmic markers, respectively (figure 4.10A). As expected, most BRAF35 was detected in the nuclear fraction, whereas a limited amount was found in the cytoplasmic fraction of mock-treated cells (sictrl) (figure 4.10A). Analysis of whole cell lysates processed in parallel with subcellular fractions confirmed the increase of BRAF35 total protein level after MID1 depletion. Interestingly, results from nuclear and cytoplasmic fractions protein quantification highlighted a predominant accumulation of BRAF35 in the cytoplasm of MID1

depleted cells compared to the mock-treated sample. The increase was not comparable to the slight decrease in the nuclear fraction indicating that this increase in the cytoplasm was not, or not predominantly, the result of BRAF35 mislocalization (figure 4.10B). All these observations suggest a precise role for MID1 in regulating BRAF35 level in the cytoplasmic compartment.

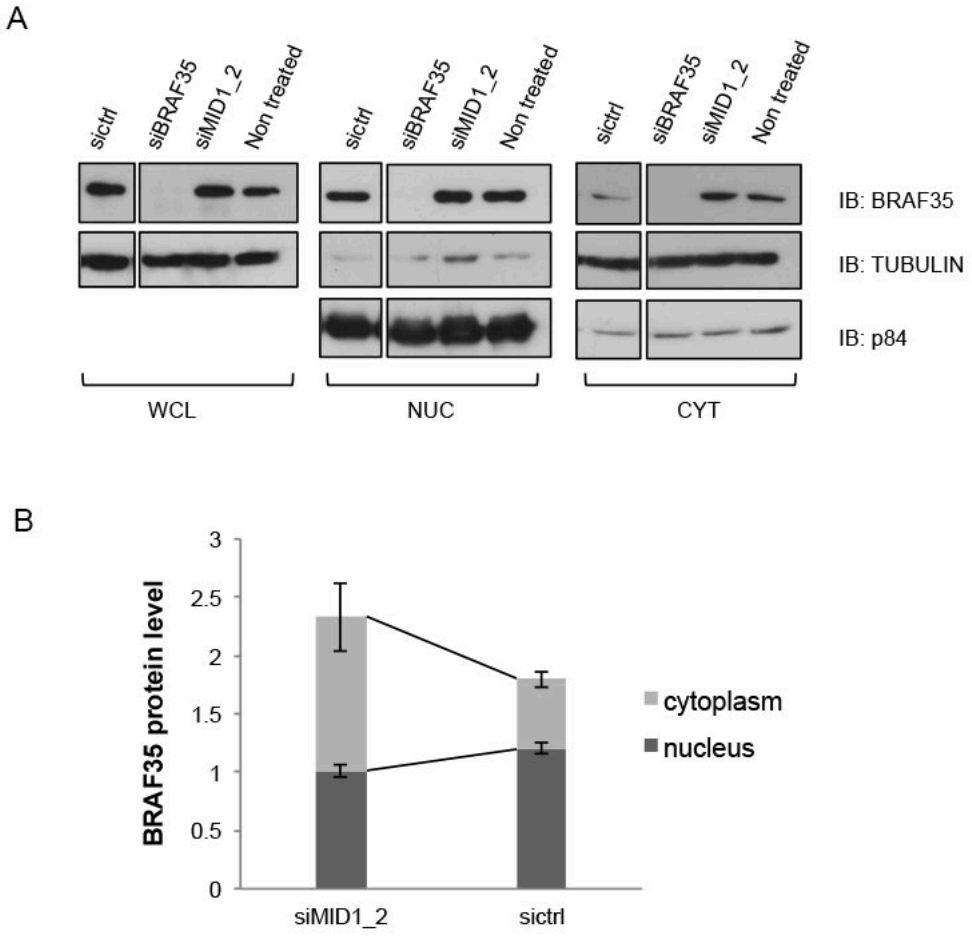


Figure 4.10: MID1 regulates BRAF35 level in the cytoplasm. A) Representative immunoblot analysis of whole cell lysate (WCL), nuclear (NUC) and cytoplasmic (CYT) extracts prepared from HeLa cells treated for 72h with non-targeting (sictrl), BRAF35 (siBRAF35) or MID1 (siMID1_2) siRNA. Samples were analysed by immunoblot with BRAF35, tubulin and nuclear matrix (p84) antibodies. Blots were cropped to remove two lanes corresponding to samples that were not included in this work. B) BRAF35 levels from nucleus and cytoplasmic fractions were quantified relative to the mean of three bands in the ponceau staining. Results from three independent experiments were plotted (bars= sem).

To further investigate if MID1 and its E3 ligase activity are responsible for BRAF35 level regulation we overexpressed MycGFP-tagged MID1 or an E3 ligase incompetent mutant (ΔRING) in HeLa cells and analysed BRAF35 endogenous level by immunoblot (figure 4.11A). As shown in the quantification plot depicted in figure 4.11B, MID1 overexpression causes a slight decrease in BRAF35 level respect to the empty vector. Interestingly, overexpression of the E3 ligase incompetent mutant leads to an accumulation of BRAF35, likely due to a dominant negative effect on the endogenous MID1.

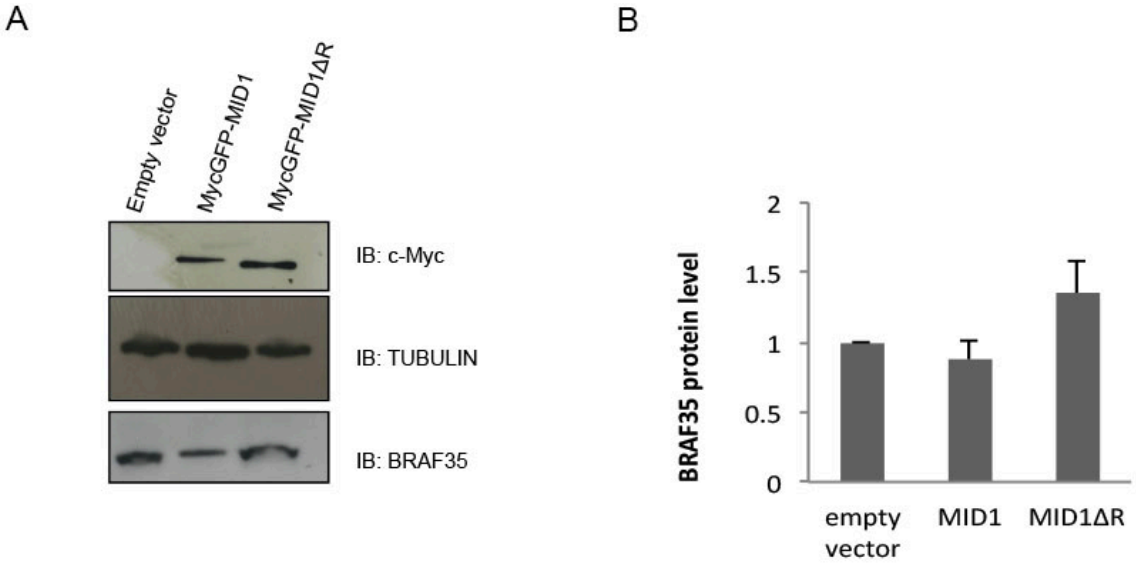


Figure 4.11: MID1 overexpression leads to a decrease in BRAF35 level. A) Representative immunoblot of HeLa cells transfected with MycGFP-tagged MID1 or the E3 ligase incompetent mutant (ΔRING) for 48h and then lysed and analysed by immunoblotting with the indicated antibodies. B) BRAF35 levels were measured relative to tubulin and data from two independents experiments were plotted considering BRAF35 abundance in empty-vector transfected cells as 1 (bars= sem).

In conclusion the results obtained in the above-described experiments suggest a specific role for MID1 in regulating BRAF35 abundance, especially in the cytoplasm.

### 4.2.2 MID1 regulates BRAF35 post-translational modification

It is likely that BRAF35 is degraded via the ubiquitin/proteasome system and that MID1 is involved in this pathway as suggested by the experiments described so far. At this point, we asked if BRAF35 could be a new target for MID1-dependent ubiquitination. Thus we decided to co-overexpress HA-tagged BRAF35 with MycGFP-MID1 or the ΔRING mutant (E3 ligase incompetent) in HEK293T cells and to block the proteasome and look for BRAF35 shift in SDS-PAGE migration indicating post-translational modifications (PTMs). Samples were prepared lysing cells in denaturing conditions, in order to limit reversing of PTMs. Then, immunoblotting with anti-HA antibody was performed to reveal BRAF35 signal. Interestingly, a series of high molecular weight (HMW) bands appeared, with dimensions compatible with ubiquitination (figure 4.12A). The bands were more evident in samples treated with MG132 confirming that that BRAF35 PTM is linked to proteasome function. We also noticed that the pattern of bands was different between samples: the intensity of the first upper band above BRAF35 (~ 45 kDa) was stronger where MID1 was overexpressed with respect to empty vector transfected cells. Moreover, expression of the ΔRING mutant resulted in a decrease of all HMW bands intensity (figure 4.12A). To further understand the connection between BRAF35 modification and MID1 activity we repeated the assay using both full-length and a truncated mutant of BRAF35 lacking the C-terminal region containing the coiled-coil domain (BRAF35 C1) (figure 4.12B). This mutant should not be able to bind MID1 (as indicated by the interaction mating assay). As demonstrated in the immunoblot in figure 4.12 C, the pattern of high molecular weight bands present on full length BRAF35 was absent on the BRAF35 C1 mutant. This data suggested that physical interaction between BRAF35 and MID1 was required in order for PTMs to occur. Alternatively, these results may indicate that lysines targeted by PTM are localized in BRAF35 C-terminus, missing in BRAF35 C1 mutant.

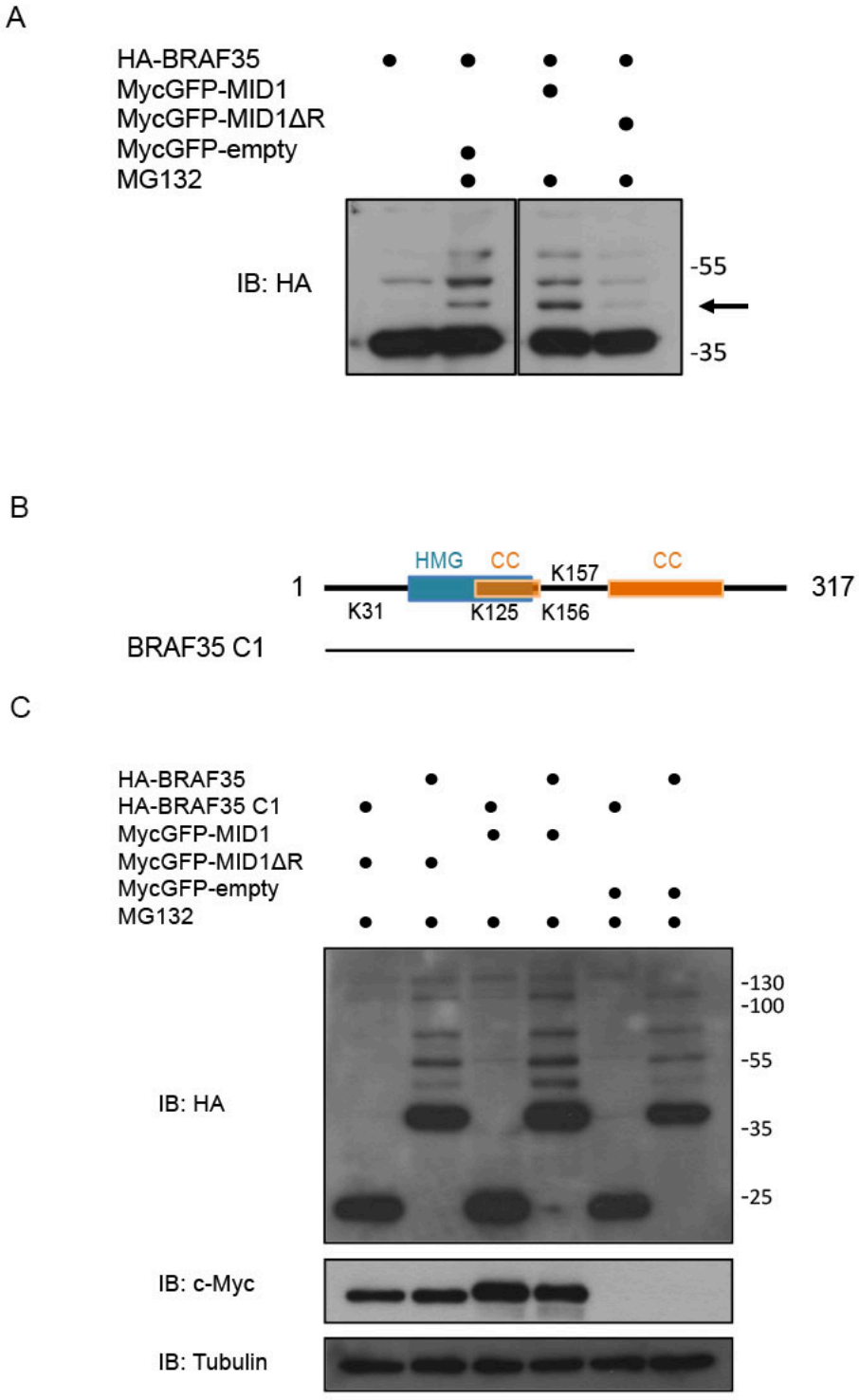


Figure 4.12: BRAF35 is subjected to MID1-dependent post-translational modification. A) HEK293T cells were transfected with HA-BRAF35 alone or together with MycGFP-tagged empty vector, MID1 or the E3 ligase incompetent mutant (ΔRING) for 48h. Where indicated cells were treated with MG132 for two hours and lysates were prepared under denaturing conditions. Immunoblot with HA antibody was performed to reveal BRAF35 high molecular weight bands alteration. B) Schematic representation of BRAF35 C1 mutant. Position of lysine 31, 125, 156 and 157 on the full-length protein is indicated. C) Immunoblot analysis with the indicated antibodies performed after a 48h

overexpression of MycGFP-tagged empty vector, MID1 or the E3 ligase incompetent mutant (ΔRING) together with HA-BRAF35 or a Δcoiled-coil mutant of BRAF35 (BRAF35 C1) using the conditions as in A. Treatment with the proteasome inhibitor MG132 for two hours is indicated.

### 4.2.3 BRAF35 is a substrate for MID1-dependent ubiquitination

In order to further confirm if BRAF35 is a target for MID1-dependent ubiquitination, in vivo ubiquitination assays were performed. HEK293T cells were transfected with FLAG-BRAF35 and HA-ubiquitin in the presence of MycGFP-tagged full-length MID1 or the E3 ligase incompetent mutants ΔRING and ΔRING-Bboxes (ΔRBB). MycGFP-empty vector or no vectors were used as negative controls for the assay (figure 4.13A and B). After incubation with MG132, cells were lysed in denaturing conditions to preserve ubiquitin chains and disrupt any non-covalent protein interactions and then immunoprecipitation was performed. All ubiquitinated proteins were immunoprecipitated with anti-HA affinity matrix and BRAF35 presence was revealed with immunoblot analysis with anti-BRAF35 antibody. Total amount of ubiquitinated proteins and inputs were checked with anti-HA, anti-myc and anti-FLAG antibodies (figure 4.13A). The faint smear present in empty vector-transfected cells indicated the basal level of BRAF35 ubiquitination. Overexpression of MID1 significantly enhanced BRAF35 ubiquitination, as expected. BRAF35 was mainly observed in the mono-ubiquitinated form, but a smear corresponding to poly-ubiquitinated BRAF35 was also detected. The intensity of the smear gradually decreased when domain deleted MID1 ΔRING and mainly ΔRBB mutants were overexpressed, indicating that the E3 ligase activity of MID1 is required for BRAF35 ubiquitination (figure 4.13A). An analogous *in vivo* ubiquitination experiment was also performed immunoprecipitating BRAF35 with anti-FLAG antibody. Results obtained were the same as previous described: a prominent mono-ubiquitination of BRAF35 upon overexpression of MID1 was observed on immunoblot with anti-HA together with a HMW smear corresponding to poly-ubiquitinated BRAF35. The pattern of poly-ubiquitinated form of BRAF35 was reduced in presence of MID1 ΔRING and ΔRBB mutants (figure 4.13B). All these observations indicate that BRAF35 is a target for MID1-dependent ubiquitination and that its E3 ligase activity is necessary but not exclusive for poly-ubiquitin chain linkage.

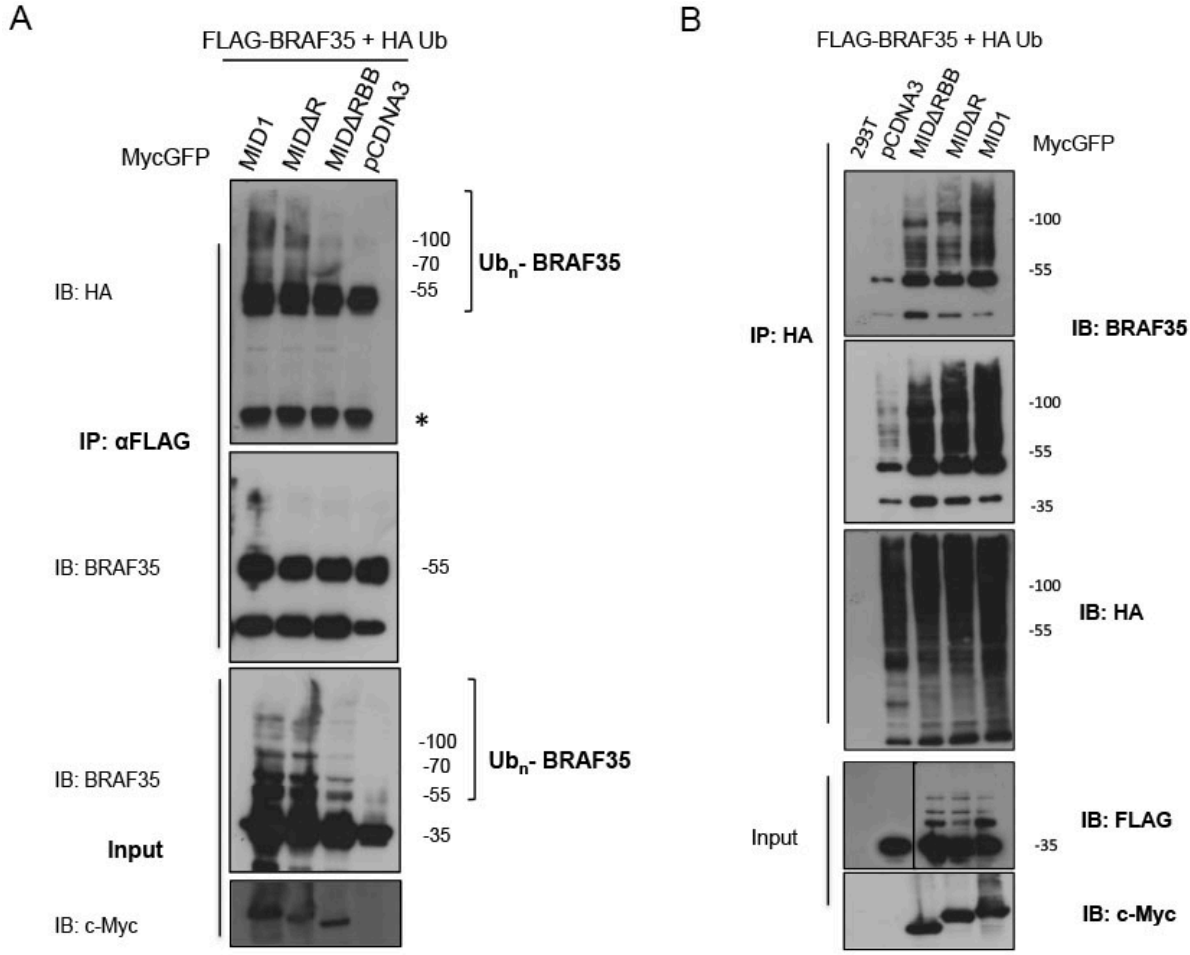


Figure 4.13: MID1 promotes BRAF35 ubiquitination. A and B) Immunoblots of BRAF35 in vivo ubiquitination after MycGFP-MID1 or domain-deleted E3 incompetent MID1 mutants (ΔRING and ΔRBB) overexpression in HEK293T cells. Cells were incubated with MG132 for two hours and lysed in denaturing conditions. After BRAF35 (A) or HA-ubiquitin (B) immunoprecipitation, the specific pattern of BRAF35 ubiquitination was revealed with the indicated antibodies. * indicates Ig light chain.

### 4.2.4 MID1-dependent BRAF35 ubiquitination is unrelated to sumoylation or iBRAF binding

BRAF35 is modified by SUMO in order to exert its antineurogenic function in the context of the LSD1-coREST complex. It has been also demonstrated that BRAF35 heterodimerizes with iBRAF, a paralogue of BRAF35, and that the interaction is mediated by their respective coiled-coil regions. Formation of iBRAF-BRAF35 heterodimer affects BRAF35 sumoylation in a negative manner, impairing its neuronal repressor activity (Ceballos-Chavez et al., 2012).

The experiment described in figure 4.12C not only indicated that BRAF35-MID1 heterodimerization was required for BRAF35 modification, but also suggested that MID1 is not implicated in BRAF35 sumoylation. The BRAF35 C1 mutant in fact still contains the four lysines (K31, K125, K156, K157 see figure 4.12B) that are modified by sumoylation. We reasoned that BRAF35 C1 was not only incapable to bind MID1, but also unable to heterodimeryze with the BRAF35 paralogue iBRAF *in vivo*. Therefore we wanted to test if iBRAF-inhibiting activity on BRAF35 sumoylation was necessary for MID1 to promote BRAF35 ubiquitination. To this aim, FLAG-BRAF35 and MycGFP-MID1 were co-overexpressed in HEK293T cells together with HA-iBRAF or HA-tagged empty vector (HA-empty). Then cells were incubated with DMSO or MG132 and lysed in denaturing conditions. Immunoblot with anti-FLAG antibody revealed the presence of BRAF35 high molecular weight band that were observed in previous experiments upon MID1 overexpression. This indicates that iBRAF activity and/or binding were not interfering with MID1-dependent BRAF35 PTM, as the pattern of the bands was unchanged (4.14A). An alternative explanation of this result could also be that MID1 overexpression impairs BRAF35-iBRAF heterodimerization, preventing sumoylation inhibition. To test this hypothesis we performed a co-IP experiment on ectopic expressed FLAG-BRAF35 and HA-iBRAF in the presence of increasing amounts of MycGFP-MID1. Immunoblots with both anti-HA and anti-FLAG antibodies were performed on immunoprecipitated FLAG-BRAF35 and HA-iBRAF proteins, respectively, revealing the presence of BRAF35 and iBRAF as complex (figure 4.14B).

Taken together, these results indicate that MID1 influences BRAF35 in a post-translational manner compatible with ubiquitination and suggest that BRAF35-iBRAF heterodimerization is still occurring and iBRAF presence does not inhibit MID1 activity.

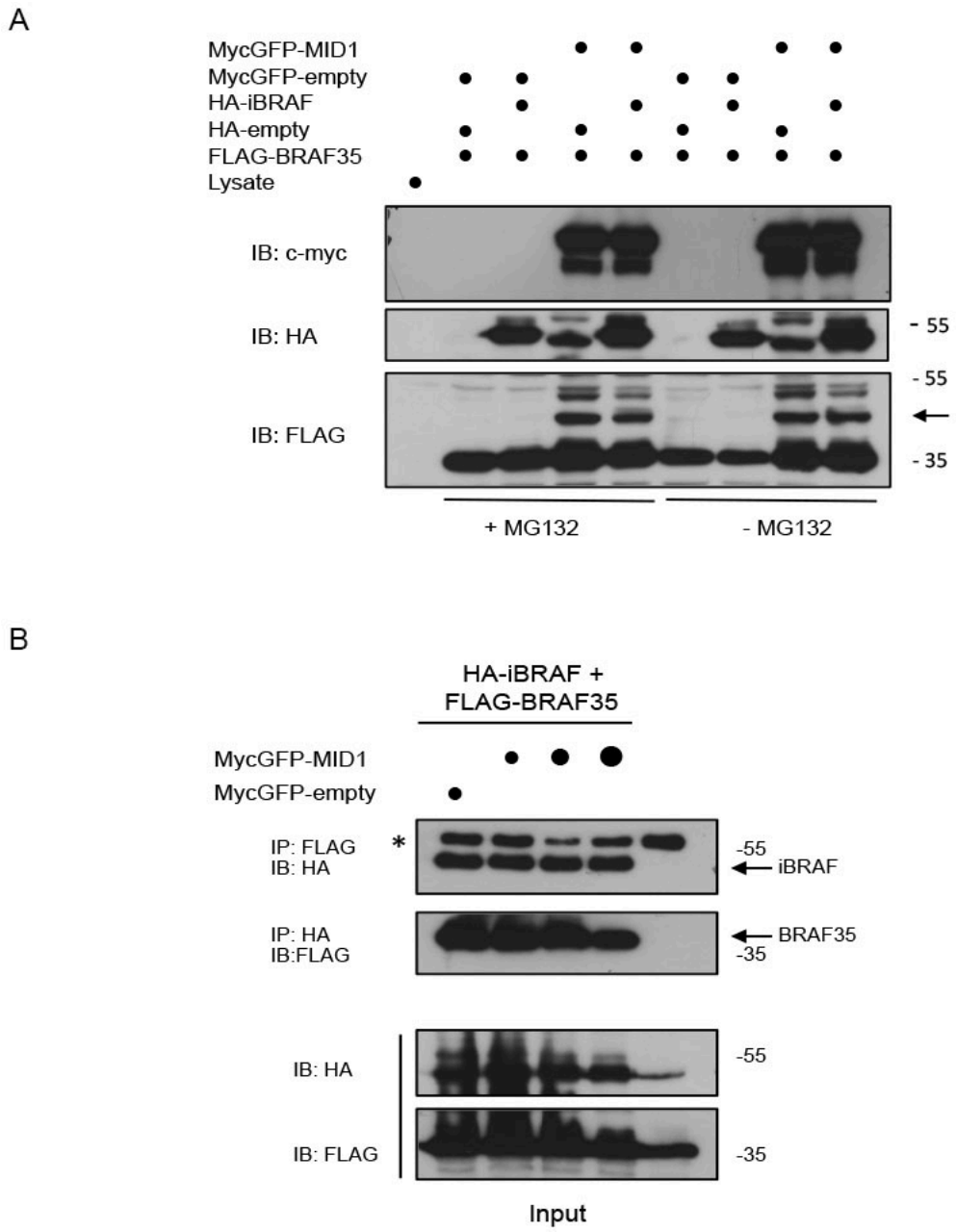


Figure 4.14: iBRAF does not interfere with MID1-dependent BRAF35 modification. A) Immunoblot analysis showing co-overexpression of MycGFP-MID1 and HA-iBRAF in the presence or absence of the proteasome inhibitor (MG132). Lysates were prepared under denaturing conditions and analysed with the indicated antibodies. Arrow indicates BRAF35 high molecular weight band considered as MID1-dependent. B) HA-iBRAF and FLAG-BRAF35 were co-overexpressed together with MycGFP-empty vector or increasing amounts of MycGFP-MID1 in HEK293T. Lysates were prepared and split to perform IP with HA-matrix and anti-FLAG antibody. The presence of co-immunoprecipitated BRAF35 and iBRAF in the reciprocal IP was analysed with HA and FLAG antibodies. * indicates Ig heavy chain.

We decided to further investigate if BRAF35 sumoylation is related in some way to its ubiquitination in order to deeply elucidate the interplay between the two PTMs and, moreover, to start mapping the lysines that are modified in the protein. We performed an *in vivo* ubiquitination assay overexpressing in HEK293T cells not only full-length but also a non-sumoylatable BRAF35 mutant in which the SUMO-targeted lysines at position 31, 125, 156 and 157 (figure 4.12B) are substituted with an arginine residue (BRAF35 4KR) (Ceballos-Chavez et al., 2012). HA-Ub and MycGFP-MID1 were co-transfected and treatment with MG132 was performed before denaturing lysis. Like in previous experiments, several MID1 mutants were employed: ΔRING, ΔRBB and RBCC-only mutants were expresses alternatively to full length MID1. Immunoblot analysis with anti-FLAG on immunoprecipitated HA-ubiquitin, i.e. all the ubiquitinated proteins, proved that both BRAF35 and BRAF35 4KR are targeted for MID1-dependent ubiquitination (figure 4.15). Again, the mono-ubiquitinated form of BRAF35 was the most abundant, although a series of higher bands on the immunoblot indicated the existence of multi mono- and/or poly-ubiquitinated forms of both BRAF35 and BRAF35 4KR. The pattern between BRAF35 and BRAF35 4KR ubiquitination upon overexpression of MID1 mutants was comparable: even though all of them could bind BRAF35 (or BRAF35 4KR, data not shown), the absence of one or more domain in MID1 protein impaired the correct linkage of ubiquitin chains on BRAF35 (figure 4.15). Altogether these data not only confirm that sumoylation of BRAF35 is independent from MID1-related ubiquitination, but also suggest that K31, K125 K156 and K157 are not the main target for ubiquitination.

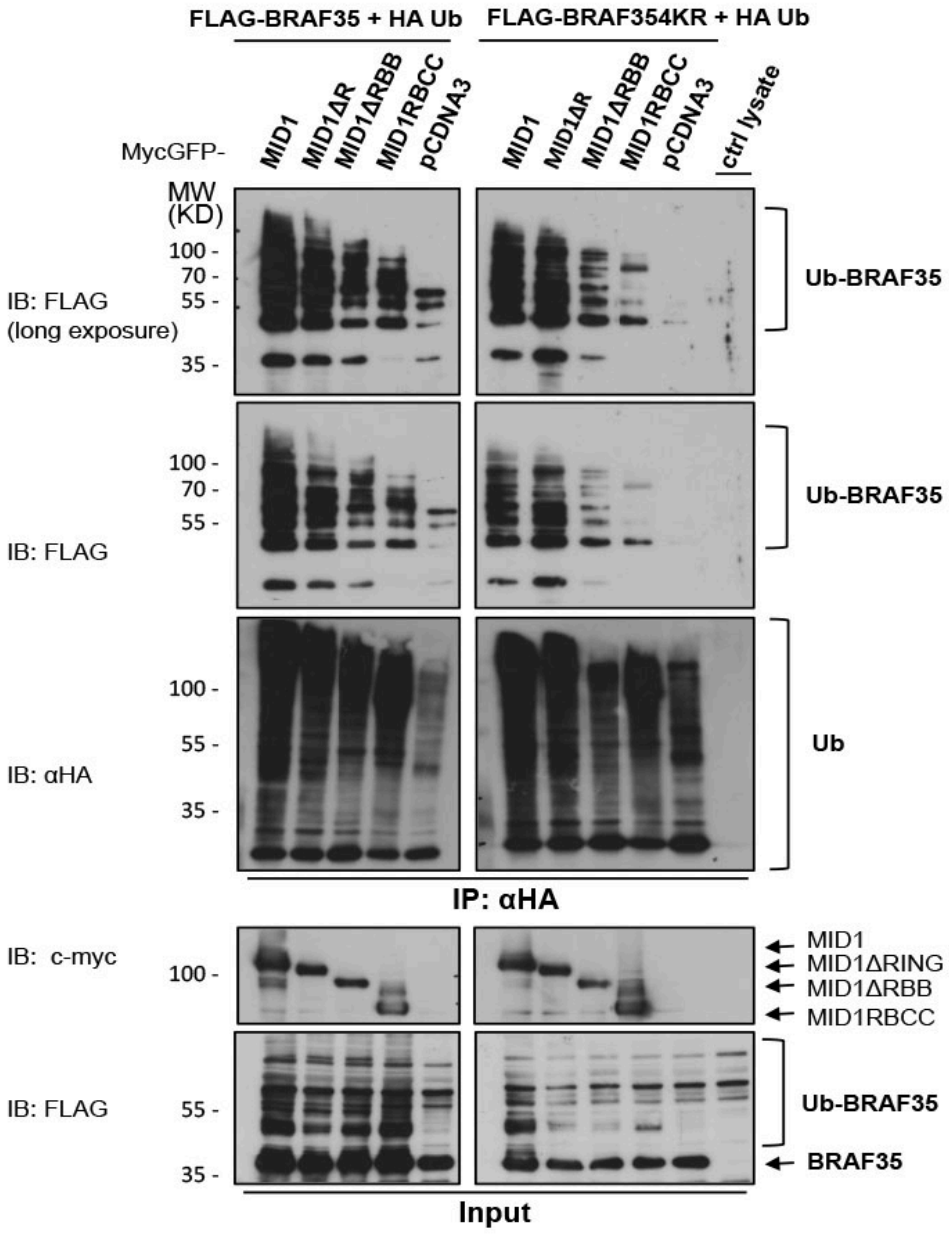


Figure 4.15: MID1-dependent BRAF35 ubiquitination occurs independently from sumoylation. HEK293T cells were transfected with HA-ubiquitin, MycGFP-MID1 (full length and mutants) and either FLAG-BRAF35 (left hand panels) or BRAF35 4KR non sumoylatable mutant (right hand panels) and treated with MG132 for 2 hours. Ubiquitinated BRAF35 species were visualized with anti-FLAG antibody after immunoprecipitation with anti-HA. Immunoprecipitation of ubiquitin was confirmed with anti-HA immunoblot. Inputs were checked with anti-FLAG and anti-myc antibodies.

### 4.2.5 MID1 stimulates lysine 63-linked polyubiquitination of BRAF35

E3 ubiquitin ligases can poly-ubiquitinate target proteins promoting the formation of chains on any of the seven lysines present on the Ub molecules. Different poly-Ub structures linked to the substrate represent specific signals that define the fate of the ubiquitinated protein. Whereas K48-linked chains mediate proteasomal degradation, K63-linked chains mainly act in non-proteasomal degradatie and non-proteolitic events like endosomal trafficking to the lysosome, intracellular signalling, and DNA repair (Xu et al., 2009). We decided to start investigating whether canonical K48 or unconventional K63 linkages are catalysed in MID1-dependent BRAF35 ubiquitination. Thus, we performed an *in vivo* ubiquitination assay taking advantage of expression constructs for ubiquitin mutants in which all lysines but K48 or K63 were changed in arginine (UbK48 and UbK63) (figure 4.16A). Wild type ubiquitin (Ub WT) was included as control. HEK293T cells were transfected with FLAG-BRAF35 together with HA-WT or mutant ubiquitin in the presence of MycGFP-MID1. Cells were incubated with the proteasome inhibitor, although this was not necessary for K63-linked Ub-chain accumulation. As expected, a strong poly-ubiquitination (and/or multi-monoubiquitination) of BRAF35 with wild type ubiquitin was promoted by MID1 overexpression (figure 4.16B). Intriguingly, the use of mutants with only one lysine available for polymerization (K48 and K63) suggested that lysine 63 was preferred to lysine 48 for MID1-dependent BRAF35 poly-ubiquitination (figure 4.16B). Taken together, these results suggest that MID1 promotes mono- and multi mono-ubiquitination but also BRAF35 poly-ubiquitination predominantly through K63-linked chains.

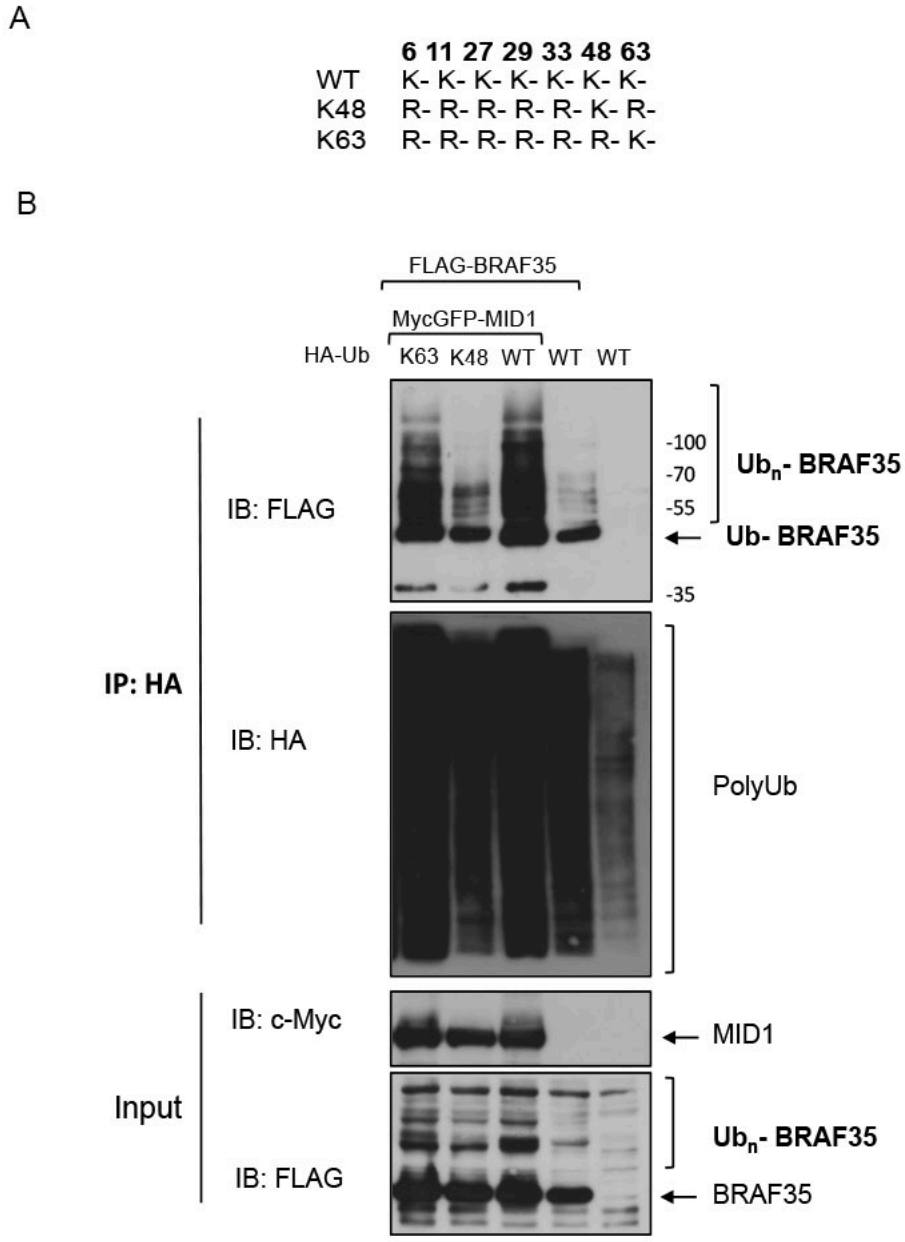


Figure 4.16: MID1 facilitates polyubiquitination of BRAF35 via Lys63 of Ubiquitin. A) Diagram of ubiquitin lysine mutants used in the assay to distinguish mono-, multi mono- or polyubiquitinated BRAF35. B) HA–ubiquitin constructs with either K48 or K63 only lysine residues were used for ubiquitination assay with MycGFP-MID1 and FLAG–BRAF35. Wild-type ubiquitin (WT) was used as positive controls. Immunoprecipitated and lysates were analysed with anti-FLAG and anti-HA antibodies.

## 4.3 Functional role of MID1 and BRAF35 in cytokinesis

### 4.3.1 MID1 and BRAF35 co-localize during cytokinesis

Cytokinesis is the last step in the cell cycle in which coordinated actions of the cytoskeleton, membrane systems and well-organized factors provide precise control of the physical separation of one cell into two. Cytokinesis can be divided in different sub-processes based on timing and morphology, comprising the reorganization of microtubules and formation of the midzone, cleavage plan specification, assembly of a contractile ring, cleavage furrow ingression and abscission, after midbody formation (Eggert et al., 2006). Even though it was known that MID1 occupies microtubules of the mitotic spindle during mitosis and that locates on the midbody at cytokinesis (Cainarca et al., 1999), at the beginning of this project no direct observation for BRAF35 on the midbody was reported even if a role for this protein in cytokinesis was soon postulated (Lee et al., 2011).

Besides colocalization in interphase cells (figure 4.8 and 4.9), our IF experiments showed a characteristic staining of MID1 and BRAF35, at the intercellular bridge and the midbody region in dividing HeLa cells (figure 4.17). In particular, we noticed that during anaphase endogenous BRAF35 was concentrating from the cytoplasm to the midzone where it colocalized with MycGFP-MID1. In telophase and cytokinetic cells the two proteins were concentrated at the midbody region occupying the intercellular bridge, where their localisation partially overlaps (figure 4.17 and inset). This was the first evidence for BRAF35 localization on the cleavage furrow and at the midbody. Interestingly, a report describing a cancer-associated mutation in BRAF35 that disrupts its localization at the midbody and correct function in cytokinesis was recently published (Lee and Venkitaraman, 2014), further confirming our observations. We therefore decided to further investigate BRAF35 regulation during cell cycle.

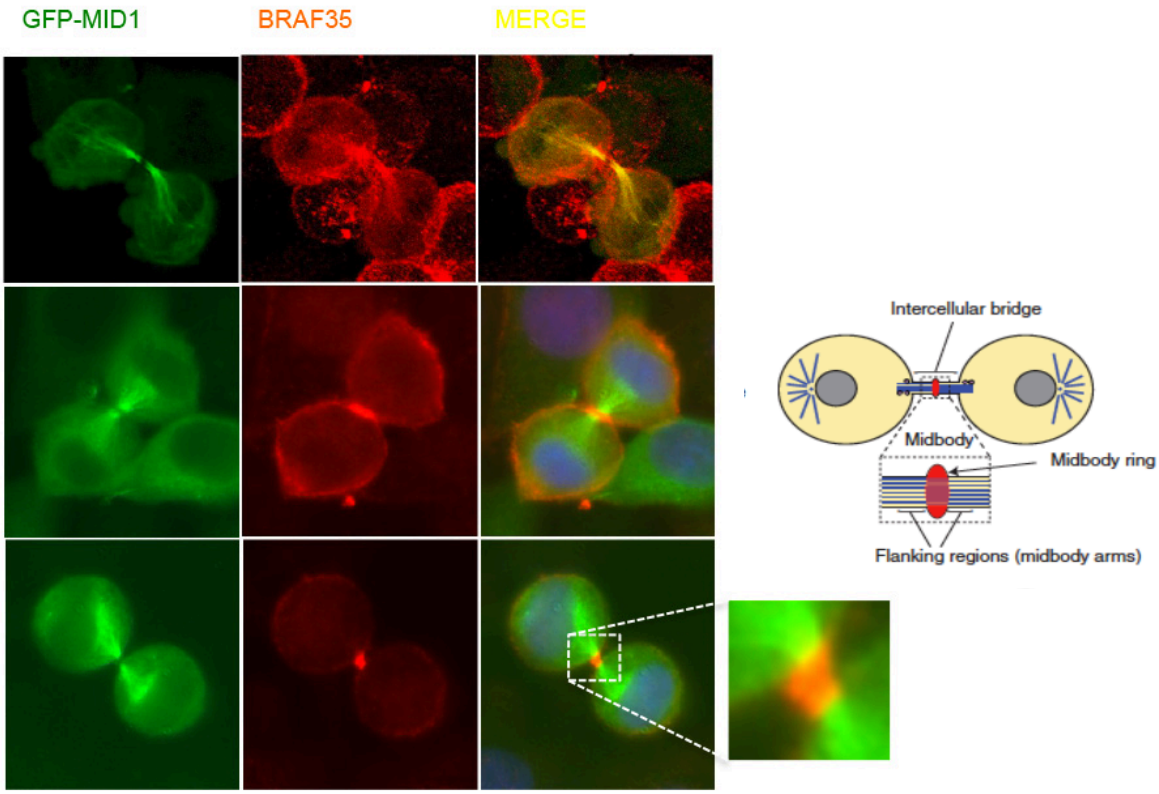


Figure 4.17: MID1 co-localize with BRAF35 at the midbody during cytokinesis**.** Representative images of immunofluorescence experiments at different cytokinetic stages showing endogenous BRAF35 (red) partially co-localizing with MycGFP-MID1 (green) on the intercellular bridge (upper panel), at the actomyosin ring (middle panel) and the midbody region (lower panel and magnification). For better comprehension of the figure, a cartoon indicating the intercellular bridge and the midbody of dividing cells is shown (adapted from D'Avino et al., 2015).

### 4.3.2 BRAF35 amount and distribution is regulated during cell cycle

The data from CHX-chase experiments and subcellular fractionation indicate that MID1 regulates BRAF35 abundance in the cytoplasm of HeLa cells. Moreover, the colocalization observed in the cytoplasm and on the midbody corroborates the hypothesis for a specific effect exerted by MID1 on BRAF35 to control cytokinesis. The midbody in fact can be considered as a platform for ubiquitination that is essential for the irreversibility of mitotic exit (Pohl and Jentsch, 2009). To begin addressing the possibility that BRAF35 is specifically degraded during different phases of the cell cycle, we compared cycling versus S-phase- (thymidine block) or G2/M -arrested (nocodazole treatment) and progressing through mitosis (released from nocodazole block) HeLa cells. Indeed, immunoblotting revealed a strong reduction of BRAF35 levels in G2/M arrested cells. Moreover, enrichment in mitotic population with shake-off technique indicated that BRAF35 protein level remains low during M phase with respect to asynchronous cells (figure 4.18A). In order to further

investigate whether this reduction was also observed during normal cell cycle progression, we synchronized HeLa cells using a double thymidine block/release protocol (figure 4.18B). Cyclin A and cyclin B1 were used as G2/M markers (Sullivan and Morgan, 2007). Despite variability among independent experiments, we reproducibly noticed a trend for a decrease in BRAF35 level in M phase compared to asynchronous cells. This reduction occurred between 10 and 12 hours after release from thymidine block, when cyclin A starts to be degraded (metaphase) until cyclin B1 degradation occurs (anaphase) (figure 4.18 B).

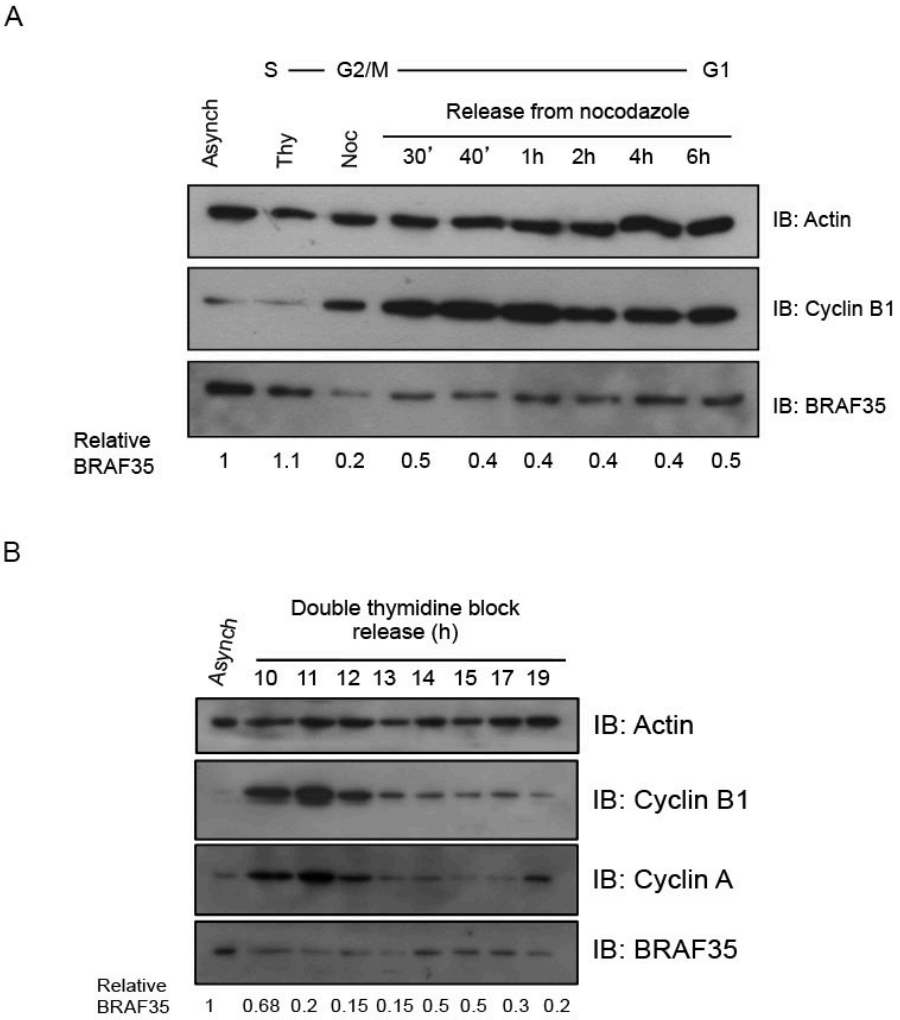


Figure 4.18: BRAF35 is a cell cycle regulated protein. A) Immunoblot analysis for cycling (asynch), thymidine S phase arrested (thy), nocodazole G2/M arrested (Noc) and synchronized mitotic HeLa cells collected at the indicated time points after nocodazole release and mitotic shake-off. Antibodies are indicated. B) HeLa cells were synchronized with a standard double thymidine block protocol and released. Samples were prepared at the indicated periods and lysates were analysed by immunoblotting with anti-actin (loading control), anti-cyclinB1 (G2/M marker) and anti-BRAF35 antibodies. Quantifications of BRAF35 level relative to actin considering asynchronous cells as 1 are indicated below the immunoblots in A and B.

The observation that BRAF35 is partially degraded during late mitosis and cytokinesis onset, has also been suggested by IF experiments on synchronized HeLa cells analysed with anti-BRAF35 antibody. The staining revealed the presence of the endogenous protein in the midzone of dividing cells as localized on the cleavage furrow during late telophase and cytokinesis (figure 4.19). Then, during abscission BRAF35 is located in the midbody region of the intercellular bridge that separates the two daughter cells (figure 4.19). This prominent association with the midbody of BRAF35 concomitant with its reduction in G2/M suggests a fine mechanism of regulation of the necessary BRAF35 removal from other cellular compartments for the cell division to correctly proceed.

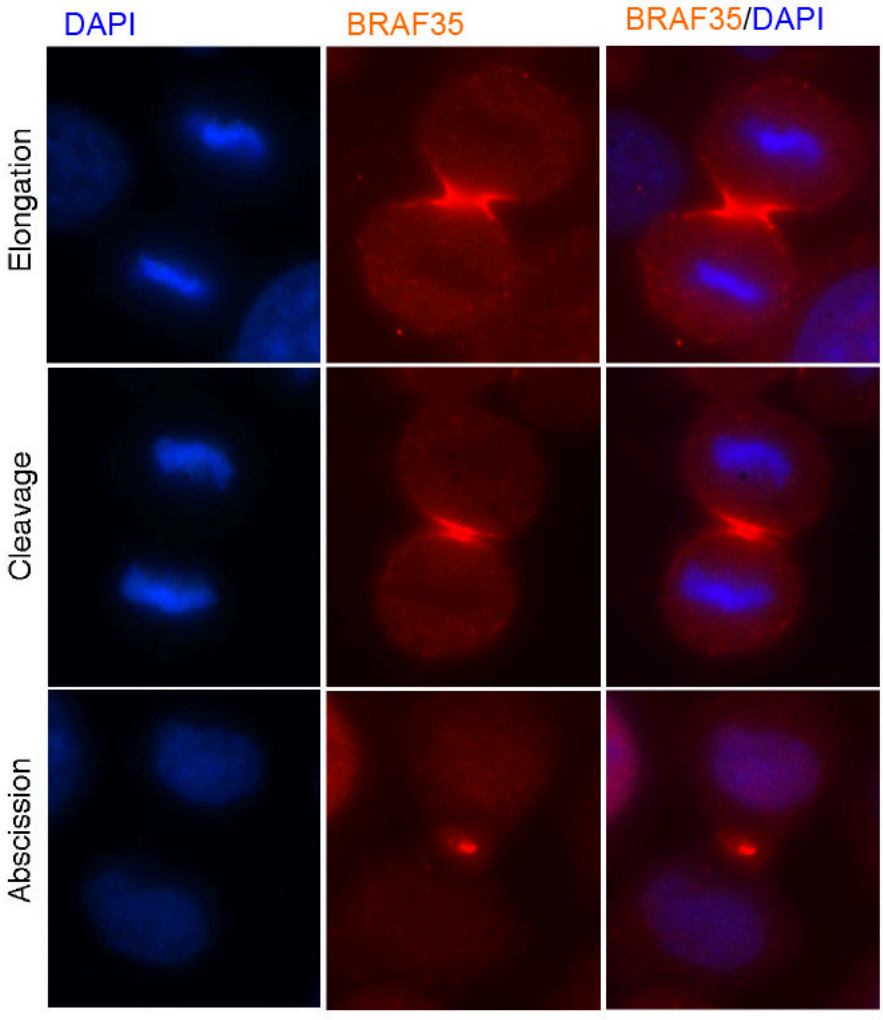


Figure 4.19: BRAF35 localizes at the cleavage furrow and midbody during cell division. Endogenous BRAF35 (red) localizes at the cleavage furrow of HeLa cells in telophase. Immunofluorescence staining also shows BRAF35 localization on the midbody during late telophase and cytokinetic abscission (red). Nuclei are stained with DAPI (blue).

### 4.4.3 MID1 depletion rescues the cytokinetic defect caused by BRAF35 silencing

It has been previously demonstrated that BRAF35 is required for the correct completion of cell division (Lee et al., 2011). In fact, BRAF35 depletion in HeLa cells results in an extended time taken from anaphase to cytokinetic abscission. Moreover, a high percentage of mitotic cells fail to divide, becoming multinucleated. It is well known that an abortive cytokinesis produces binucleate cells and that polyploidy can trigger carcinogenesis (Sagona and Stenmark, 2010). More recently, a cancer-associated mutation in BRAF35 has been described as deleterious for the correct function of endogenous BRAF35 in cytokinesis, promoting aneuploidy in HeLa cells (Lee and Venkitaraman, 2014). Considering all data on MID1 and BRAF35 interaction and ubiquitination, we started to investigate a possible mechanism of MID1-mediated BRAF35 regulation in the context of cell division.

To examine if MID1 plays a role in cytokinesis in relation to BRAF35 function, its expression was down-regulated in HeLa cells with a siRNA (siMID1_2) alone or in combination with BRAF35 siRNA (siBRAF35). The effect of MID1 depletion was examined after 72 hours of siRNA transfection with record of binucleated and multinucleated cells from bright-field microscopy images (figure 4.20A). Knock-down of BRAF35 was used as a positive control for the experiment. As reported, also in our experimental conditions, BRAF35 silencing elicited a cytokinetic defect that resulted in a 3-fold increase of bi- and multinucleated cells compared to non-treated cells (figure 4.20B). By contrast, cells treated with MID1 siRNA did not show a variation from basal bi-and multinucleation level observed in non-treated and mock-treated cells (Figure 4.20B). Importantly, concomitant depletion of BRAF35 and MID1 (siBRAF35 + siMID1) was sufficient to reduce the proportion of multinucleate cells compared to BRAF35 depleted cells (figure 4.20C). Thus, the abscission defect observed upon downregulation of BRAF35 could be rescued by co-depletion of MID1, suggesting that MID1-mediated regulation of BRAF35 contributes to the correct separation of the daughter cells.

A

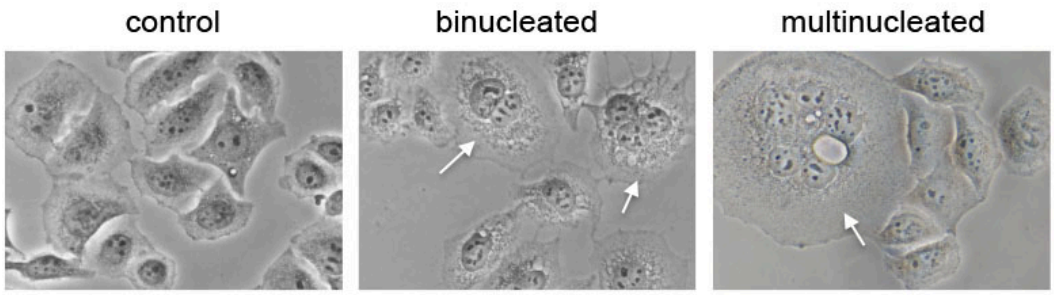


B

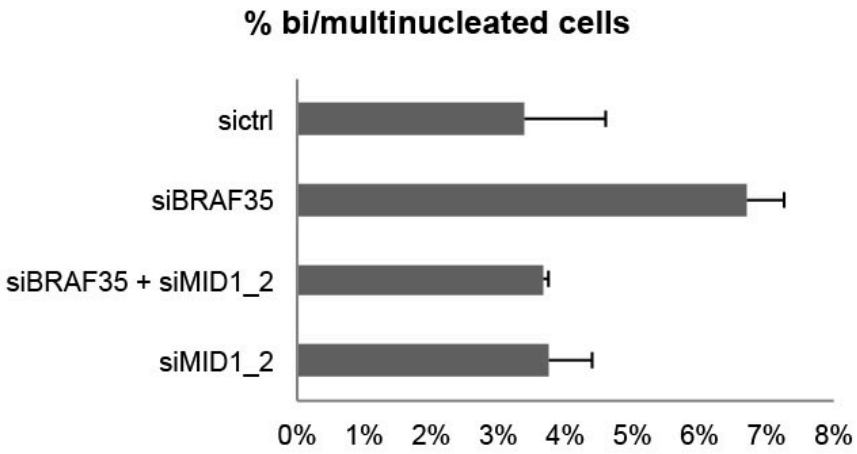


Figure 4.20: Loss of MID1 decreases multinucleation in BRAF35 depleted cells. A) Representative pictures of normal, binucleate and multinucleate HeLa cells. C) HeLa cells were transfected with different combinations of non-targeting (sictrl), BRAF35 siRNA (siBRAF35 and MID1 siRNA (siMID1_2) for 72h. For each condition, the final concentration of siRNAs was 10 nM. Cells were fixed and random picture were taken. For each condition ~ 400 random cells were observed and those with two or more nuclei were counted. Percentage of bi- and multi-nucleated cells is shown (mean of three independent experiments; bars: sem)

4.4.4 MID1 silencing stimulates membrane blebbing during cell division

Membrane blebs are round-shaped membrane protrusions produced by actomyosin cortex contraction that occur under many physiological conditions. Blebs are in fact frequently observed during cytokinesis, apoptosis and migration (Charras and Paluch, 2008). Analysis of images produced in the experiment described in par. 4.4.3 also revealed a characteristic phenotype after MID1 depletion: cells exhibited increased membrane blebbing (figure 4.21 and 4.22A).

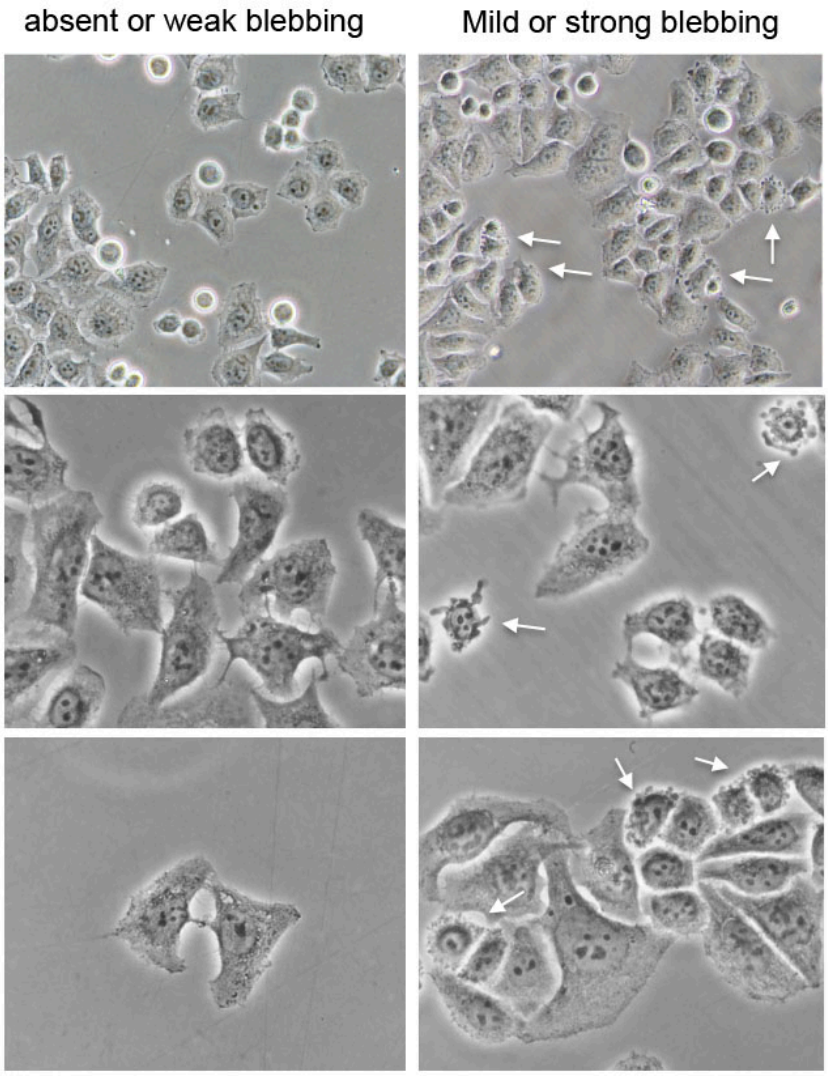


Figure 4.21: Representative pictures of interphase and cytokinetic HeLa cells with absent or weak blebbing (left panel) or exhibiting mild or strong blebbing (right panel, white arrows).

Since abnormal blebbing during cytokinesis perturbs symmetric cell division resulting in cleavage furrow displacement and aneuploidy (Sedzinski et al., 2011), we recognized this phenotype as a possible additional cytokinetic defect further implicating MID1 in cell division. All images from silencing experiments were re-analysed for blebbing alterations, in order to understand the relationship between BRAF35 depletion-driven cytokinesis failure and membrane blebbing increase. Control cells exhibited weak membrane blebbing, while this phenotype was more frequent in cells treated with BRAF35 siRNA (siBRAF35) and in MID1 depleted cells (figure 4.22A). Notably, these were prevalently prophase or interphase cells, some of them likely apoptotic cells. We then focused on the analysis of blebbing only in cells that were recognized as progressing from telophase to cytokinesis. Interestingly, among all MID1-depleted dividing cells, at least 35% presented with a pronounced membrane blebbing (figure 4.22B). This phenotype was less frequent in dividing cells treated with non-targeting or BRAF35 siRNA. These findings suggest that MID1 is involved in the regulation of membrane blebs formation during cytokinesis.

The data presented indicate a new interaction between the TRIM protein MID1 and the poorly characterized protein BRAF35. Our findings demonstrate that MID1 promotes BRAF35 mono- and/or poly-ubiquitination mainly regulating its cytoplasmic abundance.
Our data suggest a MID1-dependent regulation of BRAF35 during cytokinesis that is the result of regulated proteasomal degradation but implicates also a K63-polyUb dependent signalling. Finally, we reveal the possibility of an additional new role for MID1 in regulating cell division and cytoskeleton dynamics. All these data can explain some mechanisms altered in Opitz Syndrome pathogenesis and in the postulated MID1 pro-tumorigenic role.

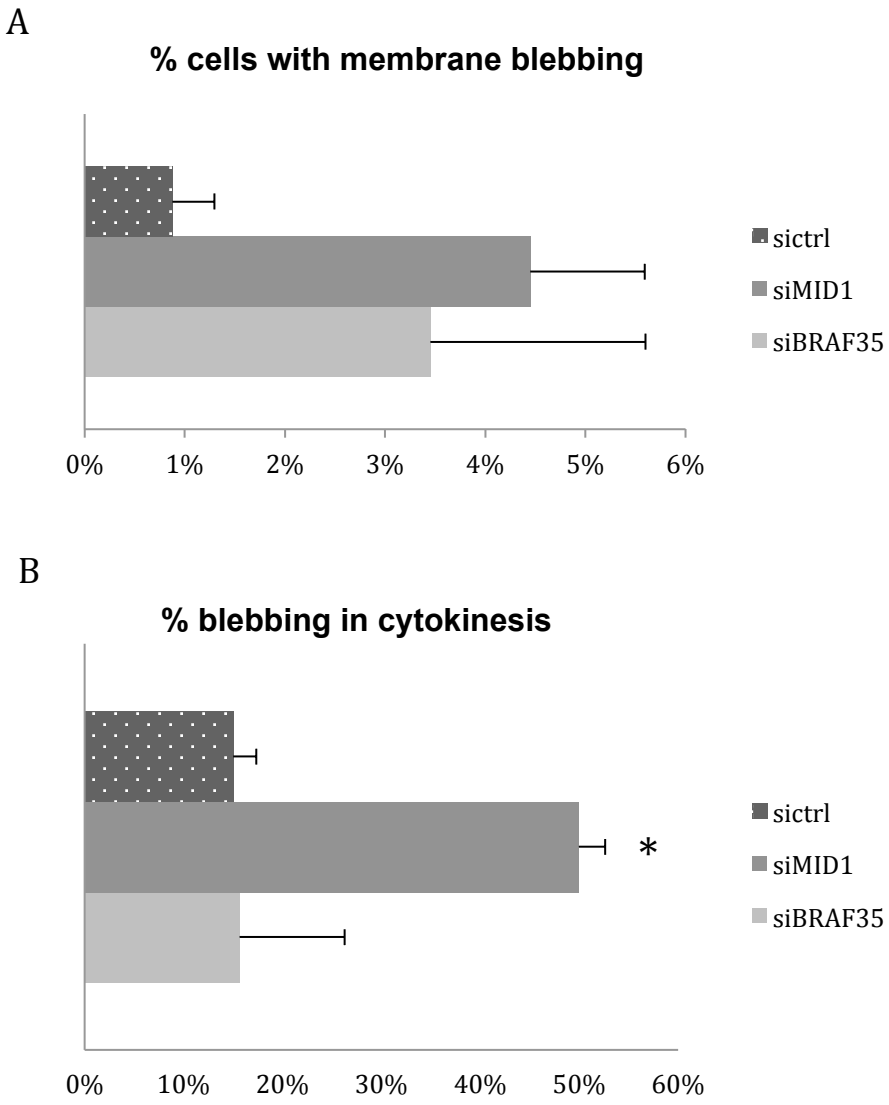


Figure 4.22: MID1 depleted cells exhibit a membrane blebbing phenotype. A) HeLa cells were fixed 72h after treatment with different combinations of non-targeting (sictrl), BRAF35 siRNA (siBRAF35) and MID1 siRNA (siMID1). Approximately 400 cells of random-taken images from three independent experiments were analysed and cells with membrane blebbing were counted. (bars: sem) B) Experiments as in B, but only dividing cells were considered. Bars: sem; t-test: *$p<0.05$)

.

# 5. DISCUSSION

The aim of this thesis work was to investigate novel MID1 protein functions in order to further elucidate the molecular mechanisms that cause the X-linked Opitz syndrome. This developmental disease, characterized by midline defects and mental retardation, is caused by loss of function mutations in the MID1 gene but the pathogenetic mechanism is still undefined. Here, we report that MID1 interacts directly with the BRCA2-Associated Factor *35* (BRAF35) promoting its ubiquitination and regulating its abundance in the cytoplasm of HeLa cells. Moreover, we found that MID1 and BRAF35 partially colocalize not only during interphase but also at the intercellular bridge during cytokinesis. Consistent with this observation, we observed a cell cycle-related regulation of BRAF35 protein level. Moreover, MID1 depletion rescued the cytokinetic defect caused by BRAF35 silencing, leading to a decrease of binucleation, but promoted a blebbing phenotype in dividing cells, suggesting an additional and new role for MID1 in cytokinesis regulation.

In this work, we present BRAF35 as a new interactor of MID1. MID1 is a member of the TRIM family of E3 ubiquitin ligases. We demonstrated that BRAF35 is partially degraded via proteasome and that its protein level is regulated by MID1 presence. Depletion and overexpression of MID1 in fact provoked a slight increase and a decrease, respectively, of BRAF35 abundance. The E3 ligase activity of MID1 is implicated in this regulation as demonstrated by the rescue of BRAF35 degradation upon overexpression of a MID1 E3 ligase incompetent mutant. The fact that MID1-dependent BRAF35 degradation is not very pronounced could be explained by the observation that protein level regulation mainly concerns the cytoplasmic fraction of BRAF35, the one that colocalizes with MID1 and is less abundant with respect to the nuclear fraction. We demonstrated that BRAF35 is ubiquitinated. We determined that MID1 E3 ligase activity is necessary for BRAF35 ubiquitination and, although we did not perform an *in vitro* experiment, our findings suggest that MID1 directly ubiquitinates BRAF35. We cannot exclude that other E3 ligases can ubiquitinate BRAF35 as suggested by the basal level of BRAF35 ubiquitination observed in the assays performed. Whether this is dependently or not from MID1 function is still to be investigated. Ubiquitination can target a protein not only for proteasomal degradation but also for non-proteolytic fates such as influencing protein-protein interaction, subcellular localization or activity (Komander and Rape, 2012). Our findings suggested an additional function for MID1-mediated BRAF35 ubiquitination dependent on K63-linked polyUb

chains. Whether this is necessary to target BRAF35 towards alternative proteolytic pathways such as autophagic or lysosomal degradation is still unknown. One alternative hypothesis is that the MID1-mediated K63 polyUb modification on BRAF35 is recognized by a UBD protein to mediate its recruitment towards a particular compartment/function.

It was previously reported that BRAF35 is sumoylated and that this modification is necessary for its association with the LSD1–CoREST complex, where it is needed as a stabilizer on the chromatin to repress neuronal genes in non-neuronal tissues and neuronal progenitors. BRAF35 sumoylation is inhibited by heterodimerization with its paralogue iBRAF, which impairs the antidifferentiation effect of BRAF35 (Ceballos-Chavez et al., 2012). It is possible that MID1-mediated ubiquitination opposes BRAF35 sumoylation or, alternatively, that one PTM is necessary for the other. Despite *in silico* prediction of the presence of at least one SIM in MID1 (unpublished observations), our data suggest that sumoylation of BRAF35 is not required, or it does not interfere, with its ubiquitination mediated by MID1. Moreover, we showed that K31, K125, K156 and K157, which are the lysines involved in sumoylation, are not targeted for MID1-mediated polyubiquitin chain linkage. Another possibility is that, given the absence of specific consensi for ubiquitination, other lysine residues in the surrounding regions of the BRAF35 4KR mutant are ubiquitinated due to the unavailability of those mutated.

We can also hypothesize that the two different PTMs, ubiquitination and sumoylation, are required to regulate BRAF35 in the different cellular compartments where it exerts its functions, i.e. cytoplasm and nucleus.

Considering the cellular context, we can speculate that MID1-dependent ubiquitination is needed in order to regulate BRAF35 subcellular localization and availability for interaction with its cellular partners. It has been shown in fact that iBRAF is an alternative subunit of the LSD1-coREST complex and that it cooperates with SNAI1 to repress epithelial genes such as CXADR, CLDN12 and KRT18 during TGF-β-driven epithelial-to-mesenchymal transition (EMT) to promote cell migration and invasiveness (Rivero et al., 2015). The presence of BRAF35 and iBRAF in the LSD1-coREST complex is mutually exclusive therefore there should be a fine equilibrium between BRAF35-iBRAF dimer, BRAF35 in the LSD1-coREST complex versus its presence in the BRCA2-containing complex, and possibly free or other complexes-associated BRAF35. MID1 is a candidate to participate in this regulation that could affect BRAF35 availability in the nucleus versus the cytoplasm during the different processes in which its function is required. During this thesis work, the role for

MID1/BRAF35 in the context of the BRCA2 complex and in cytokinesis has been addressed but it will be interesting to further investigate in the future a possible MID1 role within LSD1-coREST-associated BRAF35 and its neuronal transcriptional control.

Concerning the role of MID1/BRAF35 in the context of the BRCA2 complex and in cytokinesis that we investigated during this thesis work, at the beginning of the project, immunofluorescence experiments revealed an interesting pattern of colocalization of MID1 and BRAF35 not only in the cytoplasm of interphase cells but also at the intercellular bridge of dividing HeLa cells. This particular localization was expected for MID1, which associates to microtubular structures during all cell cycle (Cainarca et al., 1999), but not for BRAF35, which was described only as a nuclear protein (Marmorstein et al., 2001). Our observation is consistent with reported data about a possible role for BRAF35 in regulating mitotic progression and completion of cytokinesis: indeed depletion of BRAF35 causes a cytokinetic defect resulting in delayed cell division or bi/multinucleation (Lee et al., 2011). Further, a recent publication confirmed our findings on BRAF35 localization at the intercellular bridge indicating also that a BRAF35 cancer-associated mutation impairs its localization on the midbody and its interaction with BRCA2 (Lee and Venkitaraman, 2014). It will be interesting to further investigate if that mutation in BRAF35 is able to disrupt its interaction with MID1, supporting a possible involvement for MID1 in regulating BRAF35 localization at the midbody. Our detailed analysis on BRAF35 subcellular distribution indicated that the protein localizes first at the cleavage furrow to move then on the midbody of the intercellular bridge as the contractile ring constricts during cytokinesis progression. Consistent with a cell cycle fine regulation, we found that BRAF35 protein level is downregulated with a specific timing during cell cycle, starting from G2/M transition until cell division is completed.
We observed that depletion of MID1 together with BRAF35 reduced the number of bi/multinucleated cells caused by BRAF35 silencing that was reported and confirmed in our hands. Considering these data, together with the biochemical data reported above, we propose a model in which MID1 is the E3, or one of the E3s, responsible for BRAF35 ubiquitination and regulated degradation in the cytoplasm at the onset of cytokinesis and/or its regulated relocation to different subcellular structures. Therefore simultaneous depletion of both BRAF35 and MID1 could result in a partial rescue of BRAF35 protein level that should be sufficient to exert its function and contribute to completion of the division process. Inversely, we might speculate that an upregulation of MID1 activity in a tissue specific context could

provoke an abnormal degradation of BRAF35, leading to cytokinesis failure (figure 5.1). Polyploidy caused by cytokinetic failure can trigger tumourigenesis (Sagona and Stenmark, 2010) and consistently, high levels of MID1 protein were found in prostate cancer tissues (Kohler et al., 2014).

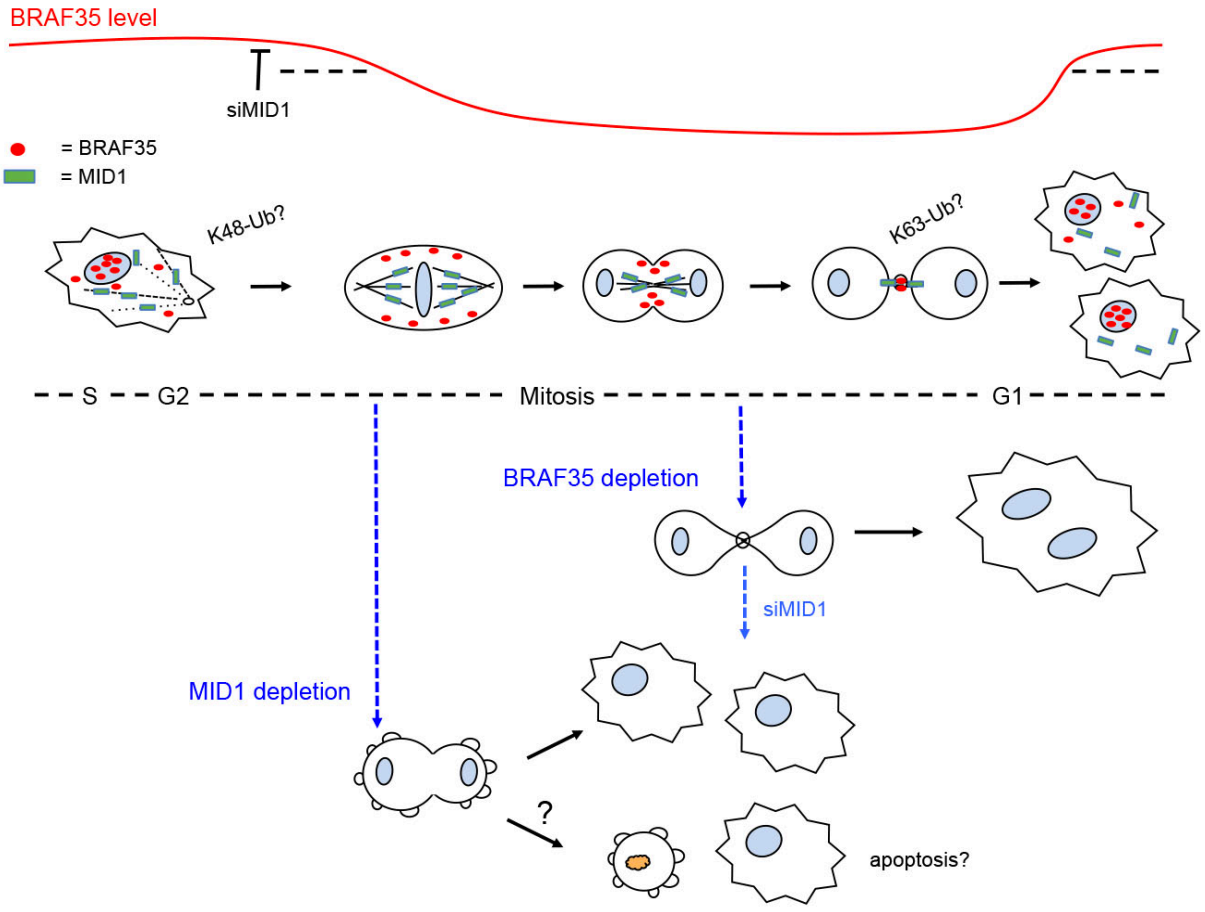


Figure 5.1: Model for MID1 regulation of BRAF35 during cytokinesis. BRAF35 protein is regulated through MID1-dependent ubiquitination, leading to its degradation or correct localization at the midbody during cell division (upper part). MID1 depletion influences not only BRAF35 protein level but also promotes membrane blebbing during cytokinesis, affecting the correct progressing of the process (light blue, DNA; red, BRAF35; green, MID1; dotted black lines, microtubules).

BRCA2 is recruited on the midbody by Filamin A and is necessary for correct localization of other midbody proteins such as MKLP1, MKLP2 and PRC1. On the midbody it forms a complex with CEP55, Alix, and Tsg101 and is required for recruitment of the ESCRT machinery necessary for abscission (Mondal et al., 2012). It is possible that BRAF35 and MID1 are recruited together on the midbody by binding BRCA2 and cooperate within this

complex. Further investigation to address if MID1 interact with BRCA2 and experiments to determine if MID1 or BRCA2 depletion affects BRAF35 localization will be required.

Another candidate protein that could intervene in BRAF35/MID1 function and the cytokinetic process is the kinesin KIF4A. KIF4A has been identified as a BRAF35 interacting partner (Lee and Kim, 2003) but the nature of their relationship is still unknown. MID1 is associated with microtubules and is transported along them by the counteraction of dynein and kinesins (Aranda-Orgilles et al., 2008). Moreover, KIF4A phosphorylation by Aurora B activates its microtubule-stimulated ATPase activity and enhances KIF4A binding to PRC1 during midzone assembly in order to regulate central spindle length (Hu et al., 2011) (Nunes Bastos et al., 2013). Since several mitotic spindle proteins lose affinity for microtubules as the cell enters cytokinesis phase, and several known midzone and microtubule plus-end tracking proteins (+TIPs gain affinity, it is possible that MID1 and BRAF35, together with KIF4A, are important in this transition phase of microtubular reorganization (Ozlu et al., 2010). Consistently, MID1, alone or together with MID2, is required for reorganization and stabilization of microtubules during neural tube closure (Suzuki et al., 2010) and in cells when associated to MIG12 (Berti et al., 2004). Newly published data support the hypothesis that MID1 activity in organizing microtubules is necessary for correct cytokinesis progression. MID1 (and MID2) binding to the microtubule-bundling/organizing protein Astrin has been reported, although the role of MID1 and the meaning of this interaction remain to be determined (Gholkar et al., 2016).

To add complexity to the picture, we can also consider phosphatase activity of PP2A. KIF4A is required to target PP2A-B56 $\gamma$ to the central spindle during anaphase and PP2A-B56 $\gamma$ is the phosphatase that counteracts Aurora B phosphorylation on KIF4A. The balance of KIF4A phosphorylation and dephosphorylation is essential to control central spindle length (Bastos et al., 2014). Since MID1 regulates PP2Ac level, disregulation of MID1 activity could lead to an unbalanced dephosphorylation of PP2A targets such as KIF4A.

Besides the interplay with BRAF35 in cytokinesis, we observed that MID1 depletion increases membrane blebbing, chiefly in association with cell division. Blebs are spherical membrane protrusions that are produced by contractions of the actomyosin cortex. Blebs occurs physiologically during cytokinesis, where they appear at the poles of dividing cells, during cell spreading or migration of tumour and embryonic cells; dynamic blebbing is associated with the execution phase of apoptosis (Charras, 2008). Mechanical studies indicate

that during cytokinesis the polar cortex regulates cleavage dynamics by generating resistive forces that slow furrow ingression (Sedzinski et al., 2011). Our observation suggests that MID1 is involved in the mechanism of cell division with a possible additional role to that exerted together with BRAF35. In fact, a similar blebbing phenotype has been reported occurring after TBC1D15 depletion. TBC1D15 is required for the proper localization of RhoA during anaphase for the ingression of the cytokinetic furrow. Activation of RhoA and its effector kinase, Rho-associated kinase (ROCK), promotes the phosphorylation of myosin light chain, which induces actomyosin contraction (Takahara et al., 2014). Interestingly, mTORC1 has been shown to regulate the Rho–ROCK pathway. Depletion of the mTOR inhibitor DEPTOR, hyperactivates mTORC1 that promote ROCK1 activity, producing a surface blebbing associated cytokinetic defect and polyploidy (Peterson et al., 2015). MID1 depletion has been shown to disrupt mTOR/Raptor association via PP2A hyperactivation and consequently inhibits mTORC1 signalling (Liu et al., 2011). Therefore with MID1 silencing the opposite outcome of mTORC1 hyperactivation should be expected, although the process could be more complex and further investigations are required.

The increased number of cells showing membrane blebbing that we observed while progressing into cytokinesis could be also the consequence of a delayed division. However, the fact that MID1 depletion does not increase bi/multinucleation means that in absence of MID1 either the cells divide slowly but eventually correctly complete abscission or the cells die before completing abscission. We will evaluate both possibilities following cells undergoing cytokinesis through live cell imaging. This will help to understand if MID1 is involved in the regulation of cytoskeleton dynamics not only during cell division, but also in other processes, such as migration and adhesion.

In conclusion, our findings indicate a new role for MID1 in regulating BRAF35 in the context of cell division. Moreover, they suggest an independent implication of MID1 in cell morphology definition and cytoskeleton organization. We think that all these data will be helpful to contribute to the understanding of the pathogenesis of Opitz syndrome and MID1 role in embryogenesis. Further, like several other developmental genes, a role of MID1 as pro-tumorigenic factor is also emerging. Therefore the knowledge of the mechanism underlying MID1-mediated regulation of BRAF35 will be of relevance to further understand both developmental and tumourigenic processes.

# 6. REFERENCES


Agromayor, M., and Martin-Serrano, J. (2013). Knowing when to cut and run: mechanisms that control cytokinetic abscission. Trends Cell Biol *23*, 433-441.

Aranda-Orgilles, B., Aigner, J., Kunath, M., Lurz, R., Schneider, R., and Schweiger, S. (2008). Active transport of the ubiquitin ligase MID1 along the microtubules is regulated by protein phosphatase 2A. PLoS One *3*, e3507.

Bastos, R.N., Cundell, M.J., and Barr, F.A. (2014). KIF4A and PP2A-B56 form a spatially restricted feedback loop opposing Aurora B at the anaphase central spindle. J Cell Biol *207*, 683-693.

Beck, J., Maerki, S., Posch, M., Metzger, T., Persaud, A., Scheel, H., Hofmann, K., Rotin, D., Pedrioli, P., Swedlow, J.R., *et al*. (2013). Ubiquitylation-dependent localization of PLK1 in mitosis. Nat Cell Biol *15*, 430-439.

Bell, J.L., Malyukova, A., Holien, J.K., Koach, J., Parker, M.W., Kavallaris, M., Marshall, G.M., and Cheung, B.B. (2012). TRIM16 acts as an E3 ubiquitin ligase and can heterodimerize with other TRIM family members. PLoS One *7*, e37470.

Berndsen, C.E., and Wolberger, C. (2014). New insights into ubiquitin E3 ligase mechanism. Nat Struct Mol Biol *21*, 301-307.

Berti, C., Fontanella, B., Ferrentino, R., and Meroni, G. (2004). Mig12, a novel Opitz syndrome gene product partner, is expressed in the embryonic ventral midline and co-operates with Mid1 to bundle and stabilize microtubules. BMC Cell Biol *5*.

Birgisdottir, A.B., Lamark, T., Johansen, T. (2013) The LIR motif – crucial for selective autophagy. J Cell Sci 2013 126: 3237-3247

Boding, L., Hansen, A.K., Meroni, G., Johansen, B.B., Braunstein, T.H., Bonefeld, C.M., Kongsbak, M., Jensen, B.A., Woetmann, A., Thomsen, A.R., *et al*. (2014a). Midline 1 directs lytic granule exocytosis and cytotoxicity of mouse killer T cells. Eur J Immunol *44*, 3109-3118.

Boding, L., Hansen, A.K., Nielsen, M.M., Meroni, G., Braunstein, T.H., Woetmann, A., Odum, N., Bonefeld, C.M., and Geisler, C. (2014b). Midline 1 controls polarization and migration of murine cytotoxic T cells. Immunity, inflammation and disease *2*, 262-271.

Bosanac, I., Phu, L., Pan, B., Zilberleyb, I., Maurer, B., Dixit, V.M., Hymowitz, S.G., and Kirkpatrick, D.S. (2011). Modulation of K11-linkage formation by variable loop residues within UbcH5A. J Mol Biol *408*, 420-431.

Budhidarmo, R., Nakatani, Y., and Day, C.L. (2012). RINGs hold the key to ubiquitin transfer. Trends Biochem Sci *37*, 58-65.

Burroughs, A. M., Jaffee, M., Iyer, L. M., & Aravind, L. (2008). Anatomy of the E2 ligase fold: implications for enzymology and evolution of ubiquitin/Ub-like protein conjugation. Journal of Structural Biology, 162(2), 205–218.

Cainarca, S., Messali, S., Ballabio, A., and Meroni, G. (1999). Functional characterization of the Opitz syndrome gene product (midin): evidence for homodimerization and association with microtubules throughout the cell cycle. Hum Mol Genet *8*, 1387-1396.

Cano, F., Rapiteanu, R., Sebastiaan Winkler, G., and Lehner, P.J. (2015). A non-proteolytic role for ubiquitin in deadenylation of MHC-I mRNA by the RNA-binding E3-ligase MEX-3C. Nature communications *6*, 8670.

Ceballos-Chavez, M., Rivero, S., Garcia-Gutierrez, P., Rodriguez-Paredes, M., Garcia-Dominguez, M., Bhattacharya, S., and Reyes, J.C. (2012). Control of neuronal differentiation by sumoylation of BRAF35, a subunit of the LSD1-CoREST histone demethylase complex. Proc Natl Acad Sci U S A *109*, 8085-8090.

Charras, G., and Paluch, E. (2008). Blebs lead the way: how to migrate without lamellipodia. Nat Rev Mol Cell Biol *9*, 730-736.

Charras, G.T. (2008). A short history of blebbing. Journal of microscopy *231*, 466-478.

Chen, C.T., Ettinger, A.W., Huttner, W.B., and Doxsey, S.J. (2013). Resurrecting remnants: the lives of post-mitotic midbodies. Trends Cell Biol *23*, 118-128.

Chen, Z.J., and Sun, L.J. (2009). Nonproteolytic functions of ubiquitin in cell signaling. Mol Cell *33*, 275-286.

Christianson, J.C., and Ye, Y. (2014). Cleaning up in the endoplasmic reticulum: ubiquitin in charge. Nat Struct Mol Biol *21*, 325-335.

Chu, Y., and Yang, X. (2010). SUMO E3 ligase activity of TRIM proteins. Oncogene *30*, 1108-1116.

Ciechanover, A., Heller, H., Elias, S., Haas, A.L., and Hershko, A. (1980). ATP-dependent conjugation of reticulocyte proteins with the polypeptide required for protein degradation. Proc Natl Acad Sci U S A *77*, 1365-1368.

Clague, M.J., Barsukov, I., Coulson, J.M., Liu, H., Rigden, D.J., and Urbe, S. (2013). Deubiquitylases from genes to organism. Physiol Rev *93*, 1289-1315.

Clague, M.J., Heride, C., Urbe, S. (2015). The demographics of the ubiquitin system. Trends Cell Biol *25*, 417-426.

Clague, M.J., and Urbe, S. (2010). Ubiquitin: same molecule, different degradation pathways. Cell *143*, 682-685.

Cubenas-Potts, C., and Matunis, M.J. (2013). SUMO: a multifaceted modifier of chromatin structure and function. Dev Cell *24*, 1-12.

D'Avino, P.P., Giansanti, M.G., and Petronczki, M. (2015). Cytokinesis in animal cells. Cold Spring Harb Perspect Biol *7*, a015834.

Demir, U., Koehler, A., Schneider, R., Schweiger, S., and Klocker, H. (2014). Metformin anti-tumor effect via disruption of the MID1 translational regulator complex and AR downregulation in prostate cancer cells. BMC cancer *14*, 52.

Denuc, A., and Marfany, G. (2010). SUMO and ubiquitin paths converge. Biochemical Society transactions *38*, 34-39.

Deshaies, R.J., and Joazeiro, C.A. (2009). RING domain E3 ubiquitin ligases. Annu Rev Biochem *78*, 399-434.

Dikic, I., Wakatsuki, S., and Walters, K.J. (2009). Ubiquitin-binding domains - from structures to functions. Nat Rev Mol Cell Biol *10*, 659-671.

Dionne, L.K., Wang, X.J., and Prekeris, R. (2015). Midbody: from cellular junk to regulator of cell polarity and cell fate. Curr Opin Cell Biol *35*, 51-58.

Dou, H., Buetow, L., Sibbet, G.J., Cameron, K., and Huang, D.T. (2012). BIRC7-E2 ubiquitin conjugate structure reveals the mechanism of ubiquitin transfer by a RING dimer. Nat Struct Mol Biol *19*, 876-883.

Du, H., Huang, Y., Zaghlula, M., Walters, E., Cox, T.C., and Massiah, M.A. (2013). The MID1 E3 ligase catalyzes the polyubiquitination of Alpha4 (alpha4), a regulatory subunit

of protein phosphatase 2A (PP2A): novel insights into MID1-mediated regulation of PP2A. J Biol Chem *288*, 21341-21350.

Eggert, U.S., Mitchison, T.J., and Field, C.M. (2006). Animal cytokinesis: from parts list to mechanisms. Annu Rev Biochem *75*, 543-566.

Eisenhardt, N., Chaugule, V.K., Koidl, S., Droescher, M., Dogan, E., Rettich, J., Sutinen, P., Imanishi, S.Y., Hofmann, K., Palvimo, J.J., *et al*. (2015). A new vertebrate SUMO enzyme family reveals insights into SUMO-chain assembly. Nat Struct Mol Biol *22*, 959-967.

Eletr, Z.M., Huang, D.T., Duda, D.M., Schulman, B.A., and Kuhlman, B. (2005). E2 conjugating enzymes must disengage from their E1 enzymes before E3-dependent ubiquitin and ubiquitin-like transfer. Nat Struct Mol Biol *12*, 933-934.

Fededa, J.P., and Gerlich, D.W. (2012). Molecular control of animal cell cytokinesis. Nat Cell Biol *14*, 440-447.

Finley, D. (2009). Recognition and processing of ubiquitin-protein conjugates by the proteasome. Annu Rev Biochem *78*, 477-513.

Finley, R.L., Jr., and Brent, R. (1994). Interaction mating reveals binary and ternary connections between Drosophila cell cycle regulators. Proc Natl Acad Sci U S A *91*, 12980-12984.

Fontanella, B., Russolillo, G., and Meroni, G. (2008). MID1 mutations in patients with X-linked Opitz G/BBB syndrome. Hum Mutat *29*, 584-594.

Gholkar, A. A., Senese, S., Lo, Y.-C., Vides, E., Contreras, E., Hodara, E., … Torres, J. Z. (2016). The Mid2 X-linked Intellectual Disability Ubiquitin Ligase Associates with Astrin and Regulates Astrin Levels to Promote Cell Division. *Cell Reports*, *14*(2), 180–188

Grabbe, C., and Dikic, I. (2009). Functional roles of ubiquitin-like domain (ULD) and ubiquitin-binding domain (UBD) containing proteins. Chemical reviews *109*, 1481-1494.

Graham, F.L., and van der Eb, A.J. (1973). A new technique for the assay of infectivity of human adenovirus 5 DNA. Virology *52*, 456-467.

Hakimi, M.A., Bochar, D.A., Chenoweth, J., Lane, W.S., Mandel, G., and Shiekhattar, R. (2002). A core-BRAF35 complex containing histone deacetylase mediates repression of neuronal-specific genes. Proc Natl Acad Sci U S A *99*, 7420-7425.

Han, X., Du, H., and Massiah, M.A. (2011). Detection and Characterization of the In Vitro E3 Ligase Activity of the Human MID1 Protein. J Mol Biol *407*, 505-520.

Hatakeyama, S. (2011). TRIM proteins and cancer. Nat Rev Cancer *11*, 792-804.

Hayashi, M.T., and Karlseder, J. (2013). DNA damage associated with mitosis and cytokinesis failure. Oncogene *32*, 4593-4601.

Herquel, B., Ouararhni, K., Khetchoumian, K., Ignat, M., Teletin, M., Mark, M., Bechade, G., Van Dorsselaer, A., Sanglier-Cianferani, S., Hamiche, A., *et al*. (2011). Transcription cofactors TRIM24, TRIM28, and TRIM33 associate to form regulatory complexes that suppress murine hepatocellular carcinoma. Proc Natl Acad Sci U S A *108*, 8212-8217.

Hershko, A., Ciechanover, A., and Varshavsky, A. (2000). Basic Medical Research Award. The ubiquitin system. Nat Med *6*, 1073-1081.

Hochstrasser, M. (2009). Origin and function of ubiquitin-like proteins. Nature *458*, 422-429.

Hu, C.K., Coughlin, M., Field, C.M., and Mitchison, T.J. (2011). KIF4 regulates midzone length during cytokinesis. Curr Biol *21*, 815-824.

Huibregtse, J.M., Scheffner, M., Beaudenon, S., and Howley, P.M. (1995). A family of proteins structurally and functionally related to the E6-AP ubiquitin-protein ligase. Proc Natl Acad Sci U S A *92*, 5249.

Jacobson, A.D., Zhang, N.Y., Xu, P., Han, K.J., Noone, S., Peng, J., and Liu, C.W. (2009). The lysine 48 and lysine 63 ubiquitin conjugates are processed differently by the 26 s proteasome. J Biol Chem *284*, 35485-35494.

James, L.C., Keeble, A.H., Khan, Z., Rhodes, D.A., and Trowsdale, J. (2007). Structural basis for PRYSPRY-mediated tripartite motif (TRIM) protein function. Proc Natl Acad Sci U S A *104*, 6200-6205.

Kimura, T., Jain, A., Choi, S.W., Mandell, M.A., Schroder, K., Johansen, T., and Deretic, V. (2015). TRIM-mediated precision autophagy targets cytoplasmic regulators of innate immunity. J Cell Biol *210*, 973-989.

Kitagawa, M., and Lee, S.H. (2015). The chromosomal passenger complex (CPC) as a key orchestrator of orderly mitotic exit and cytokinesis. Frontiers in cell and developmental biology *3*, 14.

Kleiger, G., and Mayor, T. (2014). Perilous journey: a tour of the ubiquitin–proteasome

system. Trends in Cell Biology, 24(6), 352–359.

Kohler, A., Demir, U., Kickstein, E., Krauss, S., Aigner, J., Aranda-Orgilles, B., Karagiannidis, A.I., Achmuller, C., Bu, H., Wunderlich, A., *et al*. (2014). A hormone-dependent feedback-loop controls androgen receptor levels by limiting MID1, a novel translation enhancer and promoter of oncogenic signaling. Molecular cancer *13*, 146.

Komander, D., and Rape, M. (2012). The ubiquitin code. Annu Rev Biochem *81*, 203-229.

Kraft, C., Peter, M., and Hofmann, K. (2010). Selective autophagy: ubiquitin-mediated recognition and beyond. Nat Cell Biol *12*, 836-841.

Krauss, S., Griesche, N., Jastrzebska, E., Chen, C., Rutschow, D., Achmuller, C., Dorn, S., Boesch, S.M., Lalowski, M., Wanker, E., *et al*. (2013). Translation of HTT mRNA with expanded CAG repeats is regulated by the MID1-PP2A protein complex. Nature communications *4*, 1511.

Krauss, S., So, J., Hambrock, M., Kohler, A., Kunath, M., Scharff, C., Wessling, M., Grzeschik, K.H., Schneider, R., and Schweiger, S. (2009). Point mutations in GLI3 lead to misregulation of its subcellular localization. PLoS One *4*, e7471.

Kuo, T.C., Chen, C.T., Baron, D., Onder, T.T., Loewer, S., Almeida, S., Weismann, C.M., Xu, P., Houghton, J.M., Gao, F.B., *et al*. (2011). Midbody accumulation through evasion of autophagy contributes to cellular reprogramming and tumorigenicity. Nat Cell Biol *13*, 1214-1223.

Kurasawa, Y., Earnshaw, W.C., Mochizuki, Y., Dohmae, N., and Todokoro, K. (2004). Essential roles of KIF4 and its binding partner PRC1 in organized central spindle midzone formation. EMBO J *23*, 3237-3248.

Lancioni, A., Pizzo, M., Fontanella, B., Ferrentino, R., Napolitano, L.M., De Leonibus, E., and Meroni, G. (2010). Lack of Mid1, the mouse ortholog of the Opitz syndrome gene, causes abnormal development of the anterior cerebellar vermis. J Neurosci *30*, 2880-2887.

Landry, J.R., Rouhi, A., Medstrand, P., and Mager, D.L. (2002). The Opitz syndrome gene Mid1 is transcribed from a human endogenous retroviral promoter. Mol Biol Evol *19*, 1934-1942.

Lascano, J., Uchil, P.D., Mothes, W., and Luban, J. (2015). TRIM5 Retroviral Restriction Activity Correlates with the Ability To Induce Innate Immune Signaling. J Virol *90*, 308-316.

Lee, M., Daniels, M.J., Garnett, M.J., and Venkitaraman, A.R. (2011). A mitotic function for the high-mobility group protein HMG20b regulated by its interaction with the BRC repeats of the BRCA2 tumor suppressor. Oncogene *30*, 3360-3369.

Lee, M., and Venkitaraman, A.R. (2014). A cancer-associated mutation inactivates a region of the high-mobility group protein HMG20b essential for cytokinesis. Cell Cycle *13*, 2554-2563.

Lee, Y.M., and Kim, W. (2003). Association of human kinesin superfamily protein member 4 with BRCA2-associated factor 35. Biochem J *374*, 497-503.

Lee, Y.M., Shin, H., Choi, W., Ahn, S., and Kim, W. (2002). Characterization of human SMARCE1r high-mobility-group protein. Biochim Biophys Acta *1574*, 269-276.

Lekomtsev, S., Su, K.C., Pye, V.E., Blight, K., Sundaramoorthy, S., Takaki, T., Collinson, L.M., Cherepanov, P., Divecha, N., and Petronczki, M. (2012). Centralspindlin links the mitotic spindle to the plasma membrane during cytokinesis. Nature *492*, 276-279.

Li, W., Tu, D., Brunger, A.T., and Ye, Y. (2007). A ubiquitin ligase transfers preformed polyubiquitin chains from a conjugating enzyme to a substrate. Nature *446*, 333-337.

Li, Y., Wu, H., Wu, W., Zhuo, W., Liu, W., Zhang, Y., Cheng, M., Chen, Y.G., Gao, N., Yu, H., *et al*. (2014). Structural insights into the TRIM family of ubiquitin E3 ligases. Cell research *24*, 762-765.

Lima, C.D., and Schulman, B.A. (2012). Structural biology: A protein engagement RING. Nature *489*, 43-44.

Liu, E., Knutzen, C.A., Krauss, S., Schweiger, S., and Chiang, G.G. (2011). Control of mTORC1 signaling by the Opitz syndrome protein MID1. Proc Natl Acad Sci U S A *108*, 8680-8685.

Liu, J., Prickett, T.D., Elliott, E., Meroni, G., and Brautigan, D.L. (2001). Phosphorylation and microtubule association of the Opitz syndrome protein mid-1 is regulated by protein phosphatase 2A via binding to the regulatory subunit alpha 4. Proc Natl Acad Sci U S A *98*, 6650-6655.

Lu, T., Chen, R., Cox, T.C., Moldrich, R.X., Kurniawan, N., Tan, G., Perry, J.K., Ashworth, A., Bartlett, P.F., Xu, L., *et al*. (2013). X-linked microtubule-associated protein, Mid1, regulates axon development. Proc Natl Acad Sci U S A *110*, 19131-19136.

Mandell, M.A., Jain, A., Arko-Mensah, J., Chauhan, S., Kimura, T., Dinkins, C., Silvestri, G., Munch, J., Kirchhoff, F., Simonsen, A., *et al*. (2014). TRIM proteins regulate autophagy and can target autophagic substrates by direct recognition. Dev Cell *30*, 394-409.

Marmorstein, L.Y., Kinev, A.V., Chan, G.K., Bochar, D.A., Beniya, H., Epstein, J.A., Yen, T.J., and Shiekhattar, R. (2001). A human BRCA2 complex containing a structural DNA binding component influences cell cycle progression. Cell *104*, 247-257.

McDowell, G.S., and Philpott, A. (2013). Non-canonical ubiquitylation: mechanisms and consequences. The international journal of biochemistry & cell biology *45*, 1833-1842.

Meroni, G., and Diez-Roux, G. (2005). TRIM/RBCC, a novel class of 'single protein RING finger' E3 ubiquitin ligases. Bioessays *27*, 1147-1157.

Mondal, G., Rowley, M., Guidugli, L., Wu, J., Pankratz, V.S., and Couch, F.J. (2012). BRCA2 localization to the midbody by filamin A regulates cep55 signaling and completion of cytokinesis. Dev Cell *23*, 137-152.

Mukai, A., Mizuno, E., Kobayashi, K., Matsumoto, M., Nakayama, K.I., Kitamura, N., and Komada, M. (2008). Dynamic regulation of ubiquitylation and deubiquitylation at the central spindle during cytokinesis. J Cell Sci *121*, 1325-1333.

Napolitano, L.M., Jaffray, E.G., Hay, R.T., and Meroni, G. (2011). Functional interactions between ubiquitin E2 enzymes and TRIM proteins. Biochem J *434*, 309-319.

Napolitano, L.M., and Meroni, G. (2012). TRIM family: Pleiotropy and diversification through homomultimer and heteromultimer formation. IUBMB Life *64*, 64-71.

Nayak, A., and Muller, S. (2014). SUMO-specific proteases/isopeptidases: SENPs and beyond. Genome Biol *15*, 422.

Nisole, S., Stoye, J.P., and Saib, A. (2005). TRIM family proteins: retroviral restriction and antiviral defence. Nat Rev Microbiol *3*, 799-808.

Niu, J., Shi, Y., Iwai, K., and Wu, Z.H. (2011). LUBAC regulates NF-kappaB activation upon genotoxic stress by promoting linear ubiquitination of NEMO. EMBO J *30*, 3741-3753.

Nunes Bastos, R., Gandhi, S.R., Baron, R.D., Gruneberg, U., Nigg, E.A., and Barr, F.A. (2013). Aurora B suppresses microtubule dynamics and limits central spindle size by locally activating KIF4A. J Cell Biol *202*, 605-621.

Opitz, J.M. (1987). G syndrome (hypertelorism with esophageal abnormality and hypospadias, or hypospadias-dysphagia, or "Opitz-Frias" or "Opitz-G" syndrome)--perspective in 1987 and bibliography. Am J Med Genet *28*, 275-285.

Ozato, K., Shin, D.M., Chang, T.H., and Morse, H.C., 3rd (2008). TRIM family proteins and their emerging roles in innate immunity. Nat Rev Immunol *8*, 849-860.

Ozlu, N., Monigatti, F., Renard, B.Y., Field, C.M., Steen, H., Mitchison, T.J., and Steen, J.J. (2010). Binding partner switching on microtubules and aurora-B in the mitosis to cytokinesis transition. Mol Cell Proteomics *9*, 336-350.

Peterson, T.R., Laplante, M., Van Veen, E., Van Vugt, M., Thoreen, C.C., and Sabatini, D.M. (2015). mTORC1 regulates cytokinesis through activation of Rho-ROCK signaling. arXivorg *arXiv:1506.04437*.

Petronczki, M., Glotzer, M., Kraut, N., and Peters, J.M. (2007). Polo-like kinase 1 triggers the initiation of cytokinesis in human cells by promoting recruitment of the RhoGEF Ect2 to the central spindle. Dev Cell *12*, 713-725.

Pickart, C.M., and Eddins, M.J. (2004). Ubiquitin: structures, functions, mechanisms. Biochim Biophys Acta *1695*, 55-72.

Pinheiro, D., and Bellaiche, Y. (2014). Making the most of the midbody remnant: specification of the dorsal-ventral axis. Dev Cell *28*, 219-220.

Plechanovova, A., Jaffray, E.G., Tatham, M.H., Naismith, J.H., and Hay, R.T. (2012). Structure of a RING E3 ligase and ubiquitin-loaded E2 primed for catalysis. Nature *489*, 115-120.

Pohl, C., and Jentsch, S. (2008). Final stages of cytokinesis and midbody ring formation are controlled by BRUCE. Cell *132*, 832-845.

Pohl, C., and Jentsch, S. (2009). Midbody ring disposal by autophagy is a post-abscission event of cytokinesis. Nat Cell Biol *11*, 65-70.

Poyurovsky, M.V., Priest, C., Kentsis, A., Borden, K.L., Pan, Z.Q., Pavletich, N., and Prives, C. (2007). The Mdm2 RING domain C-terminus is required for supramolecular assembly and ubiquitin ligase activity. EMBO J *26*, 90-101.

Quaderi, N.A., Schweiger, S., Gaudenz, K., Franco, B., Rugarli, E.I., Berger, W., Feldman, G.J., Volta, M., Andolfi, G., Gilgenkrantz, S., *et al*. (1997). Opitz G/BBB syndrome, a defect of midline development, is due to mutations in a new RING finger gene on Xp22. Nature Genetics *17*, 285-291.

Reymond, A., Meroni, G., Fantozzi, A., Merla, G., Cairo, S., Luzi, L., Riganelli, D., Zanaria, E., Messali, S., Cainarca, S., *et al*. (2001). The tripartite motif family identifies cell compartments. Embo J *20*, 2140-2151.

Rivero, S., Ceballos-Chavez, M., Bhattacharya, S.S., and Reyes, J.C. (2015). HMG20A is required for SNAI1-mediated epithelial to mesenchymal transition. Oncogene *34*, 5264-5276.

Sagona, A.P., and Stenmark, H. (2010). Cytokinesis and cancer. FEBS Lett *584*, 2652-2661.

Sanchez, J.G., Okreglicka, K., Chandrasekaran, V., Welker, J.M., Sundquist, W.I., and Pornillos, O. (2014). The tripartite motif coiled-coil is an elongated antiparallel hairpin dimer. Proc Natl Acad Sci U S A *111*, 2494-2499.

Sardiello, M., Cairo, S., Fontanella, B., Ballabio, A., and Meroni, G. (2008). Genomic analysis of the TRIM family reveals two groups of genes with distinct evolutionary properties. BMC Evol Biol *8*, 225.

Scaglione, K.M., Basrur, V., Ashraf, N.S., Konen, J.R., Elenitoba-Johnson, K.S., Todi, S.V., and Paulson, H.L. (2013). The ubiquitin-conjugating enzyme (E2) Ube2w ubiquitinates the N terminus of substrates. J Biol Chem *288*, 18784-18788.

Schmidt, O., and Teis, D. (2012). The ESCRT machinery. Curr Biol, 22(4), R116–R120.

Schuh, A. L. and Audhya, A. (2014). The ESCRT machinery: From the plasma membrane to endosomes and back again. Critic Rev Biochem Mol Biol 49(3), 242–261.

Schulman, B.A., and Harper, J.W. (2009). Ubiquitin-like protein activation by E1 enzymes: the apex for downstream signalling pathways. Nat Rev Mol Cell Biol *10*, 319-331.

Schumacher, F.R., Wilson G., Day, C.L. (2013). The N-Terminal Extension of UBE2E Ubiquitin-Conjugating Enzymes Limits Chain Assembly, J Mol Biol, 425, Issue 22, 4099-4111.

Schweiger, S., Dorn, S., Fuchs, M., Kohler, A., Matthes, F., Muller, E.C., Wanker, E., Schneider, R., and Krauss, S. (2014). The E3 ubiquitin ligase MID1 catalyzes ubiquitination and cleavage of Fu. J Biol Chem *289*, 31805-31817.

Sedzinski, J., Biro, M., Oswald, A., Tinevez, J.Y., Salbreux, G., and Paluch, E. (2011). Polar actomyosin contractility destabilizes the position of the cytokinetic furrow. Nature *476*, 462-466.

Shaid, S., Brandts, C.H., Serve, H., and Dikic, I. (2013). Ubiquitination and selective autophagy. Cell Death Differ *20*, 21-30.

Short, K.M., and Cox, T.C. (2006). Sub-classification of the rbcc/trim superfamily reveals a novel motif necessary for microtubule binding. J Biol Chem.

Short, K.M., Hopwood, B., Yi, Z., and Cox, T.C. (2002). MID1 and MID2 homo- and heterodimerise to tether the rapamycin- sensitive PP2A regulatory subunit, Alpha 4, to microtubules: implications for the clinical variability of X-linked Opitz GBBB syndrome and other developmental disorders. BMC Cell Biol *3*, 1.

Stros, M., Launholt, D., and Grasser, K.D. (2007). The HMG-box: a versatile protein domain occurring in a wide variety of DNA-binding proteins. Cellular and molecular life sciences : CMLS *64*, 2590-2606.

Sullivan, M., and Morgan, D.O. (2007). Finishing mitosis, one step at a time. Nat Rev Mol Cell Biol *8*, 894-903.

Suryadinata, R., Roesley, S.N., Yang, G., and Sarcevic, B. (2014). Mechanisms of generating polyubiquitin chains of different topology. Cells *3*, 674-689.

Suzuki, M., Hara, Y., Takagi, C., Yamamoto, T.S., and Ueno, N. (2010). MID1 and MID2 are required for Xenopus neural tube closure through the regulation of microtubule organization. Development *137*, 2329-2339.

Takahara, Y., Maeda, M., Hasegawa, H., Ito, S., Hyodo, T., Asano, E., Takahashi, M., Hamaguchi, M., and Senga, T. (2014). Silencing of TBC1D15 promotes RhoA activation and membrane blebbing. Molecular and cellular biochemistry *389*, 9-16.

Tao, H., Simmons, B.N., Singireddy, S., Jakkidi, M., Short, K.M., Cox, T.C., and Massiah, M.A. (2008). Structure of the MID1 tandem B-boxes reveals an interaction reminiscent of intermolecular ring heterodimers. Biochemistry *47*, 2450-2457.

Tatham, M.H., Geoffroy, M.C., Shen, L., Plechanovova, A., Hattersley, N., Jaffray, E.G., Palvimo, J.J., and Hay, R.T. (2008). RNF4 is a poly-SUMO-specific E3 ubiquitin ligase required for arsenic-induced PML degradation. Nat Cell Biol *10*, 538-546.

Tatham, M.H., Plechanovova, A., Jaffray, E.G., Salmen, H., and Hay, R.T. (2013). Ube2W conjugates ubiquitin to alpha-amino groups of protein N-termini. Biochem J *453*, 137-145.

Tokgöz, Z., Siepmann, T. J., Streich, F., Kumar, B., Klein, J. M., and Haas, A. L. (2012). E1-E2 Interactions in Ubiquitin and Nedd8 Ligation Pathways. *The Journal of Biological Chemistry*, *287*(1), 311–321.

Trockenbacher, A., Suckow, V., Foerster, J., Winter, J., Krauss, S., Ropers, H.H., Schneider, R., and Schweiger, S. (2001). MID1, mutated in Opitz syndrome, encodes an ubiquitin ligase that targets phosphatase 2A for degradation. Nat Genet *29*, 287-294.

van Beuningen, S.F., Will, L., Harterink, M., Chazeau, A., van Battum, E.Y., Frias, C.P., Franker, M.A., Katrukha, E.A., Stucchi, R., Vocking, K., *et al*. (2015). TRIM46 Controls Neuronal Polarity and Axon Specification by Driving the Formation of Parallel Microtubule Arrays. Neuron *88*, 1208-1226.

van Wijk, S. J.L., and Timmers, H.T.M. (2010). The family of ubiquitin-conjugating enzymes (E2s): deciding between life and death of proteins. FASEB J 24:981-993.

Walczak, H., Iwai, K., and Dikic, I. (2012). Generation and physiological roles of linear ubiquitin chains. BMC Biol *10*, 23.

Watkins, G.R., Wang, N., Mazalouskas, M.D., Gomez, R.J., Guthrie, C.R., Kraemer, B.C., Schweiger, S., Spiller, B.W., and Wadzinski, B.E. (2012). Monoubiquitination promotes calpain cleavage of the protein phosphatase 2A (PP2A) regulatory subunit alpha4, altering PP2A stability and microtubule-associated protein phosphorylation. J Biol Chem *287*, 24207-24215.

Weissman A.M., Shabek N. and Ciechanover A. (2010) The predator becomes the prey: regulating the ubiquitin system by ubiquitylation and degradation. Nat Rev Mol Cell Biology 12, 605-620.

Wenzel, D.M., and Klevit, R.E. (2012). Following Ariadne's thread: a new perspective on RBR ubiquitin ligases. BMC Biol *10*, 24.

Williams R.L. and Urbè S. (2007). The emerging shape of the ESCRT machinery. Nat Rev Mol Cell Biol 8, 355-368.

Wright, M.H., Berlin, I., and Nash, P.D. (2011). Regulation of endocytic sorting by ESCRT-DUB-mediated deubiquitination. Cell biochemistry and biophysics *60*, 39-46.

Wynder, C., Hakimi, M.A., Epstein, J.A., Shilatifard, A., and Shiekhattar, R. (2005). Recruitment of MLL by HMG-domain protein iBRAF promotes neural differentiation. Nat Cell Biol *7*, 1113-1117.

Xu, P., Duong, D.M., Seyfried, N.T., Cheng, D., Xie, Y., Robert, J., Rush, J., Hochstrasser, M., Finley, D., and Peng, J. (2009). Quantitative proteomics reveals the function of unconventional ubiquitin chains in proteasomal degradation. Cell *137*, 133-145.

Ye, Y., and Rape, M. (2009). Building ubiquitin chains: E2 enzymes at work. Nat Rev Mol Cell Biol *10*, 755-764.

Yuce, O., Piekny, A., and Glotzer, M. (2005). An ECT2-centralspindlin complex regulates the localization and function of RhoA. J Cell Biol *170*, 571-582.

Zheng, N., Schulman, B.A., Song, L., Miller, J.J., Jeffrey, P.D., Wang, P., Chu, C., Koepp, D.M., Elledge, S.J., Pagano, M., *et al*. (2002). Structure of the Cul1-Rbx1-Skp1-F boxSkp2 SCF ubiquitin ligase complex. Nature *416*, 703-709.